Non-coding transcription and post-transcriptional mRNA regulation in quiescent *Saccharomyces cerevisiae*

Alison Claire Greenlaw

A dissertation

submitted in partial fulfillment of the

requirements for the degree of

Doctor of Philosophy

University of Washington

2023

Reading Committee:

Toshio Tsukiyama, Chair

Steven Hahn

David Shechner

Program Authorized to Offer Degree:

Molecular and Cellular Biology

University of Washington

Abstract

Non-coding transcription and post-transcriptional mRNA regulation in quiescent *Saccharomyces cerevisiae*

Alison Claire Greenlaw

Chair of the Supervisory Committee:
Toshio Tsukiyama
Biochemistry

Quiescence is a conserved resting state, which is required for long-term survival. Quiescent cells, far from being inert, are poised to re-enter the mitotic cell cycle when conditions are appropriate. In this thesis, I analyzed the nascent transcriptome of quiescent budding yeast and found an increase in relative abundance of non-coding transcription compared to G_1-arrested yeast. Analysis of the nascent and steady-state transcriptomes also revealed increased post-transcriptional regulation in quiescence compared to G_1-arrested cells. To further understand the role of post-transcriptional regulation and non-coding transcripts in quiescence, I investigated the nuclear exosome-NNS pathway. This pathway is known to function in the regulation of non-coding transcripts in exponentially growing yeast. My work revealed that the nuclear exosome and NNS regulate over one thousand mRNAs in quiescent cells in addition to canonical non-coding RNA

targets. RNA sequencing yeast from multiple time points revealed that the nuclear exosome functions in two distinct phases, one around the diauxic shift and the other later in quiescence entry. mRNAs regulated by the NNS-nuclear exosome pathway are enriched in functions such as protein synthesis, metabolism, cellular organization, and the cell cycle, underscoring the importance of this pathway in promoting cellular quiescence.

TABLE OF CONTENTS

LIST OF FIGURES

LIST OF TABLES

ACKNOWLEDGEMENTS

Thank you to Toshi Tsukiyama for five years of mentorship and science. He has encouraged my interest in weird RNA biology, while also helping me from falling down too many rabbit holes. I am very grateful I had the opportunity to do my graduate training in his lab. Thank you to past and present members of the lab. Thank you to Dr. Christine Cucinotta and Dr. Sarah Swugert who were crucial mentors as I learned genomics. Thank you to Rachel Dell for being a joy to share a bay with. Thank you, Dr. Kris Alavattam, for your help with bioinformatics and for taking on Trinity. I am glad to have you as a co-author. Thank you also Dr. Ishita Joshi, Dr. Rina Hirano, and Dakota Hunt for being wonderful lab mates.

Thank you to the members of my committee: Dr. David Shechner, Dr. Edith Wang, Dr. Rasi Subramaniam and Dr. Steve Hahn for their support and feedback during my graduate work. Thank you especially to David and Steve for reading this dissertation.

Thank you to the members of the Hahn lab for you feedback and help over the years. It has been wonderful to share joint lab meetings with you. Thank you to the whole first floor Weintraub community, especially the Hahn and Henikoff lab for their comradery.

Thank you to my graduate school friends, particularly to Amy, Hannah, Maddy, Cassidy and Nandita. Thank to my parents, who have been there for me and supportive every step of the way. Finally, thank you to my cat, Fitz, who has improved my life immeasurably without even trying.

Chapter 1. INTRODUCTION

1.1 QUIESCENCE

1.1.1 *G_0, stationary phase and quiescence*

In 1963, Laszlo Lajtha proposed the existence of a nondividing state where "cells would just sit, minding their own biochemical business". He named this "true resting state" G_0 based on the "gap notation" used to named G_1 and G_2 (Lajtha, 1963). Over time, G_0 as a term has come to encompass multiple exits from the mitotic cell cycle, including permanent exits like terminal differentiation and senescence (Cheung & Rando, 2013). Quiescence is a unique G_0 state because it is readily reversable. Quiescent cells remain poised to re-enter the cell cycle when conditions are favorable, allowing for long term survival. This resting but poised state is crucial to organisms across domains of life. Multi-cellular organisms need to maintain a pool of quiescent adult stem cells for tissue repair and homeostasis (de Morree & Rando, 2023). Single celled organisms must be able to survive starvation conditions, especially since most microbes are quiescent most of the time (De Virgilio, 2012; Dworkin & Harwood, 2022; Rittershaus et al., 2013). Microbes have therefore spent much of evolutionary time in this cell state which is relatively under-studied, and key to their ability to adapt to changing environments (D. Lewis & Gattie, 1991). As a result, many genes may have yet undiscovered quiescence-specific functions.

Understanding quiescence in more detail has the potential to improve human health. Proper regulation of quiescence is necessary for healthy cells to avoid becoming cancerous (Hanahan & Weinberg, 2011; Tomasin & Bruni-Cardoso, 2022). Additionally, cancer cells have been proposed to enter quiescence as a mechanism to evade treatments (Bruschini et al., 2020;

W. Chen et al., 2016; Nik Nabil et al., 2021; J. Zhang et al., 2019). Quiescence in eukaryotes also has ramifications for infectious diseases. Pathogenic fungi are estimated to cause 1.2 million deaths per year worldwide (Brown et al., 2012), making them a serious health concern. Pathogenic yeast such as *Candida albicans* rely on forming biofilms where quiescence populations can evade treatment with anti-fungal drugs (Bojsen et al., 2014; Palková & Váchová, 2016). Studying quiescence in *Saccharomyces cerevisiae,* a closely related yeast species, can help uncover both basic biology and promote more translational research.

1.1.2 *Quiescence in Saccharomyces cerevisiae*

Saccharomyces cerevisiae (hereafter yeast) is widely used model system to study quiescence. Whether quiescence in yeast is analogous to mammalian G_0 is controversial (De Virgilio, 2012). However, many similarities between quiescent yeast and mammalian cells have been observed including genome compaction (Piñon, 1978), expression of heat shock proteins (Iida & Yahara, 1984), and G_1 DNA content (Gray et al., 2004; Pardee, 1974). Additionally, conserved signaling pathways such as TOR and PKA promote quiescence in yeast and mammals (Chapman et al., 2020; De Virgilio, 2012; Dhawan & Laxman, 2015).

Generally, G_0 is conceptualized as an "off cycle" cell state (Figure 1.1). Classically, in animal cells, a single restriction point exists for commitment to the cell cycle, and cells arrest in G_1 (Pardee, 1974, 1989; Zetterberg & Larsson, 1985). Recent studies have identified G_2 neural stem cells in *Drosophila* (Otsuki & Brand, 2018), and that mouse epidermal stem cells require G_2 cells for normal calcium signaling (Moore et al., 2023), suggesting exceptions to this rule may be more common in normal tissue homeostasis than previously believed.

In yeast, conditional cell division cycle (*cdc*) mutants were used to arrest cells in different cell states as well as define which cell cycle events are dependent on one another (Hartwell et al.,

1974). If G_0 were truly a distinct "off-cycle" cell state, similar mutants should exist to arrest cells in G_0. Theses mutants would be unable to exit stationary phase under restrictive conditions but would not display other cell cycle defects (Gray et al., 2004; Werner-Washburne et al., 1993). This requirement was briefly met in 1987, when a conditional mutant for exit from stationary phase was discovered (Drebot et al., 1987). This *gcs1* mutant was unable to divide when stationary yeast cells were diluted in fresh media at the restrictive temperature of 14 °C, and were defective specifically in their ability to re-enter the cell cycle from G_0. However, later work demonstrated Gsc1 and Age2 have overlapping and essential functions in vesicular transport in exponentially growing cells (Poon et al., 2001). Therefore, the *gcs1* mutant phenotype on exit from stationary phase could be the result of low expression of Age2, rather than due to a quiescent-specific requirement (De Virgilio, 2012).

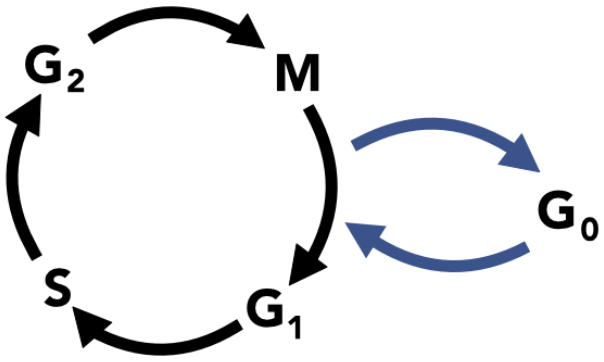

Figure 1.1 Model of G_0 as an "off-cycle" state.
Diagram of cell cycle with G_0 included.

Whether one unified quiescent state exists with essential genetic requirements, or if multiple quiescent states exist remains unknown (Breeden & Tsukiyama, 2022). Starvation from different nutrients has been studied in yeast, and limited comparative analysis suggest differences in the state reached by the cell in each case, implying that multiple quiescent states

may develop in response to nutrient limitation (Boer et al., 2010; Klosinska et al., 2011; J. Wu et al., 2004). For the purposes of this introduction, I will focus on entry into quiescence with respect to glucose exhaustion in YPD (1% yeast extract, 2% peptone, 2% glucose). All work for this thesis was performed in YPD, as historically this system has been most widely used to study quiescence in yeast (De Virgilio, 2012).

Yeast cells enter cellular quiescence over multiple days. During the first day, cells grow exponentially, fermenting glucose to support an approximately 90-minute doubling time at 30˚C (Herskowitz, 1988). Named the "Crabtree effect", yeast favor fermentation over respiration even in the presence of oxygen (Goddard & Greig, 2015; Pfeiffer & Morley, 2014). This is proposed to provide several evolutionary advantages such as increased speed of glucose consumption compared to other microbes (Pfeiffer et al., 2001), and the production of heat and toxic ethanol (Goddard, 2008). As glucose is exhausted, cells sense that nutrients will become limiting, and begin to store glucose as glycogen and later as trehalose (Lillie & Pringle, 1980). When glucose has been depleted from the media, yeast transition to post-diauxic growth, and rely on respiration to continue to grow (Werner-Washburne et al., 1993). Cells reach saturation over approximately seven days, forming a heterogenous culture with at least two distinct cell types: quiescent (Q) and non-quiescent (NQ) (Figure 1.2) (Allen et al., 2006). Allen et al. developed a method to separate these populations by density centrifugation, with the quiescent fraction going to the bottom of the gradient while the non-quiescent population stays at the top. This initial study found that these populations have distinct characteristics with non-quiescent cells having decreased longevity and thermotolerance and altered gene expression patterns compared to the quiescent fraction. In general, the quiescent yeast cells are mostly younger "daughter" cells, while older "mothers" remain in the non-quiescent fraction (Aragon et al., 2008; L. Li et al.,

2013). However, some strains have vastly different quiescence entry efficacy demonstrating this rule is not universal (Miles et al., 2019, 2023) (See Appendix A).

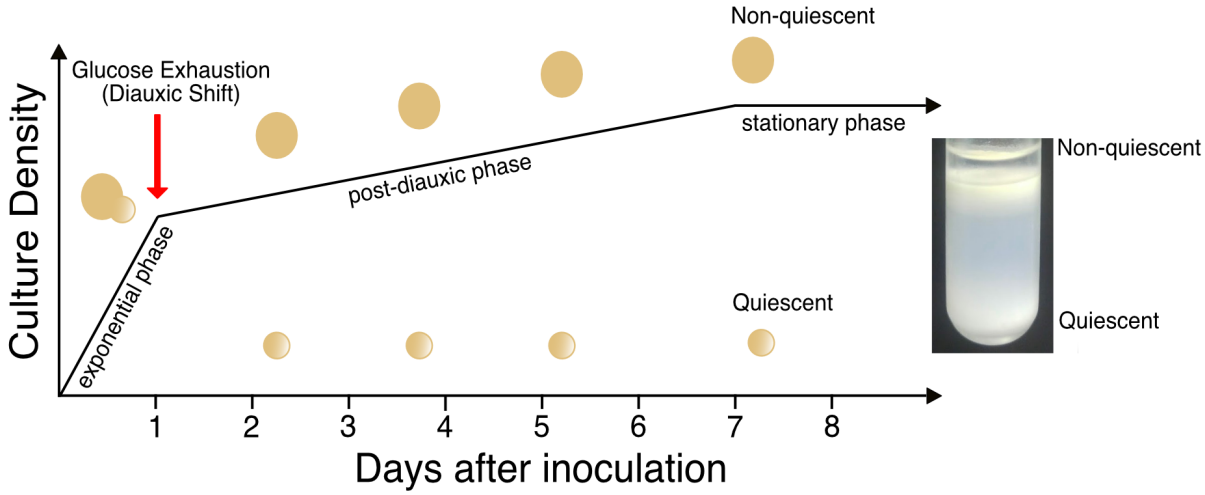

Figure 1.2 Yeast growth phase with time.
Schematic diagram of culture density, growth phase and time in yeast (left) with quiescent and non-quiescent fraction (right). Adapted from Werner-Washburne et al. 1993 and Allen et al. 2006.

The ability to isolate quiescent yeast has facilitated the study of the gene regulation during this state. Gene expression is globally altered, with an initial study using micro-arrays determining that over 1300 mRNAs distinguished quiescent and non-quiescent cells, and that expression patterns were distinct from G_1-arrested cells (Aragon et al., 2008). During entry into quiescence gene expression is globally repressed. Nucleosome depleted regions are narrowed, and histones are de-acetylated to reduce transcription (McKnight et al., 2015). While histone acetylation during quiescence entry decreases dramatically, alterations in histone methylation are more subtle and gene specific (Mews et al., 2014; Young et al., 2017). Additionally, the 3D structure of chromatin is globally compacted, resulting in a 35% smaller nucleus compared to G_1-arrested cells (Swygert et al., 2019). In concert with reduced transcription, translation is also globally repressed upon starvation (Ashe et al., 2000; L. M. Dickson & Brown, 1998; Fuge et al.,

1994). Interestingly, 5′ cap recognition factor eIF4E is dispensable for survival during starvation, but another translation initiation factor eIF4A is not (Paz & Choder, 2001). Additionally, genes with internal ribosome entry sites are translated during nitrogen starvation and stationary phase (Gilbert et al., 2007; Paz et al., 1999). Gene expression during quiescence is globally repressed, however cells retain the ability to rapidly exit, with transcription occurring within minutes of refeeding in YPD (Cucinotta et al., 2021).

1.1.3 *Post-transcriptional regulation of RNA in quiescence*

Post-transcriptional regulation of RNA is altered upon entry into quiescence. While many mechanisms involving the regulation of chromatin in quiescence have been explored, many fewer post-transcriptional mechanisms have been identified. A study using a fibroblast model of quiescence found approximately 500 mRNAs with altered half-life compared to growing fibroblasts (Johnson et al., 2017). Upon starvation from multiple nutrients yeast activate autophagy, a conserved mechanism of bulk decay (Reggiori & Klionsky, 2013). In yeast, autophagy has recently been shown to act on RNA (H. Huang et al., 2015) and be at least somewhat selective (Makino et al., 2021).

Several RNA binding proteins have been identified as regulators of quiescence. In mouse lymphocytes, RNA binding proteins ZFP36L1 and ZFP36L2 suppress the transition into S-phase (Galloway et al., 2016). Tis11, the *Drosophila* ortholog to ZFP36L1 and ZFP36L2, promotes mRNA degradation which is key to re-establishing intestinal stem cell quiescence after injury (McClelland et al., 2017). In yeast, the RNA-binding proteins Ssd1 and Mpt5 have parallel roles in promoting quiescence entry in yeast (L. Li et al., 2013). Mpt5, ZFP36L1 and ZFP36L2, and Tisll all interact with the Ccr4-Not deadenylase complex (Akiyama & Yamamoto, 2021; Fabian et al., 2013; Hook et al., 2007) which has been shown to regulate quiescence in human and

mouse immune cells (Akiyama et al., 2021). Given that this altered regulation of RNA decay is observed in multiple model systems across eukaryotic life, altered RNA stability might be a hallmark of quiescence. However, most of genes studied so far are restricted to a few of the many RNA decay pathways available to the cell, suggesting the existence of additional unknown regulators of quiescence.

RNA localization is also altered during stress conditions. The formation of phase separated RNA protein condensates is a conserved process that occurs in response to various stress conditions (Kroschwald et al., 2015; Wallace et al., 2015). Over a dozen different types of these condensates have been identified, largely based on their localization, their component proteins and their proposed functions, rather than from the perspective of their component RNAs (S. Tian et al., 2020; Wiedner & Giudice, 2021). Multiple functional RNA protein condensates have been described with functions such as ribosome biogenesis (Lafontaine et al., 2021) and regulation of translation (Parker et al., 2022). However, whether this RNA compartmentalization is necessarily functional or simply incidental in some cases is a matter of debate (Putnam et al., 2023). Current evidence suggests that some transcripts are enriched in RNA protein condensates. For example, in stationary phase yeast protease treatment of cell lysate resulted in increased abundance of over 2000 mRNAs, suggesting many RNAs are sequestered in stationary phase (Aragon et al., 2006). Which RNAs are sequestered and when the sequestration takes place is a regulated process (Escalante & Gasch, 2021). In low glucose conditions, mother cells pass processing bodies (p-bodies), a type of cytoplasmic RNA granule, on to daughter cells, resulting in larger daughters (Garmendia-Torres et al., 2014). The RNA composition of p-bodies in yeast is dependent on the stressor, and has been shown to be regulated by Mpt5 (C. Wang et al., 2018). Separately, Mpt5 has been shown to promote entry into quiescence (L. Li et al., 2013). During

transition from growth to quiescence the cytoplasmic pH drops, resulting in the cytoplasm becoming glass-like (Munder et al., 2016); this altered cytoplasm is characterized by reduced diffusion and increased protein aggregation. Interestingly, RNA concentration is a key regulator of protein aggregation, with high RNA concentration inhibiting phase separation of RNA binding proteins (Maharana et al., 2018). mRNA concentration is estimated to decrease by 30-fold on entry into quiescence (McKnight et al., 2015). Though my thesis work is on the latter, regulatory RNA sequestration and RNA decay likely work in concert to promote cellular quiescence.

1.2 NNS-NUCLEAR EXOSOME PATHWAY

1.2.1 *The nuclear RNA exosome*

The nucleus is a site of significant RNA decay, and it has even been argued that nuclear decay is the default fate of most transcription (Bresson & Tollervey, 2018). My thesis investigated the nuclear exosome, a major RNA decay pathway in the eukaryotic nucleus. The nuclear exosome is formed from the ten subunits of the core cytoplasmic exosome. Nine of these subunits form a barrel structure, with Dis3, an essential 3′to 5′ exonuclease and endonuclease associated with this barrel (Kilchert et al., 2016). The nuclear exosome has an additional exonuclease, Rrp6, which is localized to the nucleus and is non-essential in yeast (Allmang et al., 1999). The nuclear exosome, as well as many of its cofactors, are conserved in eukaryotes (Ogami et al., 2018).

Rrp6 has been implicated in the regulation of most RNA types. Genomic studies find show that Rrp6 binds rRNA, tRNA, mRNA, snRNA, snoRNA and lncRNA *in vivo* (Schneider et al., 2012; Sohrabi-Jahromi et al., 2019). 3′ end processing of structured non-coding RNAs is one of Rrp6's key roles, and in its absence 3′ extended forms of snRNAs and snoRNAs accumulate (Heo

et al., 2013; Vasiljeva & Buratowski, 2006). One of its most studied functions is in degrading non-coding transcripts, with a specific class of transcripts known as cryptic unstable transcripts (CUTs) discovered because they are readily detectible in steady state RNA when *RRP6* is deleted (Wyers et al., 2005). Additionally, Rrp6 degrades aberrant transcripts such as truncated 5S rRNA, hypo-methylated $tRNA_i^{Met}$, and improperly spliced mRNA (Kadaba et al., 2006; Lemieux et al., 2011). Most studies characterizing Rrp6 were performed in logarithmically growing cells. One report, which analyzed differential expression in *rrp6*Δ cells two hours post-diauxic shift and in early stationary phase, did not find increased mRNA abundance (Yassour et al., 2010).

1.2.2 *Transcription termination couples transcription and post-transcriptional RNA processing and decay*

Nuclear RNA decay by Rrp6 is regulated by an essential transcription termination complex−Nrd1-Nab3-Sen1 (NNS). Nrd1 and Nab3 are RNA binding proteins which interact with the nascent RNA transcript as well as the C-terminal domain (CTD) of RNA polymerase II (Pol II) (Carroll et al., 2004; Vasiljeva, Kim, Mutschler, et al., 2008). These two RNA binding proteins form an essential heterodimer (Carroll et al., 2007; Chaves-Arquero et al., 2022) and interact with RNA in a semi-specific manner (Bacikova et al., 2014) (discussed in detail below). Sen1 is an ATP dependent RNA-DNA helicase (Kim et al., 1999). *In vitro* experiments find it promotes termination by translocating along the nascent transcript and then colliding with Pol II to dislodge it (Han et al., 2017; S. Wang et al., 2019). Conserved as senataxin in humans, Sen1, also functions outside of NNS in DNA repair (Cohen et al., 2018; Hasanova et al., 2023; Yüce & West, 2013). RNA binding by Sen1 is not sequence specific, and instead interacts with Nrd1 via a CTD mimic (Han et al., 2020). However, the study which identified Sen1's CTD mimic also found it enhances, but is not necessary for transcription termination by Sen1, which instead

requires transcriptional pausing. This suggests Nab3 and Nrd1 may function to pause Pol II to recruit Sen1. Consistent with this, data using anchor away in exponentially growing yeast proposed that Nrd1 pauses Pol II transcription (Schaughency et al., 2014).

NNS mainly terminates non-coding transcripts, and directs them to the nuclear exosome for processing or decay, via a co-factor called the TRAMP complex. Trf4, a non-canonical poly(A) polymerase interacts with the Nrd1 via a CTD mimic, disrupting the interaction between Nrd1 and the Pol II CTD (Tudek et al., 2014). In *rrp6*Δ cells, Nrd1 and Nab3 accumulate on undegraded transcripts and cannot be recycled (Villa et al., 2020). This results in impaired termination of Pol II at some NNS targets *in vivo*, along with extended 3′ ends (Fox et al., 2015). Thus, while NNS is a transcriptional regulator and Rrp6 mainly functions on the level of RNA stability, the line between transcriptional and post-transcriptional is blurred in nuclear RNA metabolism.

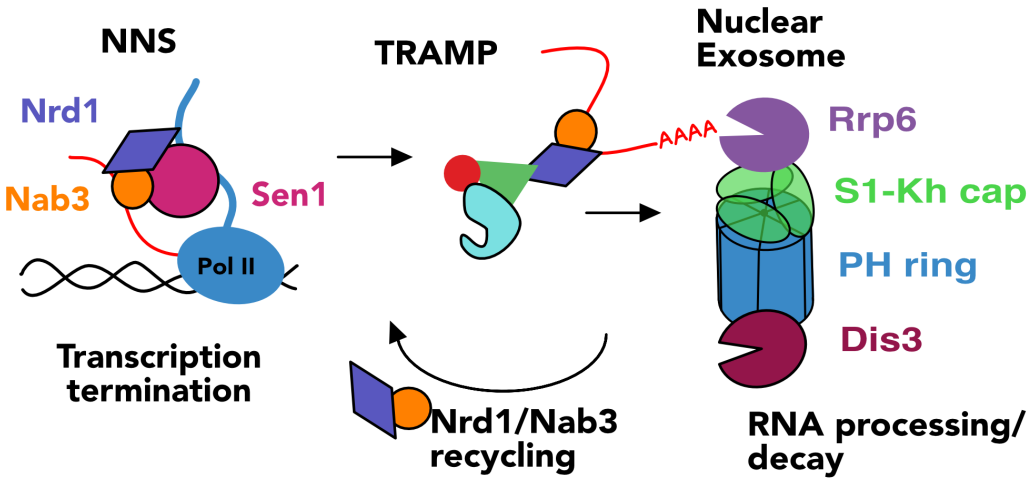

Figure 1.3 Nuclear Exosome/NNS pathway schematic.
NNS terminates transcription of RNA polymerase II transcripts. Nab3 and Nrd1 interact with the nascent transcript, and Nrd1 interacts with the CTD of Pol II. Sen1, a helicase, disrupts Pol II interaction with the DNA, terminating transcription. Nrd1, interacts with Trf4/5 of the TRAMP complex, directing transcripts for 3′ end processing or 3′ decay by nuclear exosome. Structural cartoon of the nuclear exosome shows two exonucleases, Rrp6 and Dis3, at opposite ends of the essential barrel structure. Essential genes in yeast are outlined in black. Pathway schematic

adapted from Villa and Porrua 2022. Structural cartoon of nuclear exosome adapted from Kilchert et al. 2016.

NNS acts an alternative transcription termination pathway to cleavage and polyadenylation. Cleavage and polyadenylation factor (CPF), cleavage factor IA (CFIA) and cleavage factor IB (CFIB) function in this process (Kumar et al., 2019). These two transcription termination pathways terminate most Pol II transcription in yeast (Porrua et al., 2016). Several mechanisms have been uncovered which determine whether a given transcript will be terminated by CPF or NNS.

One mechanism which discriminates between NNS and CPF pathways is post-translational modification of the Pol II CTD. This heptad repeat sequence is highly conserved across eukaryotes, and is modified as transcription progresses (P. Liu et al., 2010). Serine 5 (Ser5) phosphorylation peaks very early in transcription and diminishes quickly while serine 2 (Ser2) phosphorylation peaks towards the 3′ end of the gene (Dias et al., 2015; Mayer et al., 2012; N. Singh et al., 2022; Tietjen et al., 2010; Zaborowska et al., 2016). Ser2 phosphorylation recruits cleavage and polyadenylation complexes and is crucial for 3′ end processing in humans and yeast (Ahn et al., 2004; Davidson et al., 2014). Multiple studies have suggested that Nrd1 preferentially interacts with Ser5-phosphorylated CTD *in vitro* (Kubicek et al., 2012; Mayer et al., 2012; Vasiljeva, Kim, Mutschler, et al., 2008), and this interaction is suggested to result in NNS's preference for short loci (Gudipati et al., 2008). However, deletion of Nrd1's CTD interacting domain did not result in increased read through transcription at several snoRNA targets in one study (Vasiljeva, Kim, Mutschler, et al., 2008), though a later work found increased readthrough using Pol II ChIP (Tudek et al., 2014).

A more recent work mutated tyrosine 1 (Tyr1) of this heptad repeat to phenylalanine to block phosphorylation (Collin et al., 2019). This resulted in snoRNA read-through, without a decrease in Nrd1 recruitment to the loci. The Ser5 phospho-blocking mutant from the same study did not have any apparent readthrough transcription. This work suggested that Tyr1 phosphorylation mediated pausing, not Ser5 phosphorylation is required for efficient NNS termination *in vivo*. Nrd1 does not interact with Tyr1 phosphorylation *in vitro* (Mayer et al., 2012), further complicating the mechanism of action. While Tyr1 peaks towards the 5′end of genes in humans (Descostes et al., 2014), in yeast during logarithmic growth it peaks towards the 3′ end of genes, and prevents premature termination by polyadenylation and cleavage (Mayer et al., 2012). Re-analysis of this data has suggested this Tyr1 phosphorylation effect is likely limited to only a subset of mRNAs (Collin et al., 2019) suggesting Tyr1 phosphorylation has multiple functions.

Chromatin architecture has also been demonstrated to regulate transcription termination. 3′ nucleosome depleted regions (NDRs) form just downstream of poly(A) site and NDR width informs poly(A) site selection (Spies et al., 2009; Turner et al., 2021). A strongly positioned nucleosome is sufficient to rescue transcription termination defects (Hildreth et al., 2020). Histone post-translational modifications have also been implicated in regulation of transcription termination. In general, histone trimethylation at K4 (H3K4me3) peaks towards the 5′ end of genes while H3K4me1 peaks towards the 3′ end (Barski et al., 2007; C. L. Liu et al., 2005). Poly(A) sites have distinct chromatin signatures with decreased H3K36 trimethylation and H3K4 methylation in human cells (Khaladkar et al., 2011; C. Lee & Chen, 2013). In yeast, polyadenylation site choice is regulated by histone methyltransferases Set1 and Set2 (Kaczmarek Michaels et al., 2020). NNS mutants have been shown to have genetic interactions

with Set1 and histone demethylase, Jhd2. Increased readthrough transcription is seen when the methyltransferase activity of Set1 is removed, implying that H3K4 methylation regulates NNS termination (Terzi et al., 2011). Additionally, the "constitutively unmethylated" H3K4A amino acid substitution mutant exacerbates the temperature sensitive growth defect of Nab3 mutants (K. Y. Lee et al., 2018). Recently it was found that Set1 methylates Nab3 at a crucial regulatory site, complicating the initial finding that H3K4 methylation regulates NNS (K. Y. Lee et al., 2020).

Another mechanism of regulation is through recognition of RNA motifs on the nascent transcript. Analysis of snoRNA targets, found that Nrd1 recognizes GUA[A/G], while Nab3 recognizes UCUU (Carroll et al., 2004; Steinmetz et al., 2001). These binding motifs are highly abundant, and present in the sequence of almost every mRNA in yeast (Webb et al., 2014). However, Nrd1 has been described as only somewhat sequence specific (Bacikova et al., 2014), and Nab3 and Nrd1 binding motifs can also be targeted by the cleavage and polyadenylation pathway (Porrua et al., 2012). Multiple RNA sequences coordinate polyadenylation and cleavage, with a positioning element, efficiency element and U-rich element interacting with different subunits of the complex; these RNA motifs are degenerate, and can occur multiple times at a given location, giving rise to alternative polyadenylation (Proudfoot, 2011; B. Tian & Graber, 2012).

Given multiple RNA binding motifs on a given transcript, and global patterns of chromatin and CTD modifications, an emerging model is that transcription termination is largely a kinetic competition between multiple sites of varying efficiency. Kinetics have been demonstrated to be key in poly(A) site choice (Geisberg et al., 2020; Pinto et al., 2011; Turner et al., 2021) and several studies have found mutant "slow" Pol II alleles rescue defects in NNS

dependent termination (Collin et al., 2019; Hazelbaker et al., 2013). Crucially, where transcription is terminated and by what mechanism is a key determinate of the ultimate fate of a given RNA.

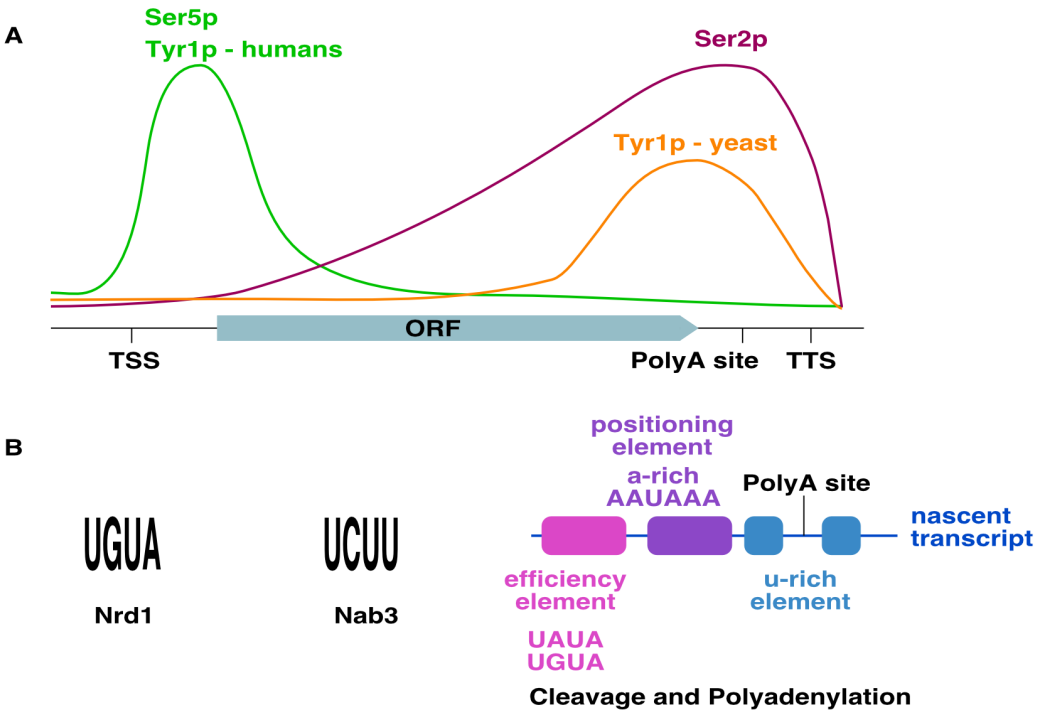

Figure 1.4 Some features which distinguish NNS and CPF site choice.
(**A**) Distribution of Pol II CTD marks. Ser5p has been implicated in NNS targeting while Ser2p has been implicated in targeting CPF. Data suggests Tyr1p regulates both NNS and CPF. Adapted from Zaborowska et al. 2016.
(**B**) RNA motifs associated with NNS termination vs. polyadenylation and cleavage. Short RNA motifs are associate with Nrd1 and Nab3 binding. CPF binding depends on multiple elements, including an efficiency element, A-rich positioning element and a U-rich element.

1.2.3 *NNS-nuclear exosome in mRNA regulation*

NNS and Rrp6 are mainly described as non-coding RNA regulators (Villa & Porrua, 2022). Despite this, accumulating evidence suggests that this pathway is also a key regulator of coding transcripts. Rrp6, Nrd1 and Nab3 have been demonstrated to bind mRNA in exponential growth

using an RNA-IP assay known as PAR-CLIP (Sohrabi-Jahromi et al., 2019; Webb et al., 2014). This is consistent with the observation that nearly all mRNAs contain Nrd1 or Nab3 RNA-binding motifs (Webb et al., 2014). However, only a small number of mRNAs have been identified as differentially expressed when either RRP6 is deleted (Arigo, Carroll, et al., 2006; Kuehner & Brow, 2008) or Nab3 is depleted (Merran & Corden, 2017) in exponentially growing cells.

Rrp6 and NNS function in quality control for many different RNA species, and this activity extends to mRNA. Incorrectly spliced mRNAs are terminated and degraded by this pathway (P. Singh et al., 2021; Steinmetz & Brow, 1998). Disrupting mRNA biogenesis in logarithmic growth results in the accumulation of aberrant mRNAs in *rrp6*Δ and NNS mutants. This has been studied by expressing bacterial Rho to perturb RNA biogenesis (Honorine et al., 2011; Moreau et al., 2019) and using conditional transcriptional mutants (P. Singh et al., 2021). Crucially, NNS's regulation of mRNA has been linked to nutrition sensing. When glucose is rapidly removed from the media, NNS binds distinct mRNA targets (Bresson et al., 2017; van Nues et al., 2017). Using anchor-away, NNS was demonstrated to regulate the transcription of mRNAs functioning in nitrogen catabolite repression (Merran & Corden, 2017). These accumulating reports suggest NNS targeting may be a crucial way in which yeast adapt their transcriptional program to various changes in nutrition.

1.3 NON-CODING RNA

1.3.1 *Pervasive transcription*

The term pervasive transcription describes the phenomenon wherein most of the genome is transcribed. Pervasive transcription is a conserved featured of eukaryotic genomes (Dinger et

al., 2009; Villa & Porrua, 2022). In humans, ~2% of the genome is devoted to open reading frames (International Human Genome Sequencing Consortium, 2004) but more than 90% is estimated to be transcribed (Pertea, 2012). Since the discovery of this widespread non-coding transcription, it has been an open question in the field if this it provides cellular functions or if pervasive transcription is a result of leaky transcription initiation (Dinger et al., 2009). Evidence is emerging that non-coding transcription is a conserved hallmark of cell state in humans, plants and invertebrates (Akay et al., 2019; Kang & Liu, 2015; Seifuddin et al., 2020). However, only a small minority of non-coding transcripts have been functionally characterized (Dinger et al., 2009; Till et al., 2018). Characterized lncRNA are sometimes only functional under certain conditions (Lenstra et al., 2015; Moretto et al., 2021). Additionally, different mechanisms and functions have been suggested by different investigators (Castelnuovo et al., 2013; Hegazy et al., 2023).

Saccharomyces cerevisiae have a gene dense genome, where the average length between open reading frames is only 536 base pairs (Hurowitz & Brown, 2004) and ~73% of the genome is devoted to open reading frames (Alexander et al., 2010). Nevertheless, pervasive transcription occurs in this gene dense landscape, with 85 % of the yeast genome transcribed in rich media (David et al., 2006). *Saccharomyces cerevisiae* have lost RNA interference (RNAi), a conserved system of recognizing and regulating double stranded RNA (dsRNA) (Drinnenberg et al., 2009). The loss of RNAi was evolutionarily advantageous to yeast because it allows for double stranded RNA killer viruses to persist in the cytoplasm (Drinnenberg et al., 2011). These viruses allow the yeast to produce a “killer-toxin”. Yeast carrying the virus are immune to it the associated killer-toxin while non-infected yeast are sensitive (Schmitt & Breinig, 2006; Wickner et al., 2013). Thus, retaining RNAi was specifically problematic to yeast as it meant they could not be infected

by these dsRNA viruses, and would be vulnerable to the resulting toxins. As a result of losing RNAi, *S. cerevisiae* have expanded antisense transcription compared to yeast species which retained RNAi (Alcid & Tsukiyama, 2016). Some of these antisense transcripts have been evolutionarily conserved among closely related yeast, suggesting that they may serve functional roles (Rhind et al., 2011; Yassour et al., 2010).

Non-coding transcription in *Saccharomyces cerevisiae* has been annotated by several different groups using different strategies. Xu et al., 2009 annotated a class of non-coding transcripts they called "stable unannotated transcripts" (SUTs) which are expressed in wild-type yeast and readily detectable in steady state RNA sequencing (Xu et al., 2009). Other class of transcripts have relied on genetic manipulation. Deleting RNA surveillance factors was an approach which stabilized "cryptic" transcripts such as cryptic unstable transcripts (CUTs; found on deletion of *RRP6*) (Vera & Dowell, 2016; Xu et al., 2009) and Xrn1-sensitive unstable transcripts (XUTs) (van Dijk et al., 2011). Alternatively, transcription regulators have been used to similar effect, creating the classes of Nrd1-unterminated transcripts (NUTs) (Schulz et al., 2013) and Set2-repressed antisense transcripts (SRATs) (Venkatesh et al., 2016). In some cases, these transcripts were annotated without consideration for if they overlapped one another, creating a technical hurdle to analysis.

1.3.2 *Functional lncRNA in Saccharomyces cerevisiae*

Several studies have attempted to understand if non-coding RNA in *S. cerevisiae* is globally functional. These studies have relied on comparing between two genotypes or two cell states, and seeing if antisense non-coding and coding expression are correlated or anti-correlated. Most of these efforts have shown that antisense transcription is weakly anti-correlated with sense transcription genome wide (Gill et al., 2020; Nevers et al., 2018; Schulz et al., 2013). However,

one recent study found change in sense and antisense to be positively correlated (Hegazy et al., 2023). Thus, which gene is used to increase non-coding transcription biases these results.

Fewer than twenty of the thousands of annotated *S. cerevisiae* ncRNA have been functionally characterized to any extent (J. Li et al., 2021; Till et al., 2018). Several mechanisms have emerged on how these transcripts function in regulating gene expression. Most well characterized non-coding RNAs in *S. cerevisiae* function in *cis* rather than in *trans*, meaning they function at the locus where they are transcribed, and expression from an ectopic locus does not confer normal function (Gil & Ulitsky, 2020; Till et al., 2018; Yamashita et al., 2016). Due to our currently limited knowledge and diverse apparent mechanisms, it is not currently reasonable to classify non-coding RNA in yeast with a set of validated categories (Till et al., 2018). I will instead focus on describing several example loci which have been characterized and discuss what is currently known about their mechanism of action.

One mechanism of function for non-coding RNA occurs when local transcription interferes with transcription from a different start site in *cis*. At the *IME4* locus, elongation of antisense non-coding RNA called *RME2* represses *IME4*, ostensibly through recruiting factors which block *IME4* elongation (Gelfand et al., 2011; Hongay et al., 2006). The transcription of this ncRNA regulates if the cell commits to meiosis. A similar mechanism occurs at *FLO11* where an upstream ncRNA *IRC1* resets *FLO11* to a basal state by blocking the binding of transcription factor Flo8 (Bumgarner et al., 2009, 2012).

Another common mechanism is through alteration of the local chromatin structure by the ncRNA. These non-coding transcripts can occur upstream of the gene, which is the case at the *SER3* locus. The serine metabolic gene is repressed by an upstream non-coding transcript called *SRG1*. Transcription of *SRG1* alters nucleosome positioning which prevents transcription factor

binding at the *SER3* locus (Hainer et al., 2011). At the *GAL* locus, transcription of *GAL10*-ncRNA results in increased H3K36 trimethylation and decreased acetylation (Houseley et al., 2008). This ncRNA functions to repress galactose metabolic genes when more preferred carbon sources such as glucose are available. Antisense transcripts can also be activating, as is the case with the antisense transcript at *CDC28*. In this case, antisense transcription promotes gene looping and activates mRNA expression (Nadal-Ribelles et al., 2014).

Finally, several potentially *trans*-activating non-coding RNAs have been identified in yeast. Deletion of *SUT457*, an intergenic transcript, results in the altered expression of 12 genes involved in telomere control by an unknown, but likely *trans*-acting mechanism (Kyriakou et al., 2016). In aged cells, the *PHO84* antisense transcript was originally proposed to repress mRNA transcription in *cis* via histone deacetylation (Camblong et al., 2007). An additional study by the same authors demonstrated that expression of the *PHO84* antisense transcript from a plasmid represses both copies of the mRNA transcript, suggesting an additional *trans* mechanism (Camblong et al., 2009). However, this locus has recently become much more controversial. These previous reports showed it functioned to repress its sense mRNA through recruiting chromatin modifiers (Camblong et al., 2007, 2009), but a new study suggests an activating rather than repressive function (Hegazy et al., 2023). Three distinct mechanisms have been proposed for how *PHO84* antisense transcription regulates *PHO84* mRNA and phosphate metabolism.

Current studies of non-coding transcription in yeast have demonstrated that it is highly context specific. The multiple mechanisms proposed for the *PHO84* locus could all be true in different contexts. At the *GAL10* locus, antisense transcription was shown to be functionally repressive only when yeast were grown in glucose or raffinose, whereas it did not affect sense transcription in the presence of galactose (Lenstra et al., 2015). What conditions a lncRNA is

studied in determines what functions may be discovered. Even some of the more well-defined non-coding loci in yeast would benefit from additional study to understand the required conditions and exact mechanisms for their function.

1.4 DISSERTATION OVERVIEW

A major goal of my thesis work was to investigate the quiescent nascent transcriptome at high resolution and sensitivity. I sought to further probe what transcription persists during quiescence, when the chromatin environment is highly repressive. These revealed over 1000 non-coding RNAs expressed in quiescence, over 200 of which had no overlap to previous non-coding annotations. Sequencing of both nascent and steady state RNA additionally allowed me to investigate post-transcriptional regulation in quiescence. This revealed that many mRNAs and non-coding RNAs have a larger difference between steady-state and nascent transcriptomes in quiescence than in G_1, demonstrating the extent of post-transcriptional regulation in quiescence. In the search for pathways that regulate this process, I identified the NNS-nuclear exosome as a key regulator of both non-coding and coding transcripts in quiescence and quiescence entry. This work expands our understanding of gene regulation in quiescence and opens the door for identifying additional mechanisms of regulation in the future.

Chapter 2. POST-TRANSCRIPTIONAL REGULATION SHAPES THE TRANSCRIPTOME OF QUIESCENT BUDDING YEAST

This chapter is adapted from "Post-transcriptional regulation shapes the transcriptome of quiescent budding yeast" which has been accepted for publication at *Nucleic Acids Research*.

AUTHORS

Alison C. Greenlaw[1, 2], Kris G. Alavattam[1], and Toshio Tsukiyama[1]*

[1] Basic Sciences Division, Fred Hutchinson Cancer Center, Seattle, WA 98109, USA

[2] Molecular and Cellular Biology Program, Fred Hutchinson Cancer Center and University of Washington

*: corresponding author Email: [ttsukiya@fredhutch.org]

2.1 ABSTRACT

To facilitate long-term survival, cells must exit the cell cycle and enter quiescence, a reversible non-replicative state. Budding yeast cells reprogram their gene expression during quiescence entry to silence transcription, but how the nascent transcriptome changes in quiescence is unknown. By investigating the nascent transcriptome, we identified over a thousand non-coding RNAs in quiescent and G_1 yeast cells, and found non-coding transcription represented a larger portion of the quiescent transcriptome than in G_1. Additionally, both mRNA and ncRNA are subject to increased post-transcriptional regulation in quiescence compared to G_1. We found that, in quiescence, the nuclear exosome-NNS pathway suppresses over one thousand mRNAs, in addition to canonical non-coding RNAs. RNA sequencing through

quiescent entry revealed two distinct time points at which the nuclear exosome controls the abundance of mRNAs involved in protein production, cellular organization, and metabolism, thereby facilitating efficient quiescence entry. Our work identified a previously unknown key biological role for the nuclear exosome-NNS pathway in mRNA regulation and uncovered a novel layer of gene-expression control in quiescence.

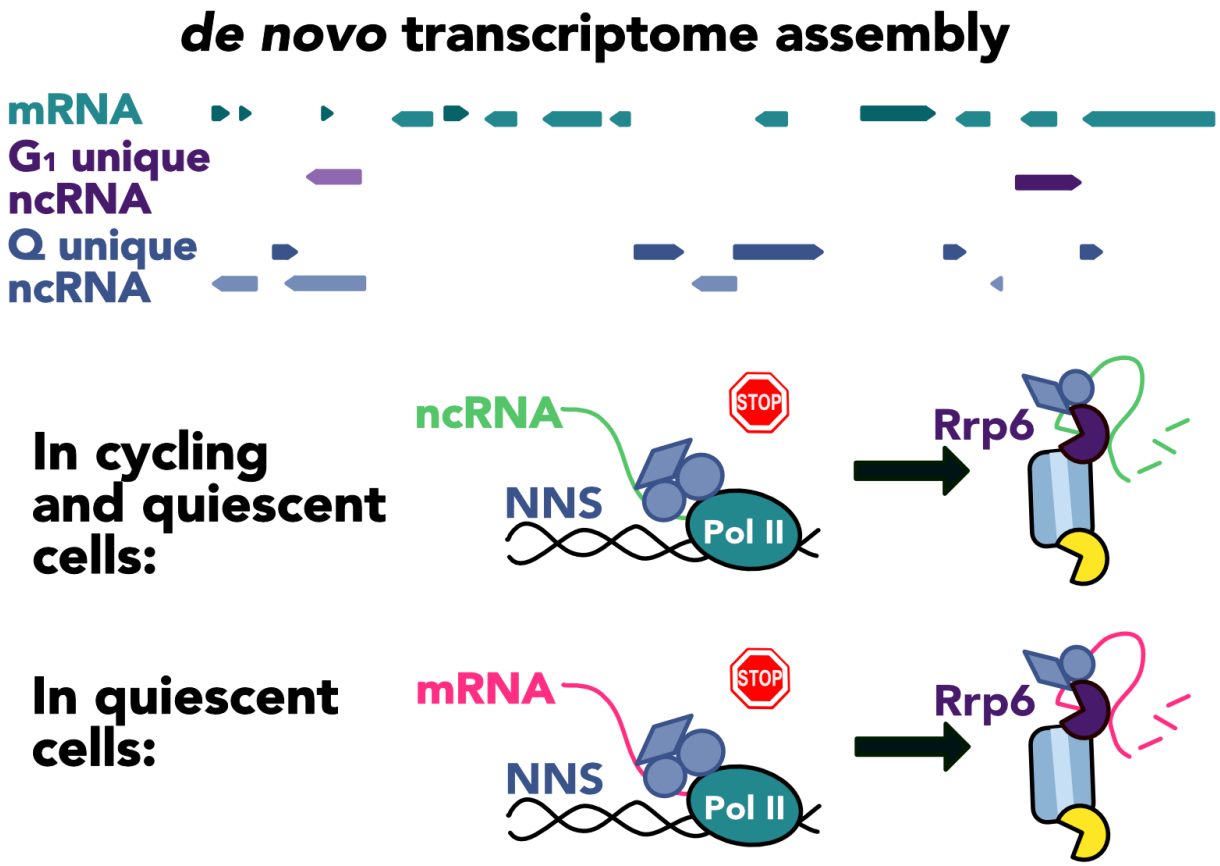

Figure 2.1 Graphical abstract for *Post-transcriptional regulation shapes the transcriptome of quiescent budding yeast*

2.2 INTRODUCTION

Cells in all kingdoms of life must be able to cease proliferation and enter a non-replicative G_0 state to allow for long-term survival. Quiescence is distinct from other G_0 states such as terminal differentiation and senescence because it is reversible, allowing cells to divide again when conditions are favorable (Breeden & Tsukiyama, 2022). Proper regulation of quiescence is crucial for single-cell organisms to survive harsh conditions (De Virgilio, 2012; Rittershaus et al., 2013) and multicellular organisms to maintain their stem cell niche (Cheung & Rando, 2013; de Morree & Rando, 2023). *Saccharomyces cerevisiae* is an ideal model organism to study quiescence because they readily exit the cell cycle when nutrients are exhausted. A long-lived quiescent population is present in heterogeneous stationary phase culture and can be separated from the non-quiescent population via density gradient centrifugation (Allen et al., 2006).

This purification method has been instrumental in expanding our understanding of the molecular mechanisms underlying quiescence. Gene expression is globally remodeled from an active to a silenced state during quiescence entry (McKnight et al., 2015; Swygert et al., 2019, 2021; Young et al., 2017). Histones are globally de-acetylated by lysine deacetylase Rpd3 (McKnight et al., 2015), which promotes quiescence-specific chromatin folding as well as transcriptional shut-off (Swygert et al., 2021). In concert with these changes, condensin-mediated chromatin loops (Swygert et al., 2019) and narrowed nucleosome depleted regions contribute to the repressed chromatin environment (McKnight et al., 2015). Additionally, a host of transcription factors collaborate to repress growth genes and activate stress-response genes during quiescence entry (T. B. Bailey et al., 2022; P. Lee et al., 2013; Miles et al., 2013). While prior studies have explored the alternative regulation of transcription and genome organization in quiescence, there has not been a detailed investigation into the changes in the nascent

transcriptome that occur in quiescence. Previous studies have largely relied on measurements of steady-state RNA and/or Pol II chromatin immunoprecipitation (ChIP) (Klosinska et al., 2011; McKnight et al., 2015; Nevers et al., 2018; Swygert et al., 2019; Young et al., 2017), neither of which capture the nascent transcriptome at high resolution or high sensitivity, nor do these assays provide information about post-transcriptional regulation.

The *S. cerevisiae* nuclear exosome is a conserved post-transcriptional regulator comprised of the 10 subunits shared by the cytoplasmic and the nuclear exosomes, as well as Rrp6, the nuclear-specific 3′- to 5′-exonuclease (Januszyk & Lima, 2014; Kilchert et al., 2016). Rrp6 regulates diverse RNA species and is responsible for 3′-end processing of structured non-coding RNAs (ncRNAs) such as snoRNAs and snRNAs, and the degradation of antisense and aberrant transcripts (Kilchert et al., 2016). Transcripts are targeted to the nuclear exosome by the transcription termination complex Nrd1-Nab3-Sen1 (NNS). The NNS complex is composed of three proteins essential for viability: the two RNA-binding proteins Nrd1 and Nab3, and the helicase Sen1 (Arndt & Reines, 2015; Villa & Porrua, 2022). This transcription termination complex is known to largely target ncRNAs such as snoRNAs, tRNAs, and antisense transcripts, which are enriched for short sequence binding motifs (Carroll et al., 2004; Schulz et al., 2013; Steinmetz et al., 2001). However, Nab3- and Nrd1-binding motifs alone are not sufficient to explain NNS activity, as the same motifs can also be targeted by the cleavage and poly-adenylation pathway (Porrua et al., 2012). Nrd1 preferentially interacts with the RNA polymerase II C-terminal domain (CTD) when phosphorylated at Ser5 (Kubicek et al., 2012; Vasiljeva, Kim, Mutschler, et al., 2008), which peaks early in transcription, and directs transcripts to early termination and decay.

Despite nearly all mRNAs containing Nrd1 or Nab3 RNA-binding motifs (Webb et al., 2014), only a small number of mRNAs are regulated by NNS in logarithmic growth via the premature termination mechanism (Arigo, Carroll, et al., 2006; Kuehner & Brow, 2008; Merran & Corden, 2017). Consistent with the role of Rrp6 and NNS in degrading incorrectly processed RNAs (Allmang et al., 2000; Kadaba et al., 2004; Wlotzka et al., 2011), improperly spliced mRNAs are also regulated by the pathway (P. Singh et al., 2021; Steinmetz & Brow, 1998). Additionally, when mRNA biogenesis is disrupted, aberrant mRNAs accumulate in the absence of Rrp6 or NNS in logarithmic growth (Honorine et al., 2011; P. Singh et al., 2021). Most relevant to the study of quiescence, NNS has been shown to degrade mRNAs when glucose is rapidly removed from the media (Bresson et al., 2017; van Nues et al., 2017) and to regulate genes involved in nitrogen metabolism (Merran & Corden, 2017). Despite accumulating reports of NNS and Rrp6 regulating mRNA, they are mainly described as regulators of non-coding transcripts (Villa & Porrua, 2022).

In this work, we investigated the nascent transcriptome in quiescent yeast, assembling and annotating transcripts in quiescent and G_1 cells. We identified many ncRNA transcripts and demonstrated that ncRNA profiles distinguish quiescent and G_1 states. We further showed that post-transcriptional regulation plays larger roles in quiescence compared to G_1. Finally, we discovered that the NNS-nuclear exosome pathway reduces the abundance of a large number of mRNAs, in addition to ncRNAs, during quiescence entry and plays key roles in proper transcriptome regulation in quiescent cells.

2.3 RESULTS

2.3.1 *Characterizing the quiescent transcriptome*

To study transcription in quiescence, we measured newly transcribed (i.e., "nascent") transcripts in quiescent and G_1-arrested cells. We used G_1 as a control because it represents an arrested state that has not silenced its genome or metabolically adapted to the absence of glucose. Furthermore, both G_1 and quiescent cells have 1c DNA content. Nascent RNA production was measured using 4tU-seq, an assay in which the uracil analog 4-thiouracil (4tU) is incorporated into newly transcribed RNAs, metabolically labeling nascent transcripts within a short label time (see Chapter 3: Materials and Methods) (Barrass et al., 2015).

We estimated steady-state mRNA abundance to be approximately 14-fold lower in quiescent versus G_1 cells (Figure 2.2). To perform this calculation, we normalized to spike-in alignments and adjusted for the varied cell amounts used in library preparation (see Chapter 3: Materials and Methods). However, we chose not to estimate nascent RNA levels due to the complexities associated with 4tU incorporation. 4tU needs to be transported into the cell and converted to UTP before becoming part of nascent transcripts (Duffy et al., 2019). This process is complicated by the thick cell walls of quiescent cells (L. Li et al., 2013; Shimoi et al., 1998) and their altered metabolic activity (Klosinska et al., 2011; Lillie & Pringle, 1980; Shi et al., 2010), factors that likely lead to different 4tU incorporation rates compared to G_1 cells. While these variations prevent the comparison of absolute transcription levels between the two cell states, 4tU-seq provides the advantage of high sensitivity to low abundance and rapidly degraded transcripts (Barrass et al., 2015). To avoid potential misinterpretation, we opted to focus on the enrichment of transcripts, examining them as proportions of nascent and steady-state RNA, rather than report on absolute RNA levels. Thus, we analyzed the proportions of processed

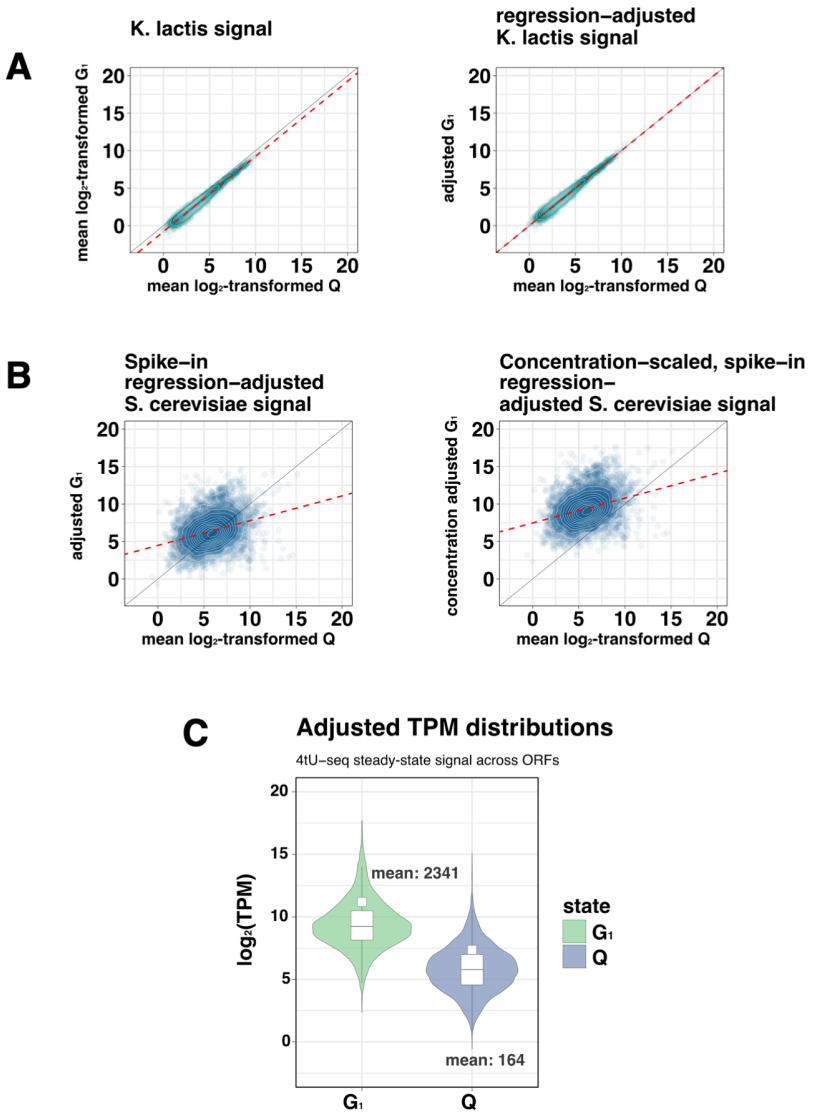

Figure 2.2 Estimating the absolute difference in RNA level between G_1 and quiescence.
(**A**) Scatter plot of mean log2-transformed counts for *K. lactis* spike in without adjustment (left) and with regression adjustment (right).
(**B**) Scatter plot of mean log2-transformed counts for *S. cerevisiae* spike in with regression adjustment (left) and scaled for concentration (right).
(**C**) Violin plot of mean log2-transformed TPM values in quiescence and G1, reflecting ~14-fold change between cell states.

paired-end 4tU-seq reads (hereafter "reads;" see Chapter 3: Materials and Methods) that align to the *Saccharomyces cerevisi*ae Ensembl R64-1-1 genome (henceforth "R64"), a high-quality annotated genome assembly (*Saccharomyces Cerevisiae S288C Genome Assembly R64*, n.d.). Based on where and what feature they align to, we assigned reads to the feature categories "gene," "snoRNA," "pseudogene," "snRNA," and "TE" (transposable element; Figure 2.3A; see Chapter 3: Materials and Methods). If reads aligned to a region with no annotation, then they were assigned the category "no feature," and if they aligned to multiple features, they were designated "ambiguous".

The annotated features that comprise R64 do not include the many ncRNAs that have been assembled and annotated by different groups using a variety of methods (Schulz et al., 2013; van Dijk et al., 2011; Venkatesh et al., 2016; Vera & Dowell, 2016; Xu et al., 2009). In some cases, these non-R64 ncRNAs were assembled and annotated without reference to one another. As a result, thousands of non-R64 non-coding transcripts partially or completely overlap one another, including cryptic unstable transcripts (CUTs) (Vera & Dowell, 2016; Xu et al., 2009), Nrd1-unterminated transcripts (NUTs) (Schulz et al., 2013), Xrn1-sensitive unstable transcripts (XUTs) (van Dijk et al., 2011), stable unannotated transcripts (SUTs) (Xu et al., 2009), and Set2-repressed antisense transcripts (SRATs) (Venkatesh et al., 2016). Reads that aligned to overlapping regions or span the boundaries of contiguous features are categorized as "ambiguous", thus obfuscating the characterization of the transcriptome. To circumvent this issue, we collapsed the non-coding transcripts into a single annotated transcriptome assembly that we refer to as "previously annotated non-coding RNA" (pa-ncRNA; Figure 2.4 and 2.5; see Chapter 3: Materials and Methods). We refrained from combining pa-ncRNA with the R64 *S.*

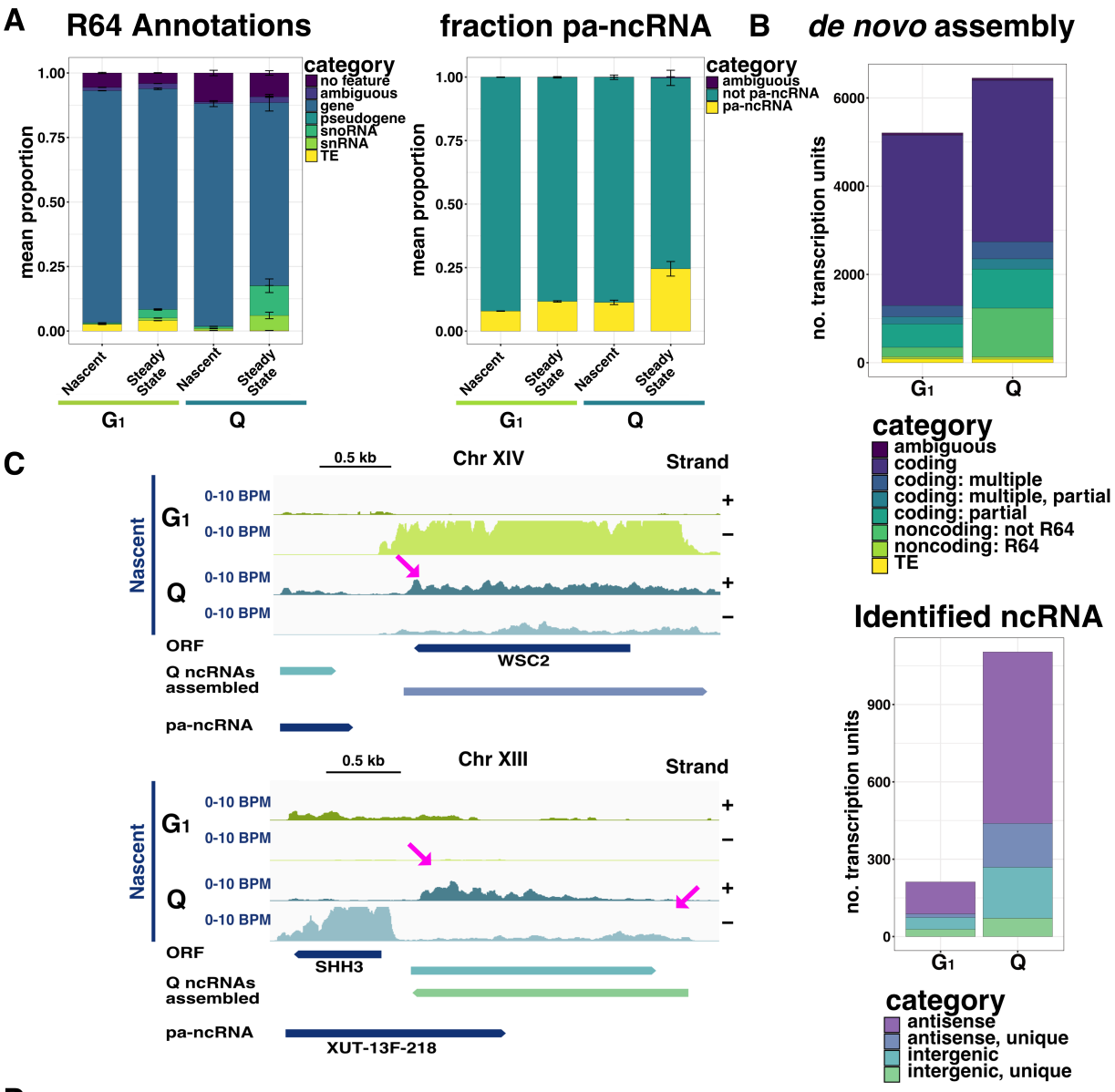
A
R64 Annotations
fraction pa-ncRNA
B
de novo assembly
mean proportion
category
no feature
ambiguous
gene
pseudogene
snoRNA
snRNA
TE
not pa-ncRNA
pa-ncRNA
no. transcription units
Nascent
Steady State
G1
Q
C
0.5 kb
Chr XIV
Strand
Nascent
0-10 BPM
ORF
WSC2
Q ncRNAs assembled
pa-ncRNA
Chr XIII
SHH3
XUT-13F-218
coding
coding: multiple
coding: multiple, partial
coding: partial
noncoding: not R64
noncoding: R64
Identified ncRNA
antisense
antisense, unique
intergenic
intergenic, unique
D
Q features
coding: misc.
noncoding: novel

Figure 2.3 The nascent transcriptome is enriched for non-coding features in quiescence.

(**A**) Mean proportions of read alignment from nascent and steady-state RNA-seq from G_1 and quiescence (Q) aligned to R64 categories (left) and pa-ncRNA (right). Error bars are SEM for n = 2 biological replicates.
(**B**) (top) The numbers of transcripts identified *de novo* with Trinity (Grabherr et al., 2011) from nascent 4tU-seq of G_1 and quiescent cells. Transcripts were defined by what feature(s) in the R64-1-1 assembly (R64) they overlapped. (bottom) Categorization of assembled non-R64 ncRNAs. Non-R64 ncRNAs were defined to be either antisense or intergenic. Antisense transcripts were defined as having 1 base pair or more antisense overlap to a known feature. All other transcripts were defined as intergenic. These ncRNAs were subsequently compared to pa-ncRNA; those having no same-strand overlap were designated as unique.
(**C**) Examples of novel non-coding transcripts at *WSC2* (top) and *SHH3* (bottom). Coverage was normalized using the deepTools (Ramírez et al., 2014) bins per million (BPM) calculation, where the bin size was set to 1 base pair. Regions blacklisted in normalization are detailed in Materials and Methods.
(**D**) Mean proportions of read alignment from nascent and steady-state RNA-seq from G_1 and quiescence aligned to the Trinity-assembled quiescent features.

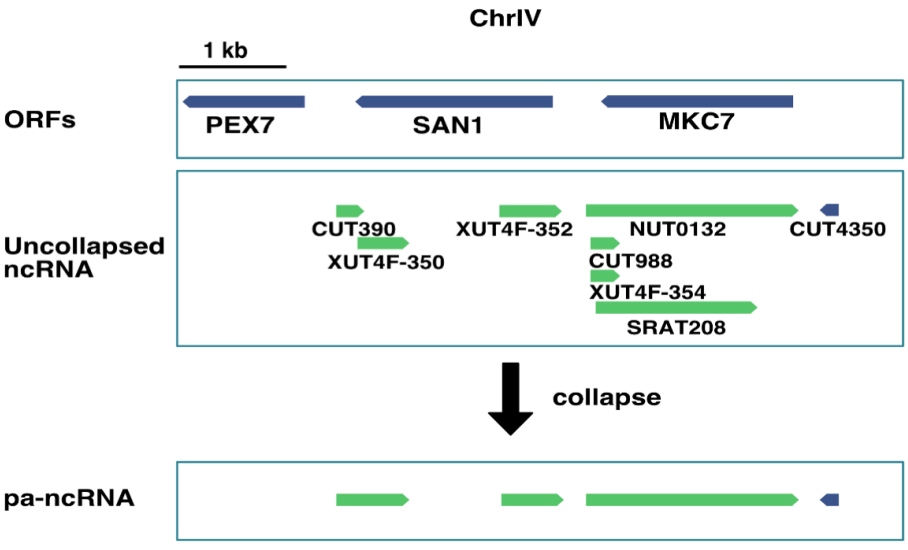

Figure 2.4 Schematic diagram of non-coding annotations overlapping 3 ORFS.
Uncollapsed non-coding annotations (middle) and collapsed pa-ncRNA (bottom) are both shown. Positive strand features in green, negative strand features in blue.

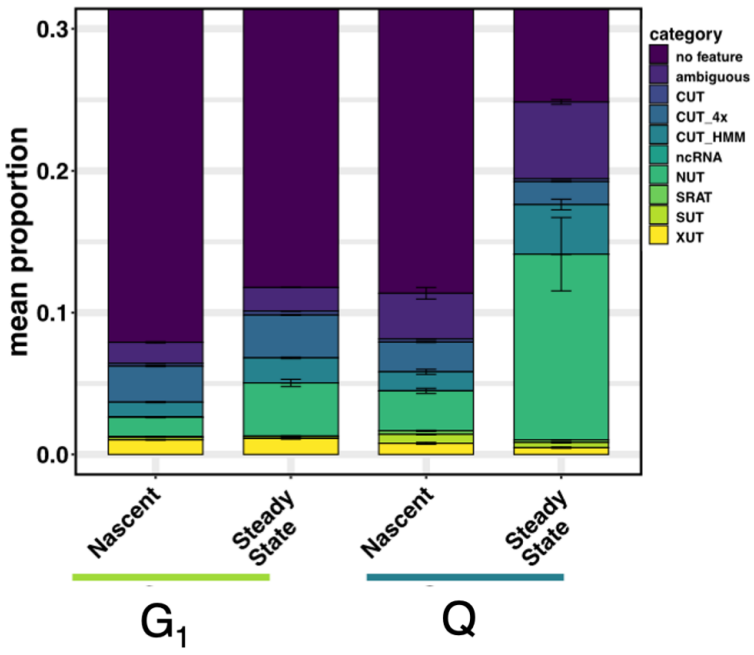

Figure 2.5 Mean proportion of aligned reads to uncollapsed ncRNA broken down by annotation.

cerevisiae features since frequent feature overlaps further ballooned the number of reads designated as ambiguous. This enabled us to separately analyze coding and non-coding features.

Compared to G_1, the nascent quiescent transcriptome has a higher fraction of reads that cannot be assigned to an R64 feature, with ~10% of reads aligned to no known features (Figure 2.3A, left: "no feature"). Sequencing of both nascent and steady-state RNA revealed that a much larger fraction of reads aligned to pa-ncRNA in quiescence than in G_1 (Figure 2.3A, right).

Due to the increase in non-coding transcription and the number of reads not assigned to a known feature—whether in R64 or pa-ncRNA—we determined that further study of transcription in quiescence required custom quiescent and G_1 transcriptome assemblies. To achieve this task, we used Trinity, a well-established and regularly updated program for *de novo*

transcriptome assembly (Grabherr et al., 2011). Using the same conservative parameters and cutoffs for both cell states, we assembled 5,228 transcripts in G1 and 6,471 in quiescence (Figure 2.3B, top). The increased number of assembled transcripts demonstrates the complexity of the nascent quiescent transcriptome. This means that the low level of global transcription in quiescence (McKnight et al., 2015; Mews et al., 2014; Young et al., 2017) is spread across a larger number and increased variety of features.

We assigned the Trinity-assembled transcripts to feature categories based on their overlap with known features in R64 (see Chapter 3: Materials and Methods). These categories include "ambiguous," "coding," "non-coding," and "TE"; the sub-category "non-coding: R64" refers to transcripts that overlap non-coding features in R64, including snRNAs, snoRNAs, and 14 additional RNAs such as the RNA subunit of the Signal Recognition Particle. Transcripts with no same-strand overlaps against R64 features were assigned to the sub-category "non-coding: not R64." The difference in the total number of transcripts between G_1 and quiescence is driven by the number of "non-coding: not R64" transcripts in each cell state: 212 G_1 transcripts and 1,104 quiescence transcripts belong to this feature category (Figure 2.3B, bottom). The majority of annotated ncRNAs were at least partially antisense to known R64 ORFs, with quiescent cells particularly enriched for this sub-category. Additional analyses of assembled transcription-unit length and expression-level distributions are shown in Figures 2.6 and 2.7.

Of these ncRNAs, we identified subsets that had no overlap with pa-ncRNA, referring to them as "unique." In both G_1 and quiescence, ~20% of ncRNAs are unique (42 in G_1 and 241 in quiescence). The number of completely unique transcripts in G_1 was more than expected given several previous reports in which ncRNAs were identified in cycling cells (Schulz et al., 2013; van Dijk et al., 2011; Venkatesh et al., 2016; Vera & Dowell, 2016; Xu et al., 2009).

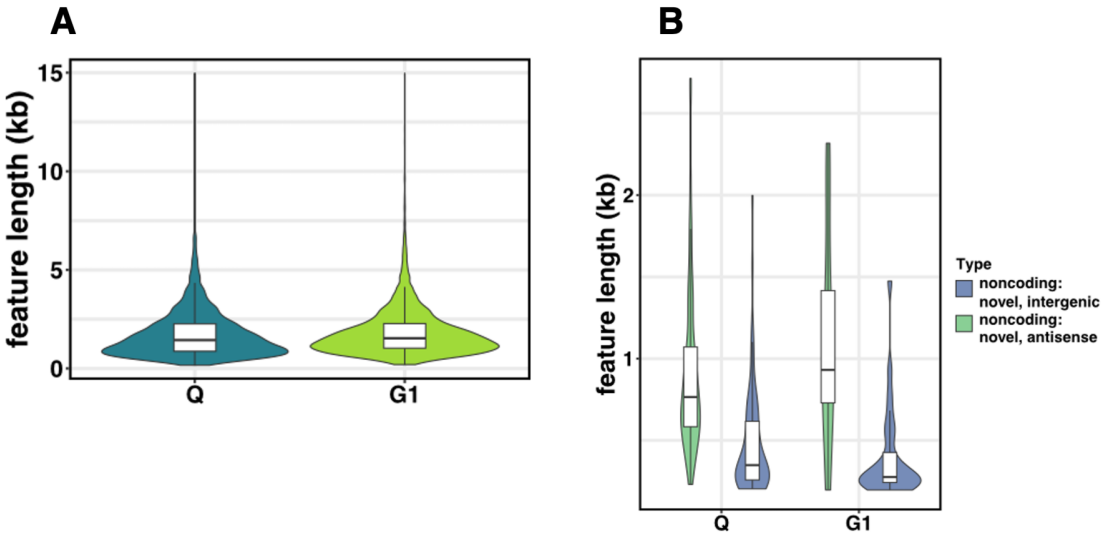

Figure 2.6 Length of Trinity *de novo* assembled transcripts.
(**A**) Violin/box and whisker plots of length for all assembled trinity transcripts for quiescence (left) and G1 (right).
(**B**) Violin/box and whisker plots of length for all unique assembled trinity transcripts for quiescence (left) and G1 (right) divided into intergenic (blue) and antisense (green).

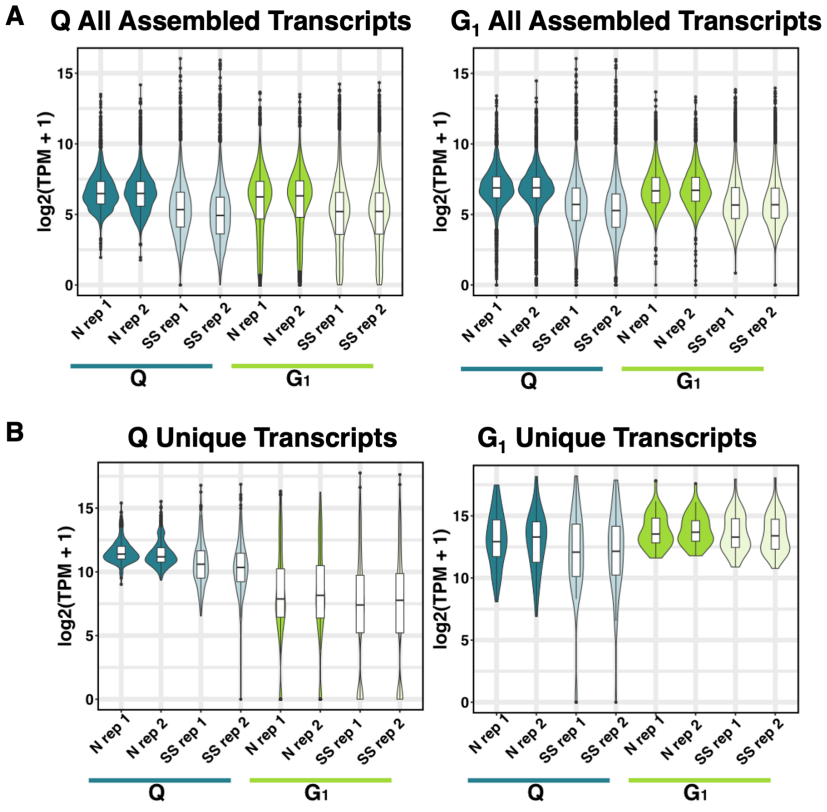

Figure 2.7 Expression level of Trinity *de novo* assembled transcripts.
(**A**) Violin/box and whisker plots of expression level for all assembled trinity transcripts for quiescence (left) and G_1 (right) for both nascent (N) and steady state (SS) expression.
(**B**) Violin/box and whisker plots of expression level for all unique assembled trinity transcripts for quiescence (left) and G_1 (right) for both nascent (N) and steady state (SS) expression.

In Figure 2.3C (top), we provide an example of a unique antisense transcript at the *WSC2* locus, a gene that encodes a cell wall protein, and a downstream intergenic transcript that overlaps a pa-ncRNA annotation (pink arrow). In Figure 2.3C (bottom), we show an example of a unique intergenic transcript upstream of *SHH3*, which codes for a putative mitochondrial inner membrane protein. In this same intergenic region, there is also an ncRNA annotation on the positive stand that overlaps an annotated XUT (a kind of pa-ncRNA) (van Dijk et al., 2011).

To evaluate the differences between G_1 and quiescence captured by our assembled transcripts, we aligned reads from each cell state to our assembly of the nascent quiescent transcriptome. This revealed that ~5% of nascent 4tU-seq reads align to ncRNAs in quiescence, a much larger fraction than in G_1 (Figure 2.3D). Taken together, these results reveal that, despite limited nutrient availability and globally repressed transcription (McKnight et al., 2015; Mews et al., 2014; Young et al., 2017), a larger fraction of transcription is devoted to non-coding transcription in quiescence than in G_1-arrested cells.

2.3.2 *A note on our transcriptome annotation*

In the subsequent sections, we do not rely on the transcriptome assemblies we generated in the above section. This is for two major reasons. The first was based on timing. Most of the analysis in the later parts of the paper were completed in part or full before the annotations were finalized. The second reason is that the analysis we attempted with these transcripts did not

reveal interesting biology. The main trend when we analyzed quiescent unique noncoding RNAs was that they were not expressed in G_1.

2.3.3 *Post-transcriptional regulation of quiescence transcriptome*

During transcriptome analyses, we observed that steady-state and nascent transcriptomes were distinct from each other in quiescence, with major differences in total composition between the two (Figure 2.3A, 2.3D). To investigate the differences between nascent and steady-state transcripts, we performed principal component analysis (PCA) of mRNAs and pa-ncRNAs. To compare between sequencing types across cell state, raw counts were normalized using the transcript per million reads (TPM) calculation and then $\log_2$-regularized prior to running PCA. When mRNAs were used in this analysis, nascent and steady-state transcriptomes cluster further apart from each other in quiescence than in G_1 (Figure 2.8A), a finding consistent with our observations in the previous section. When pa-ncRNAs were analyzed, principal component (PC) 1 separates the nascent transcriptome in quiescent cells from all other samples, and PC2 separates the steady-state transcriptome in quiescence from all other samples. These two components account for 87% of total variation in pa-ncRNA. The larger difference between steady-state and nascent transcriptomes suggests post-transcriptional regulation plays a larger role in quiescence than in G_1 across transcript types, especially for ncRNAs.

PCA of mRNA also allowed us to compare steady-state and nascent transcriptomes in G_1 and quiescence without performing differential expression analysis, a method that can be inappropriate when absolute amounts of RNA are radically different between samples (Evans et al., 2018), as is the case with quiescent and G_1 cells. Leveraging PCA in this way enabled the

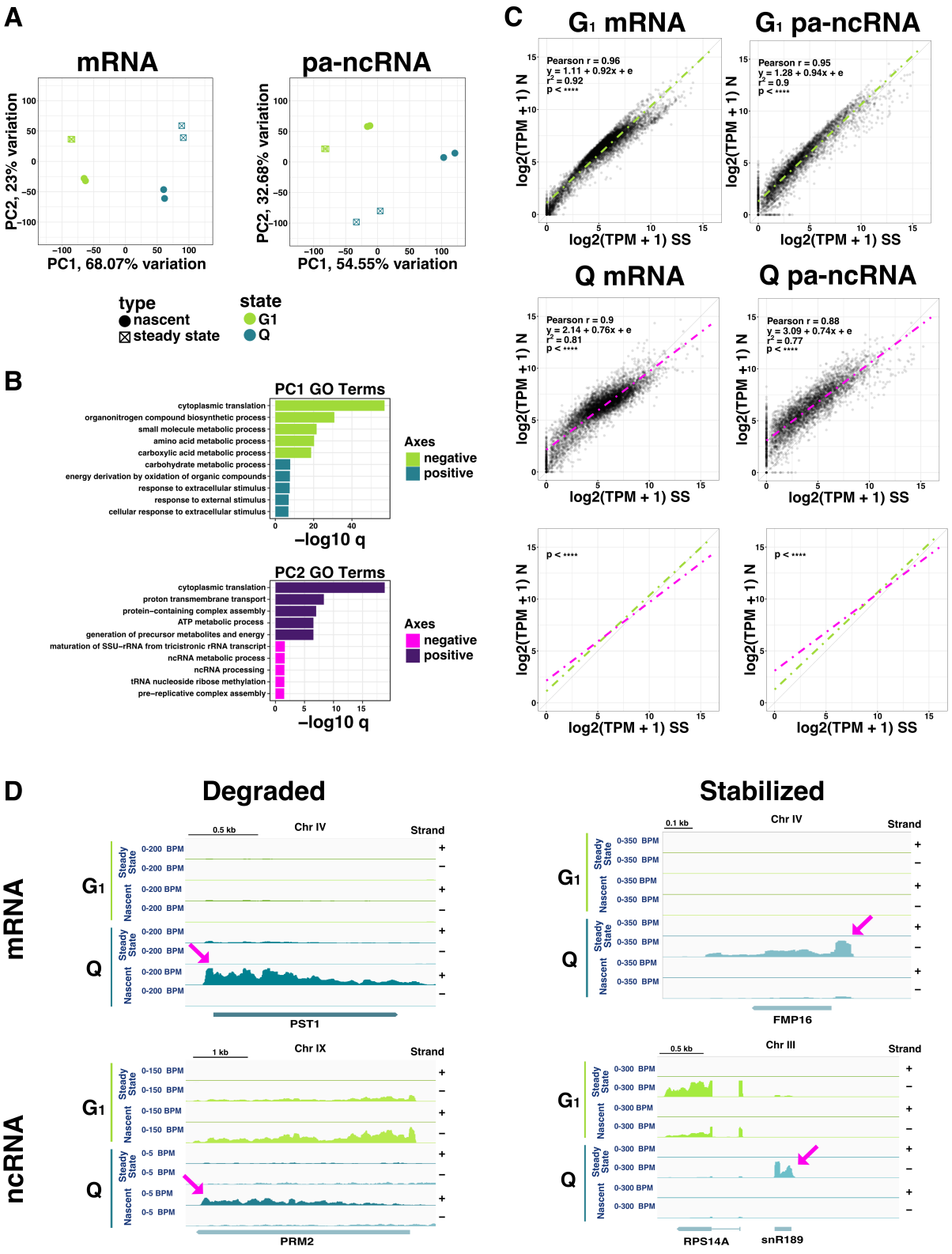
A
mRNA
pa-ncRNA
PC2, 23% variation
PC1, 68.07% variation
PC2, 32.68% variation
PC1, 54.55% variation
type
nascent
steady state
state
G1
Q
B
PC1 GO Terms
cytoplasmic translation
organonitrogen compound biosynthetic process
small molecule metabolic process
amino acid metabolic process
carboxylic acid metabolic process
carbohydrate metabolic process
energy derivation by oxidation of organic compounds
response to extracellular stimulus
response to external stimulus
cellular response to extracellular stimulus
−log10 q
Axes
negative
positive
PC2 GO Terms
cytoplasmic translation
proton transmembrane transport
protein−containing complex assembly
ATP metabolic process
generation of precursor metabolites and energy
maturation of SSU−rRNA from tricistronic rRNA transcript
ncRNA metabolic process
ncRNA processing
tRNA nucleoside ribose methylation
pre−replicative complex assembly
−log10 q
Axes
negative
positive
C
G1 mRNA
G1 pa-ncRNA
Q mRNA
Q pa-ncRNA
Pearson r = 0.96
y = 1.11 + 0.92x + e
r2 = 0.92
p < ****
Pearson r = 0.95
y = 1.28 + 0.94x + e
r2 = 0.9
p < ****
Pearson r = 0.9
y = 2.14 + 0.76x + e
r2 = 0.81
p < ****
Pearson r = 0.88
y = 3.09 + 0.74x + e
r2 = 0.77
p < ****
p < ****
p < ****
log2(TPM + 1) N
log2(TPM + 1) SS
D
Degraded
Stabilized
mRNA
ncRNA
G1
Q
Steady State
Nascent
Chr IV
Strand
0.5 kb
0-200 BPM
PST1
Chr IX
1 kb
0-150 BPM
0-5 BPM
PRM2
0.1 kb
0-350 BPM
FMP16
Chr III
0.5 kb
0-300 BPM
RPS14A
snR189

Figure 2.8 Post-transcriptional regulation is more prevalent in quiescence than G_1.
(**A**) PCA of TPM-normalized, log_2-regularized mRNA features (left) and pa-ncRNA features (right).
(**B**) Bar charts depicting adjusted p values (q) for the top 5 Gene Ontology (GO) biological process terms enriched for the top 750 mRNAs associated with PC1 axes (negative, light green; positive, teal) and PC2 axes (negative, pink; positive, purple). GO terms and q values are from hypergeometric tests with Benjamini-Hochberg corrections from YeastMine (Balakrishnan et al., 2012).
(**C**) Scatter plots of log_2 TPM + 1 values for every mRNA (left) and every pa-ncRNA (right) in G_1 (top) and quiescence (middle) for nascent (N, y-axis) and steady-state (SS, x-axis) transcription. Mann-Whitney U tests shows TPM distributions are different between steady-state and nascent in all cases (**** = $p < 0.0001$). (bottom) Comparisons of linear regressions from quiescence and G_1 mRNA (left) and pa-ncRNA (right) with p values from Mann–Whitney U tests (**** = $p < 0.0001$).
(**D**) Examples of rapidly degraded transcripts at *PST1* and *PRM2* (left), and stabilized transcripts at *FMP16* and snR189 (right). Coverage was normalized using the deepTools (72) bins per million (BPM) calculation, where the bin size was set to 1 base pair. Regions blacklisted in normalization are detailed in Materials and Methods.

identification of transcripts associated with certain conditions and not others. With that in mind, we performed Gene Ontology (GO) analysis using YeastMine (Balakrishnan et al., 2012) for the 750 mRNAs most strongly associated with the PC1 and PC2 axes. PC1 separated transcriptomes by cell state and accounted for 68.07% of variation in the data. Both nascent and steady-state transcripts from quiescent cells were associated with the PC1 positive axis, and the top 750 genes most strongly associated with the PC1 positive axis were enriched for GO terms related to carbohydrate metabolism, oxidative metabolism, and responses to stimuli (Figure 2.8B)—processes necessary to maintain cellular quiescence (De Virgilio, 2012). Both nascent and steady-state transcripts from G_1 were associated with the PC1 negative axis, and the top 750 genes most strongly associated with this axis were enriched for GO terms related to translation and multiple metabolic processes necessary to promote growth in cycling cells.

PC2 separated nascent from steady-state transcriptomes and accounted for 23% of variation. Steady-state transcripts associated with the PC2 positive axis were enriched for GO terms related to translation, proton transport, protein complex assembly and energy metabolism. Conversely, transcripts associated with the PC2 negative axis were enriched for rRNA maturation, ncRNA metabolism, and tRNA methylation—processes that are enriched in the nascent transcriptome fraction. Since ncRNAs are post-transcriptionally modified (e.g., tRNA methylation), it is logical that they are more likely to be enriched in the nascent fraction.

To further examine cell-state differences in post-transcriptional regulation, we compared the relative abundance of steady-state and nascent transcripts for each transcript across cell states. Using $\log_2$-regularized TPM-normalized counts, we compared G_1 steady-state and G_1 nascent transcriptomes, revealing strong correlations across transcript types (mRNA: Pearson r = 0.96; pa-ncRNA: Pearson r = 0.95) (Figure 2.8C, top). The correlations in quiescence were less than in G_1 for both transcript types (mRNA: Pearson r = 0.90; pa-ncRNA: Pearson r = 0.88) (Figure 2.8C, middle). Additionally, for both mRNA and pa-ncRNA, linear regressions and statistical analyses demonstrated these distributions were significantly different between cell states (Figure 2.8C, bottom). Examples of actively degraded (i.e., high in nascent but low in steady-state; left) and stabilized (i.e., low in nascent but high in steady-state; right) transcripts are shown in Figure 2.8D (pink arrows).

Taken together, these results indicate that post-transcriptional regulation plays a large role in the transcriptome of quiescent cells for both and coding and non-coding transcripts. Since post-transcriptional regulation has not been well characterized in quiescence, we next sought to test this possibility and to elucidate its underlying mechanisms.

2.3.4 *The nuclear exosome regulates mRNA abundance in quiescence*

We hypothesized the nuclear exosome is a key post-transcriptional regulator of non-coding transcripts in quiescence due to its well-established role in ncRNA decay (Kilchert et al., 2016; Vera & Dowell, 2016; Xu et al., 2009) and the number of CUTs expressed in quiescence (Figure 2.5). To test this possibility, we knocked out the nuclear exosome-specific exonuclease gene *RRP6* and performed RNA-seq in G_1-arrested and quiescent yeast cells.

In analyses of steady-state RNA in *rrp6Δ* G_1 arrested cells, we observed 1,206 upregulated pa-ncRNAs ($\log_2FC > 0.58$, adjusted p value (q) < 0.05), while only 191 mRNAs were upregulated (Figure 2.10A). This result is consistent with reports that, during logarithmic growth, the nuclear exosome plays only a minor role in mRNA regulation (Tudek et al., 2021; Wyers et al., 2005). However, in comparison to parental wild-type control cells, quiescent *rrp6Δ* cells demonstrated broadly increased levels of steady-state RNA: 928 pa-ncRNAs and 1,304 mRNAs. These results show that mRNA regulation is a major role of the nuclear exosome in quiescence (Figure 2.9A). Examples of such regulation at *ECM22* and *NCW2* genes are shown in Figure 2.9B (pink arrows).

Analysis of *RRP6*-dependent changes in RNA abundance revealed that, despite dramatically different transcriptomes, there was a strong correlation between $\log_2$ fold changes in pa-ncRNA abundance in G_1 and quiescence cells (Pearson r = 0.53) (Figure 2.9C, top). This result suggests that similar sets of non-coding transcripts are regulated by *RRP6* in G_1 and quiescence. In contrast, comparing *RRP6*-dependent changes in mRNA abundance between G_1

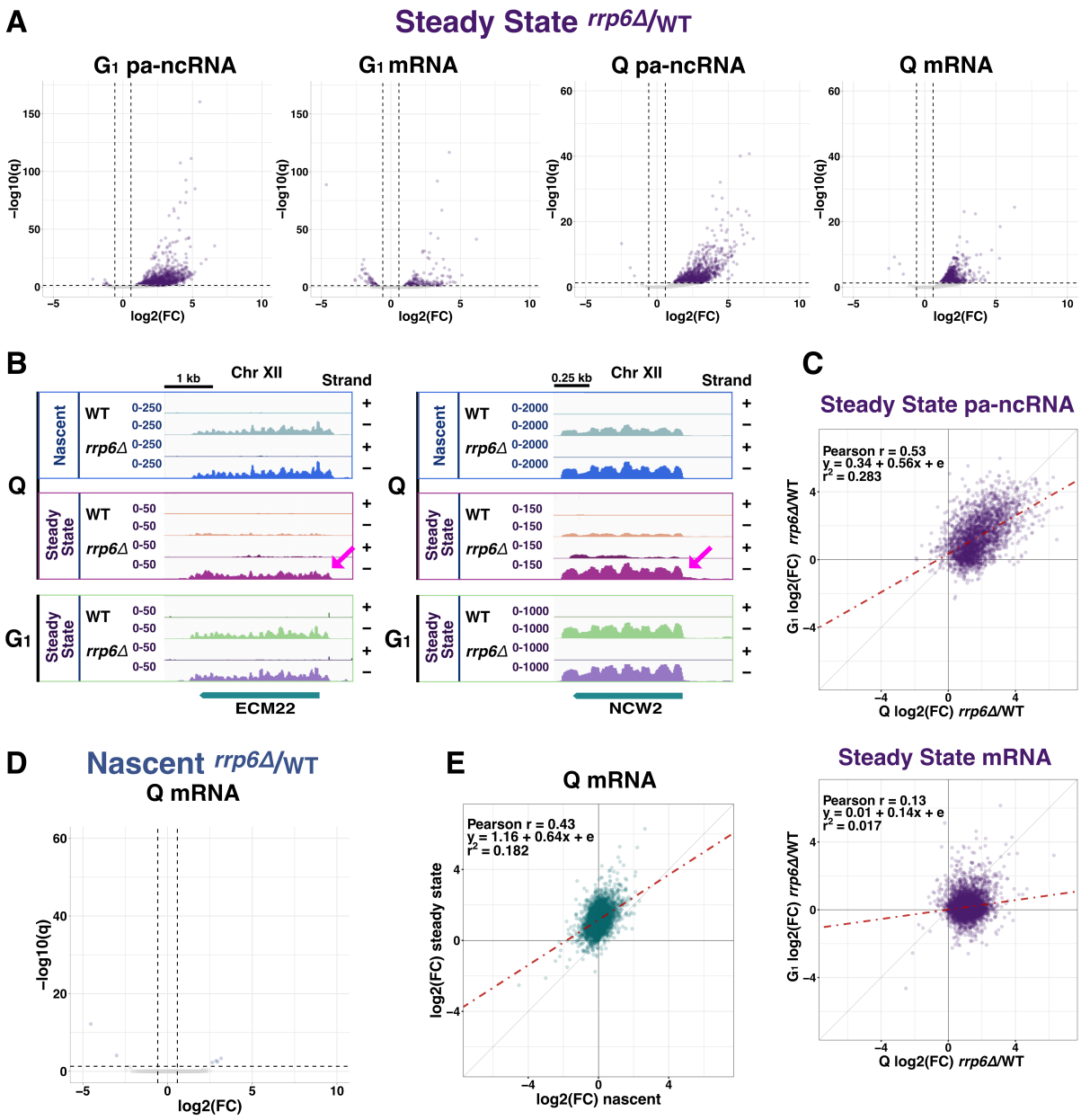

Figure 2.9 *RRP6* post-transcriptionally regulates mRNA abundance in quiescence.
(**A**) Volcano plots showing *RRP6*-dependent changes in steady-state transcript levels (*rrp6*Δ /WT). Analyses were performed using DESeq2 (Love et al., 2014), and panels show the magnitudes of *rrp6*Δ/WT $\log_2$ fold change (x-axis) versus significance ($-\log_{10}$ q value) for differentially expressed pa-ncRNA and mRNA (y-axis) in G_1 and quiescence. Significant differences were defined as $q < 0.05$ and absolute log2 fold change > 0.58. q values were obtained from Wald tests with Benjamini-Hochberg corrections. Spike-in *K. lactis* reads were used for normalization with *K. lactis* genes set as control genes in DESeq2.

(**B**) Examples of *RRP6*-regulated mRNAs in quiescence. Signal is coverage scaled using *K. lactis* size factors generated via DESeq2.
(**C**) Correlations between *RRP6*-dependent changes (*rrp6*Δ/WT) in transcript abundance between G_1 (y-axis) and quiescence (x-axis) for pa-ncRNA (top) and mRNA (bottom). The red line denotes the line of best fit from linear regression analysis.
(**D**) Volcano plot of *RRP6*-dependent changes in nascent mRNA transcript levels (*rrp6*Δ/WT). Differential expression analysis was performed as in 3a.
(**E**) Scatter plot of *RRP6*-dependent changes ($\log_2$ fold) in nascent (x-axis) and steady-state (y-axis) mRNA transcripts in quiescence.

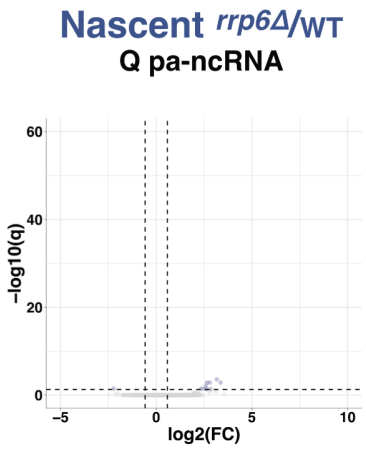

Figure 2.10 Volcano plots of *RRP6*-dependent changes in nascent transcript levels (*rrp6*Δ /WT).

Analysis was performed using DESeq2 (51) and panels show magnitude of $\log_2$ fold change of *rrp6*Δ /WT (x-axis) versus significance ($-\log_{10}$ q value) for differentially expressed pa-ncRNA (y-axis) in quiescence. Significant difference was defined as $q < 0.05$ and absolute log2 fold change > 0.58 q obtained from Wald test with Benjamini-Hochberg correction. Spike-in *K. lactis* is used for normalization with *K. lactis* genes set as control genes in DeSeq2.

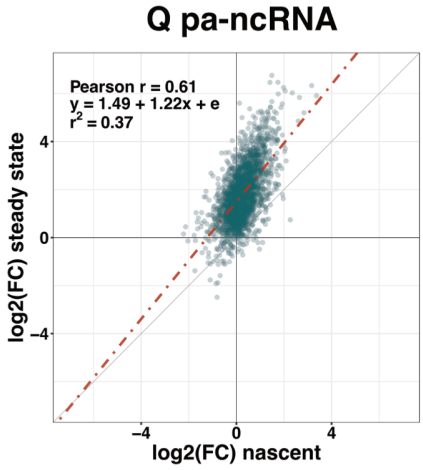

Figure 2.11 Scatter plot of *RRP6*-dependent changes (log_2 fold) in nascent (x-axis) and steady state (y-axis) pa-ncRNA transcripts in quiescence.

and quiescence revealed a poor correlation (Pearson r = 0.13), confirming *RRP6* deletion causes considerably different effects on mRNAs between G_1 and quiescence (Figure 2.9C, bottom).

Previous reports suggested that transcription termination is impaired at some loci in *rrp6Δ* mutants (Fox et al., 2015; Villa et al., 2020). To test whether *RRP6* regulates mRNA abundance in quiescence at a post-transcriptional level, we performed 4tU-seq in wild-type and *rrp6Δ* quiescent cells. Differential expression analysis revealed only 4 mRNAs were upregulated in *rrp6Δ* cells ($log_2FC > 0.58$, $q < 0.05$), showing the effect of *RRP6* deletion in quiescence on mRNAs is largely post-transcriptional (Figure 2.9D). This same pattern persisted for pa-ncRNA, with only a small number pa-ncRNAs demonstrating upregulated transcription (Figure 2.10). Examples of modest differences between nascent RNA signals in *rrp6Δ* compared to wild-type controls can be seen in the top panels of Figure 2.9B (blue box). Additionally, changes in steady-state and nascent mRNA levels are correlated (Pearson r = 0.43; Figure 2.9E; Figure 2.11),

arguing against a dramatic decrease in transcription rate in *rrp6Δ* cells (transcriptional buffering) that was previously reported (Sun et al., 2013). Taken together, our results show the nuclear exosome post-transcriptionally represses an abundance of mRNAs (~1,300) in quiescence.

2.3.5 *Altered transcription termination in quiescence*

Next, we sought to obtain mechanistic insights into how the nuclear exosome affects mRNA abundance in quiescence. Because the Nrd1-Nab3-Sen1 (NNS) complex functions upstream of *RRP6* (Arigo, Eyler, et al., 2006; Tudek et al., 2014; Villa et al., 2020) and was reported to target mRNAs upon rapid carbon source downshift (Bresson et al., 2017; van Nues et al., 2017), we hypothesized that NNS terminates mRNA transcription in quiescence. To test this possibility, the RNA-binding protein Nab3 was depleted in quiescence using an auxin inducible degron system (Nishimura & Kanemaki, 2014) (Figure 2.12). To assess changes in transcription, 4tU-seq was performed in the presence of auxin in Nab3 degron-tagged strains and, as controls, untagged parental strains.

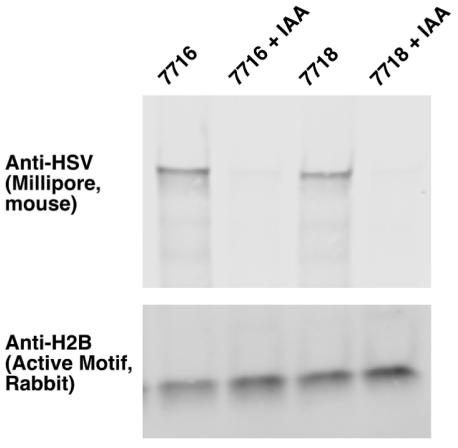

Figure 2.12 Auxin efficiently depletes Nab3-AID in quiescent yeast

Western blot of Nab3-HSV-AID to demonstrate depletion. H2B was used as a loading control.

Differential expression analyses of these strains revealed the increased transcription of both pa-ncRNA and mRNA in quiescence compared to parents, with 2,539 pa-ncRNAs and 1,417 mRNAs demonstrating increased transcription ($log_2FC > 0.58$, $q < 0.05$) (Figure 2.13A). Additionally, upon Nab3 depletion, 1,555 pa-ncRNAs and 3,255 mRNAs showed increased steady-state RNA levels. We compared log_2 fold changes in steady-state and nascent transcripts upon Nab3 depletion, revealing high correlations for mRNAs (Pearson r = 0.77) and pa-ncRNAs (Pearson r = 0.84). This suggests that NNS-independent post-transcriptional regulation plays a minor role for these transcripts (Figure 2.14).

To determine if *NAB3* and *RRP6* regulate overlapping sets of mRNAs in quiescence, we compared log_2 fold changes for *rrp6Δ* steady-state mRNAs to log_2 fold changes in wild-type Nab3-depletion nascent transcripts. *RRP6*- and *NAB3*-dependent changes were correlated (Pearson r = 0.39), implying that many of the mRNAs that are regulated by *RRP6* are also regulated by *NAB3* (Figure 2.13B; Figure 2.15). This result supports our conclusions above that the NNS-*RRP6* pathway regulates mRNA abundance in quiescence. Log_2 fold changes tended to be higher upon Nab3 depletion versus *RRP6* deletion. The larger log_2 fold changes in mRNA abundance upon Nab3 depletion was the result of increased transcription, with 770 mRNA transcripts evidencing a 2-fold-or-greater increase. In contrast, in *rrp6Δ* cells, the increase in abundance of a given transcript was limited by the level of transcription since this effect was almost entirely post-transcriptional, with only 175 mRNA transcripts exhibiting more than a 2-fold increase.

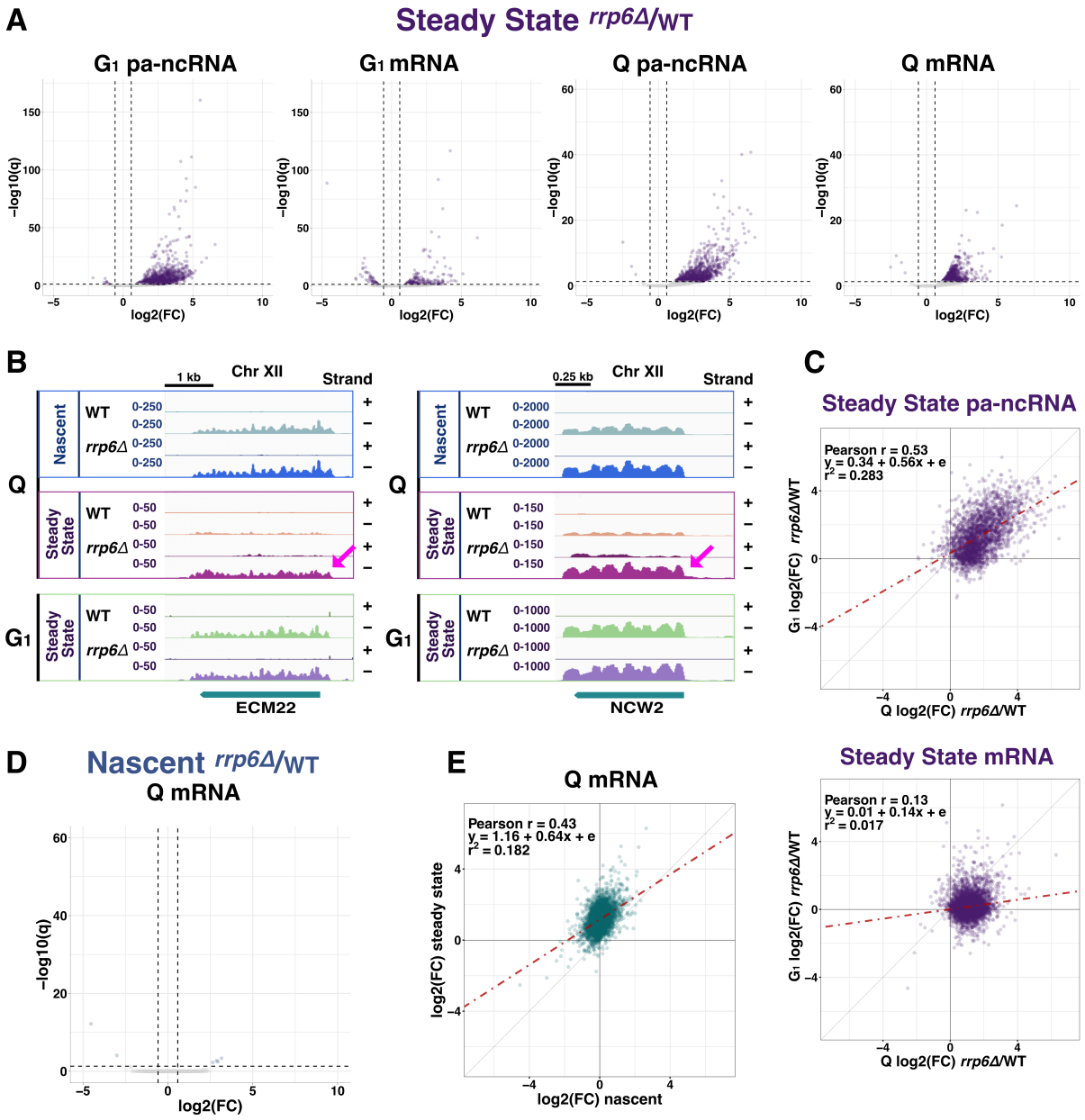

Figure 2.13 Nab3 regulates mRNA transcription in quiescence.
(**A**) Volcano plots showing *NAB3*-dependent changes in transcript levels (*NAB3-AID*/parent). Analyses were performed using DESeq2 (Love et al., 2014) , and panels show the magnitudes of *NAB3-AID*/parent $\log_2$ fold change (x-axis) versus significance ($-\log_{10}$ q value, y-axis) for nascent (left) and steady-state (right) pa-ncRNA and mRNA in quiescence. Significant differences were defined as $q < 0.05$ and absolute log2 fold change > 0.58. q values were obtained from Wald tests with Benjamini-Hochberg corrections. Spike-in *K. lactis* reads were used for normalization with *K. lactis* genes set as control genes in DESeq2.

(**B**) Correlation between *RRP6*-dependent changes (*rrp6*Δ/WT, y-axis) in steady-state transcript abundance and *NAB3*-dependent changes in nascent transcript abundance (*NAB3-AID/*parent, x-axis) in quiescence.
(**C**) Correlation between *NAB3*-dependent changes in abundance of antisense ncRNA (x-axis) and that of overlapping mRNA (y-axis).
(**D**) Loss of gene boundaries in transcription upon *NAB3* depletion. Average nascent transcription signals at 1,416 Nab3 target genes aligned at translation start (top) and stop (bottom) codons are shown. The shades around lines indicate standard error of the mean.
(**E**) Examples of Nab3-regulated mRNAs in quiescence. Signal is coverage scaled using *K. lactis* size factors generated by DESeq2.

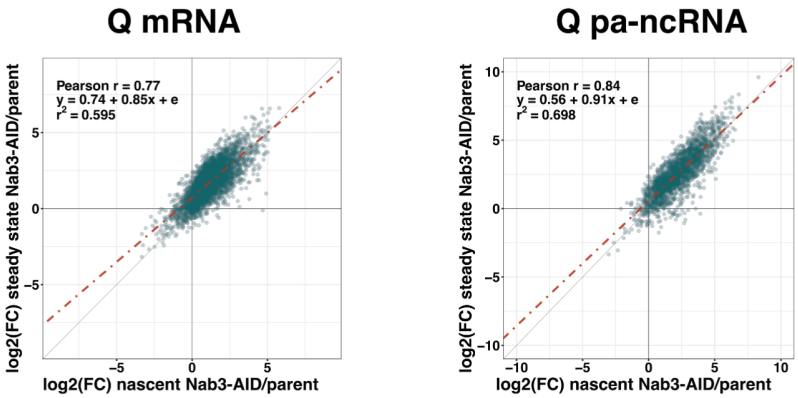

Figure 2.14 Minimal post-transcriptional compensation occurs at mRNA and pa-ncRNA in Nab3 depleted yeast.
Scatter plot of Nab3-dependent changes (log_2 fold) in nascent (x-axis) and steady state (y-axis) mRNA (left) and pa-ncRNA (right) transcripts in quiescence.

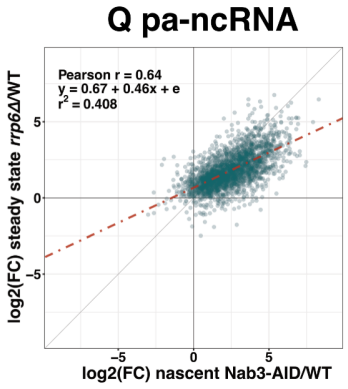

Figure 2.15 Nab3 and Rrp6 regulate similar pa-ncRNAs.

Correlation between *RRP6*-dependent changes (*rrp6*Δ /WT, y-axis) in steady-state transcript abundance and *NAB3*-dependent changes in nascent transcript abundance (*NAB3-AID* /parent, x-axis) for pa-ncRNA in quiescence.

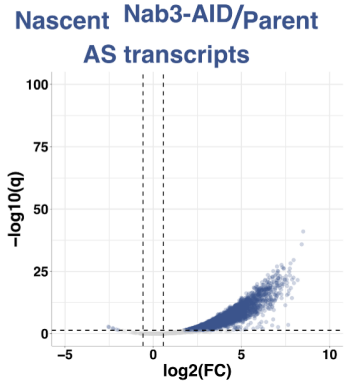

Figure 2.16 Nab3 depletion increase antisense transcription genome-wide.
Volcano plots of *NAB3*-dependent changes in transcript level (*NAB3-AID* /parent). Analysis was performed using DESeq2 (51) and panels show $\log_2$ fold change of *NAB3-AID* /parent (x-axis) versus significance ($-\log_{10}$ q value, y-axis) for nascent antisense transcripts in quiescence. Significant differences were defined as $q < 0.05$ and absolute log2 fold change > 0.58. q values were obtained from Wald test with Benjamini-Hochberg correction. Spike-in *K. lactis* is used for normalization with *K. lactis* genes set as control genes in DeSeq2.

Nuclear depletion of Nrd1 in late log phase was reported to cause increased antisense transcription, which resulted in decreased transcription of overlapping mRNAs (Schulz et al., 2013). Consistent with this, we found a dramatic increase in antisense transcription in quiescence upon Nab3 depletion (Figure 2.16), with 4,011 antisense transcripts evidencing increased expression by at least 1.5-fold ($q < 0.05$). Similar to trends reported in studies of dividing cells (Nevers et al., 2018; Schulz et al., 2013), global changes in nascent antisense transcripts weakly anti-correlated with changes in nascent sense transcripts in quiescent cells (Pearson = –0.22; Figure 2.13C). However, in contrast to other studies (Gill et al., 2020; Huber et al., 2016; Schulz et al., 2013), only 20 induced antisense transcripts were associated with a mRNA with

significantly decreased expression upon Nab3 depletion. These select antisense transcripts may control the abundance of their overlapping mRNA transcripts. Given the prevalence of non-coding transcription in quiescence (Figure 2.3A and B), it was unexpected that so few showed evidence of meaningfully repressive functions.

Metaplot analyses of Nab3-regulated mRNAs revealed poor maintenance of gene boundaries upon Nab3 depletion: both upstream and downstream transcription was increased (Figure 2.13D). The extent of upstream and downstream transcription is heterogenous, with some genes showing only slight changes in transcription initiation and termination as highlighted in Figure 2.13E at the *MDG1* locus (left panel, red boxes). Other genes show a more egregious loss of gene boundaries, such as at the *JAC1* locus, where transcription extended into neighboring genes (Figure 2.13E, right panel, pink arrow). Consistent with Figure 2.13C, increased antisense transcription at the *CKB1* locus did not have an appreciable effect on mRNA transcription, highlighting that most changes upon Nab3 depletion result in higher levels of transcription. Our results collectively showed that Nab3 suppresses mRNA transcription in quiescence, which can partially explain why the nuclear exosome suppresses mRNA abundance in this cell state.

2.3.6 *Features of Nab3-regulated mRNAs in quiescence*

We wondered why some mRNAs are affected by NNS in quiescence but not others. To address this question, we sought to identify specific features of the mRNAs repressed by Nab3 in quiescence. NNS is known to target short genes in actively dividing cells through Ser5 phosphorylation on the RNA polymerase II C-terminal domain (Kubicek et al., 2012; Vasiljeva,

Kim, Mutschler, et al., 2008), which peaks near the 5′ end of genes (Komarnitsky et al., 2000). In quiescence, gene length and Nab3-dependent changes in nascent transcription were weakly anti-correlated (Pearson = –0.19) (Figure 2.17A). While short mRNAs were more likely to be regulated by Nab3 than long ones, this is a trend rather than a rule. Of the 1,417 Nab3-regulated mRNAs we identified, 1,010 had open reading frames longer than 500 base pairs.

Independent of gene length, we found the expression level of Nab3 targets tended to be low. Changes in transcript abundance upon Nab3 depletion and expression level in parental strains were strongly anti-correlated (Pearson = –0.67) (Figure 2.17B). This suggests Nab3 further suppresses the abundance of lowly transcribed mRNAs in quiescence.

Nab3 and Nrd1 are known to bind RNA through short binding motifs. We tested whether Nab3 regulated genes are enriched for such motifs. The ten strongest Nrd1 and Nab3 motifs as identified by Schulz et al. (Schulz et al., 2013) were used for this analysis. Using simple enrichment analysis from MEME Suite (T. L. Bailey et al., 2009), we compared Nab3-regulated mRNAs to an equal number of randomly sampled genome positions (see Chapter 3: Materials and Methods). This analysis revealed that Nab3-regulated transcripts contain NNS motifs largely at or below background levels, with mean enrichment within ~25% of the background distribution in all cases (Figure 2.17C).

GO analysis of all 1,400 Nab3 regulated genes resulted in no significant term enrichment, suggesting that weakly upregulated Nab3 targets are sources of noise in the analysis. Thus, we sought to examine the GO term enrichment of strongly regulated Nab3 genes by performing differential expression analysis with $\log_2$ fold change > 1 and $q < 0.05$. This resulted in 770

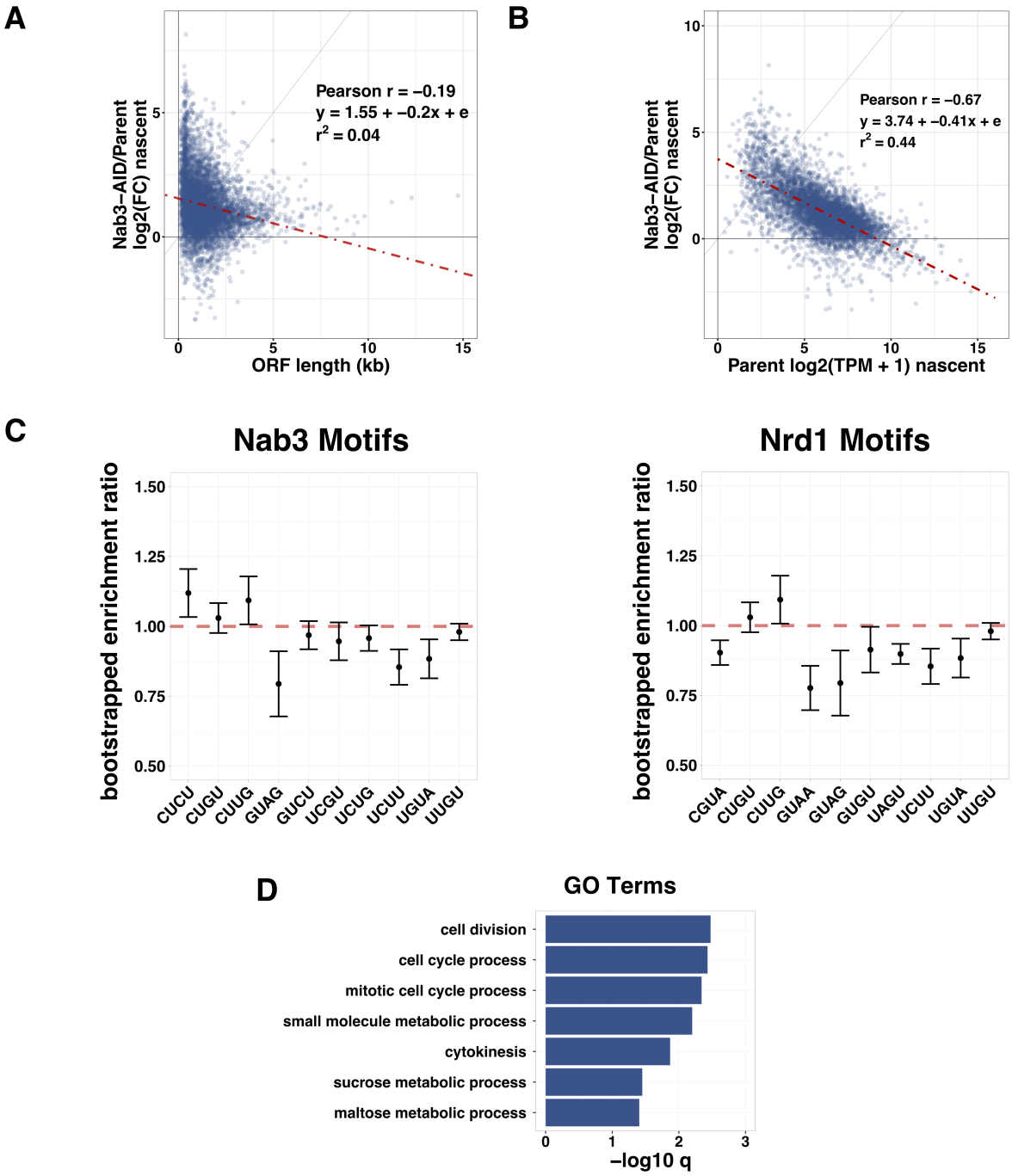

Figure 2.17 . Features of Nab3-regulated mRNAs in quiescence.
(**A**) Weak anti-correlation between *NAB3*-dependent changes in nascent RNA signals and gene length. Log_2 fold change in nascent transcript abundance (*NAB3-AID*/parent) in quiescence (y-axis) versus ORF length (x-axis) are plotted.

(**B**) Anti-correlation between *NAB3*-dependent changes in nascent RNA signals and transcription levels. Log_2 fold change in nascent transcript abundance (*NAB3-AID*/parent) in quiescence (y-axis) versus log_2 TPM + 1 values in parent strain (x-axis) are plotted.
(**C**) Lack of enrichment for Nab3- and Nrd1-binding motifs on Nab3 target mRNAs in quiescence. Bootstrapped enrichment analysis of known Nab3 and Nrd1 RNA-binding motifs was performed on Nab3-target ORFs using simple enrichment analysis from MEME Suite (T. L. Bailey et al., 2009).
(**D**) GO enrichment analysis of the top 770 Nab3-target mRNAs. GO terms and q values from hypergeometric tests with Benjamini-Hochberg corrections from YeastMine (Balakrishnan et al., 2012) are presented.

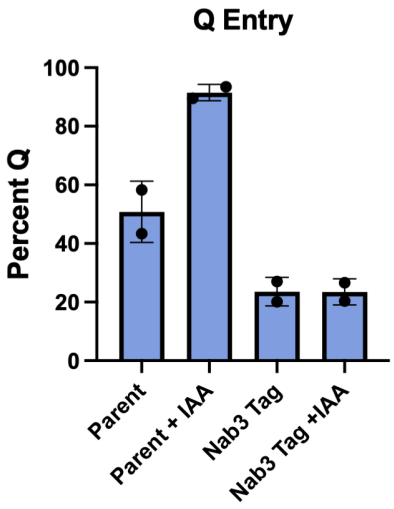

Figure 2.18 Nab3 tag and depletion impair quiescence entry.
Bar plot of Q entry for Nab3 tagged and parental strains with and without IAA added at DS+6 hours.

genes that were, in turn, enriched in GO terms associated with cell division, the cell cycle, and metabolism, suggesting Nab3 plays crucial roles in quiescence entry and/or maintenance (Figure 2.17D). Consistent with these findings, depletion of Nab3 results in significant quiescence entry defects (Figure 2.18). However, since all subunits of the NNS complex are essential for cell viability, the need for NNS in quiescence entry cannot be separated from its essential functions.

We next tested whether NNS regulates similar mRNAs in quiescence and rapid carbon source shift in which yeast cells were moved from media containing glucose to media containing glycerol and ethanol (Bresson et al., 2017). Of the mRNAs repressed by Nab3 in quiescence we found only 123 (~9%) also had increased binding by Nab3 upon rapid carbon source shift (Figure 2.19). It is possible that this discrepancy is the result of the difference in assays; Bresson et al. used an RNA IP assay known as the Cross-Linking Analysis of cDNAs (CRAC), while we used 4tUseq to measure changes in nascent transcription. Additionally, we compared mRNAs repressed by *RRP6* in quiescence to those with increased binding by Mtr4 upon rapid carbon source shift; Mtr4 is a part of the TRAMP complex and an essential cofactor of the nuclear exosome. Our analysis revealed that 237 of 1,250 *RRP6*-repressed mRNAs in quiescence were targeted by Mtr4 during rapid carbon source shift (approximately ~19%) (Figure 2.19). These results suggest the possibility that NNS and the nuclear exosome may affect different mRNAs between rapid carbon source shift and quiescence.

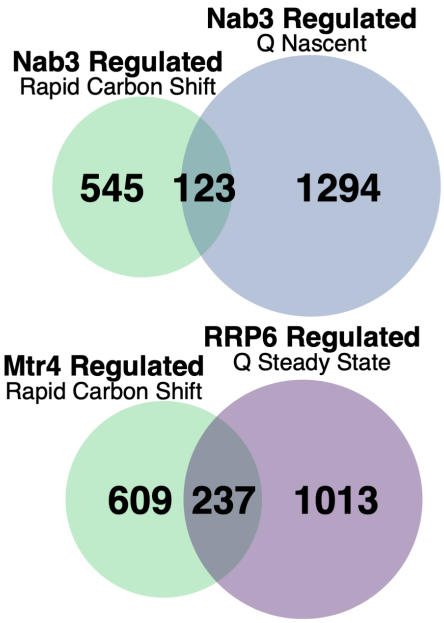

Figure 2.19 Venn diagrams of mRNAs regulated by Nab3 or Rrp6 in quiescence compared to those found on carbon source shift.

2.3.7 *Two distinct phases of post-transcriptional regulation during quiescence entry*

Our data suggest the NNS-nuclear exosome pathway plays previously unknown unique roles in quiescence. Next, we sought to determine when during the process of quiescence entry the activity of the pathway shifts from its canonical role in ncRNA regulation to the additional regulation of mRNAs. Due to challenges posed by using a depletion system during time-course experiments, we employed *rrp6Δ* mutants for these experiments. Yeast cells were harvested through quiescence entry, and steady-state RNA-seq was performed. Time points were chosen in the hours preceding and following the diauxic shift (DS), when glucose becomes undetectable in media and yeast cells switch from fermentation to respiration. Previous work demonstrated that dramatic changes in the transcriptome take place around DS (M. Spain et al., 2018).

PCA was performed on TPM-normalized, $\log_2$-regularized counts for mRNA genes across all collected time points in wild type and *rrp6Δ* (Figure 2.20A). PC1 separated transcriptomes based on timepoints and PC2 specifically separated DS+2hrs and DS+24hrs from all other time points. Together PC1 and PC2 represent 70.06% of total variation. In G_1 and at DS–2hrs, *rrp6Δ* transcriptomes were slightly closer to the transcriptomes of the parents at later timepoints, but at DS+2hrs and after, *rrp6Δ* transcriptomes were more similar to the transcriptomes of the parents at earlier time points, suggesting that, after the DS, gene expression events during quiescence entry were delayed in the absence of *RRP6*. PC3 separated mutant and wild-type samples and accounted for only 10.46% of variation, indicating growth phase and nutrient availability are stronger sources of variation than genotype.

We next sought to determine how *RRP6* affects its targets during quiescence entry. To this end, we performed a two-step cluster analysis (see Materials and Methods) of the 1,250 genes that are repressed by *RRP6* in quiescence but not G_1 ($\log_2FC > 0.58$, $q < 0.05$) and found 3 distinct clusters (Figure 2.20B). Cluster 1 was composed of 308 genes down in *rrp6Δ* at DS–2hrs and up at DS+2hrs, suggesting *RRP6* is necessary for reducing the abundance of transcripts in this cluster around the DS. The 317 genes that comprised cluster 2 had the opposite pattern as cluster 1, with increased relative expression in *rrp6Δ* at DS–2hrs and decreased expression at DS+2hrs. Cluster 3 genes had increased expression in *rrp6Δ* later in quiescence entry, with the effect on 629 genes beginning by DS+24hrs and becoming more pronounced by DS+48hrs. To test the statistical significance of *RRP6*-dependent changes, we plotted $\log_2$-transformed TPM distributions for the genes that make up each cluster (Figure 2.20C). In agreement with our cluster analysis, the differences in TPM distributions between mutant and parent in cluster 1 became significant at DS+2hrs, whereas the differences were not significant for cluster 3 until DS+48hrs. Cluster 2 was significantly different at DS–2hrs and DS+48hrs.

These clusters represented distinct functional groups, with unique sets of enriched GO terms consistent with the cellular changes during quiescence entry. Cluster 1 was strongly enriched for genes involved in protein synthesis, such as translation and ribosome biogenesis. In contrast, cluster 2 genes were more likely to be involved in metabolism, and genes from cluster 3 were involved in organization and transport (Figure 2.20D).

Consistent with the role of *RRP6* in regulating these key transitions in gene expression, *rrp6Δ* mutants exhibited a ~50% lower quiescence entry efficiency compared to their parental

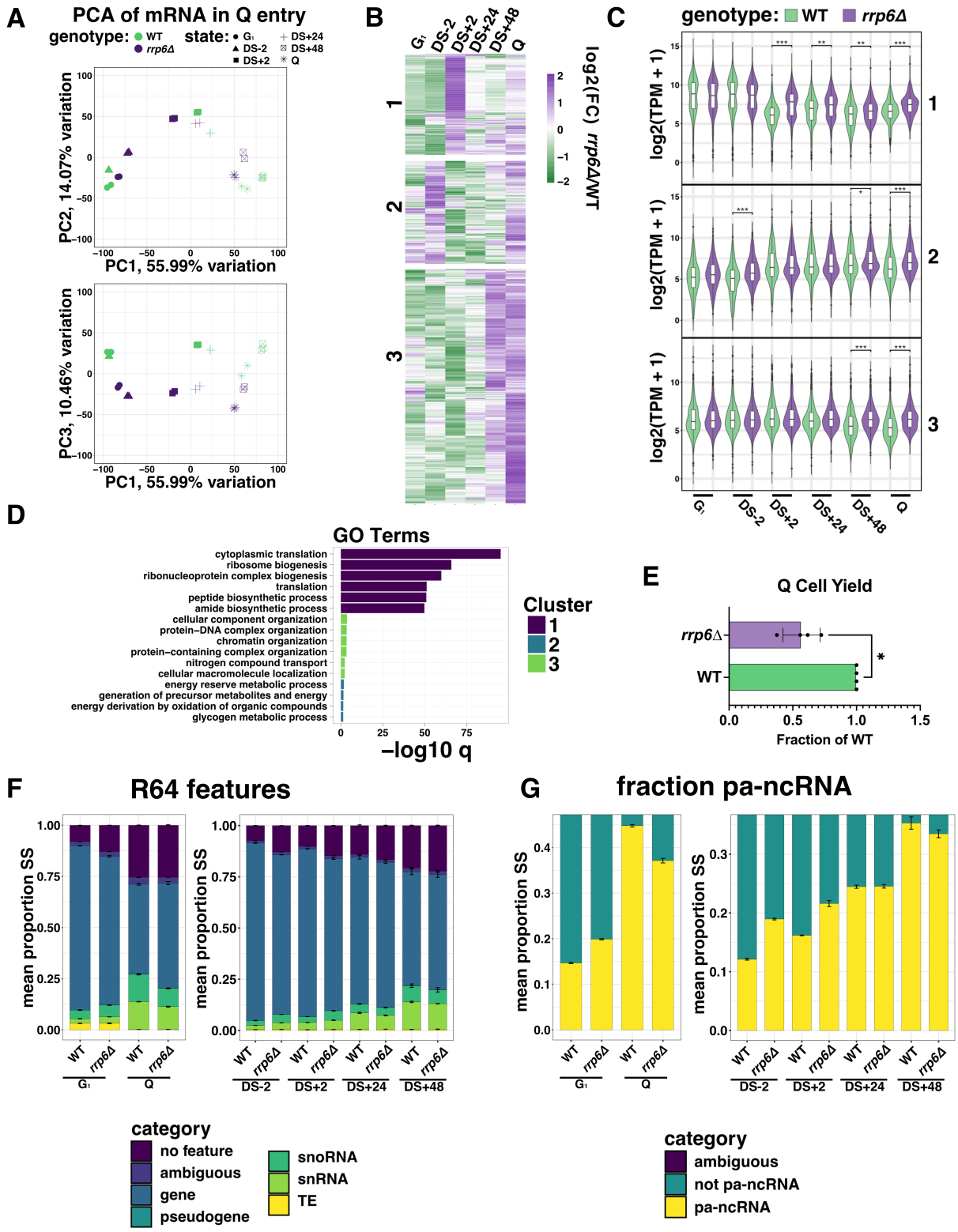

Figure 2.20 *RRP6* regulates mRNA abundance at multiple time points during quiescence entry.

(**A**) PCA of steady-state mRNA levels in wild-type and *rrp6*Δ cells during quiescence entry. PCA was performed on log_2-regularized TPM-normalized mRNA values from wild-type and *rrp6*Δ cells at 6 time points: G_1, DS–2hs, DS+2hrs, DS+24hrs, DS+48hrs, and quiescence.
(**B**) Two-step cluster analysis of *RRP6*-dependent changes in steady-state transcript levels (*rrp6*Δ/WT) during quiescence entry. The analysis was performed through quiescence entry on 1,250 mRNAs regulated by *RRP6* in quiescence but not in G_1. Log_2 fold change was calculated using log_2-regularized TPM-normalized RNA-seq data.
(**C**) Box-and-whisker/violin plots statistically validate *RRP6*-dependent mRNA control of 3 clusters from 6b. Distributions of log_2-regularized TPM-normalized RNA-seq data are stratified by genotype and state for each cluster. q values are calculated from Kolmogorov-Smirnov tests with Benjamini-Hochberg corrections: (* = $p \leq 0.05$, ** = $p \leq 0.01$. *** = $p \leq 0.001$, no asterisks= not significant).
(**D**) GO enrichment analysis of *RRP6*-regulated mRNAs from each cluster. GO terms are from YeastMine (Balakrishnan et al., 2012), as are q values from hypergeometric tests with Benjamini-Hochberg corrections.
(**E**) Bar plot for *rrp6*Δ and wild-type quiescent cell yield from two biological replicates in technical duplicate from heterogenous 8-day culture. p value is calculated from Student's t-test.
(**F**) Mean proportions of read alignment from steady-state RNA-seq from wild-type and *rrp6*Δ cells aligned to the R64-1-1 assembly from G_1 and quiescence (left), and quiescence entry time course (right). Error bars are standard error of the mean for 2 biological replicates.
(**G**) Mean proportions of read alignment from steady-state RNA-seq from wild-type and *rrp6*Δ cells aligned to pa-ncRNA in wild-type and *rrp6*Δ cells in G_1 and quiescence (left), and during quiescence entry time course (right). Error bars are standard error of the mean for 2 biological replicates.

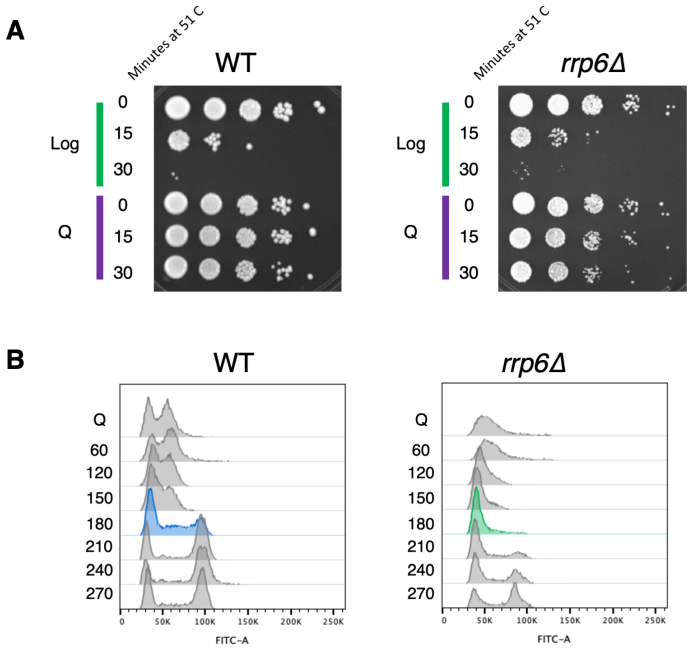

Figure 2.21 *rrp6*Δ mutants produce bona fide quiescent cells.
(**A**) Representative thermotolerance spot test for wild type and *rrp6*Δ cells from logarithmically growing and quiescence cultures.
(**B**) Representative FACs profile for Q exit for wild type and *rrp6*Δ.

wild-type cells (Figure 2.20E). Despite these impairments in quiescence entry, *rrp6Δ* quiescent cells are not dissimilar from wild-type cells. They display only slightly decreased thermotolerance and are far more thermotolerant than cells in exponential growth (Figure 2.21A). Additionally, *rrp6Δ* quiescent cells have slower kinetics during exit from quiescence (Figure 2.21B). The latter is likely due in part to slow growth defects in *rrp6Δ* cells (Stead et al., 2007). Consistent with these mild phenotypes, the transcriptome of quiescent *rrp6Δ* mutants is much closer to that of wild-type quiescent cells than cells at any time points during quiescence entry (Figure 2.20A). Therefore, while changes in mRNA abundance affect entry into quiescence, *rrp6Δ* mutants still produce *bona fide* quiescent cells.

We next analyzed whether global changes in RNA abundance coincided with changes in specific classes of mRNA transcripts. In *rrp6Δ* mutants in G_1, mRNAs made up a smaller fraction of read depth as compared to parental wild-type controls (Figure 2.20F, left). Since non-coding RNAs were elevated in abundance in G_1, mRNAs became a smaller proportion of the transcriptome. In sharp contrast, this pattern was reversed in quiescence, consistent with our finding that a key role for *RRP6* in quiescence is to repress mRNAs. During quiescence entry, *rrp6Δ* cells were more like G_1 cells in terms of mRNA proportion at DS–2hrs but became more like quiescent cells by DS+48hrs (Figure 2.20F, right). Concurrently, ncRNA exhibited a pattern opposite to mRNA, with a larger proportion of read depth corresponding to non-coding features in G_1 *rrp6Δ* cells versus wild-type controls, and a smaller portion in quiescence (Figure 2.20G,

left). During quiescence entry, *rrp6Δ* mutants and WT cells exhibited pa-ncRNA content similar to G_1 at DS–2hrs and DS+2hrs (about ~20% of read depth). By DS+48hrs, both *rrp6Δ* mutants and wild-type cells began to look similar to the quiescent state in terms of pa-ncRNA content (approaching ~40% of read depth in quiescence entry) (Figure 2.20G, right). We conclude that changes in global ncRNA levels coincide with global changes in mRNA level and that the nuclear exosome is needed to facilitate these key transitions in both classes of transcripts. We note that the proportions of read alignment from nascent and steady-state RNA from wild-type G_1 and quiescent cells are different between Figure 2.3A and Figures 2.20F and G, a difference that likely resulted from using different kits for library preparations (see Materials and Methods). This is consistent with reports that comparable results can be obtained from different kits, but kit choice can alter library complexity and numbers of transcripts detected (Sarantopoulou et al., 2019; Y. Song et al., 2018). We compared only samples prepared with the same kit to eliminate technical variations that could confound analyses.

2.4 DISCUSSION

2.4.1 *Identification of cell state-associated ncRNA*

In this study, we provide the first *de novo* assemblies of the nascent transcriptomes in quiescent and G_1 cells, which are valuable resources for those who study transcription and RNA stability in budding yeast. We identified ~1,300 ncRNAs in quiescence and G_1, about 300 of which had no overlap to previously identified ncRNAs, despite the use of stringent filters to eliminate low-count signals. We suspect the use of cells in specific cell-cycle stages, 4tU-seq, and rRNA depletion allowed us to capture cryptic transcripts without mutating RNA surveillance systems to artificially elevate their abundance. While we expected to identify unique ncRNAs in

quiescence, we were surprised to find 42 G_1-expressed ncRNAs that had no overlap with previously annotated transcripts. This might be due to the use of different strain backgrounds (S288C versus W303), different library preparation methods (poly(A) enriched versus rRNA depleted), the increased sensitivity of deep sequencing compared with tiling arrays, and/or the presence genuinely *bona fide* G_1-specific ncRNAs. Our finding suggests that despite the small genome size and previous efforts by multiple labs to identify ncRNAs in yeast, many ncRNAs are yet to be found in the budding yeast genome under different conditions.

While ncRNAs have been a subject of increasing scientific interest for the last two decades, ncRNA identification in yeast has not been systematized to the extent of mRNA. Long-term efforts to find and characterize functional ncRNAs could be accelerated by a rigorous multi-lab effort to identify yeast ncRNAs across conditions and cell states. Such an effort would address the issues caused by the multiple independent annotations and could provide a universal set of naming rules. Systematic and accurate ncRNA identification would be of high value in better understanding how yeast adapt their gene expression to cell state. Our data demonstrate that ncRNA profiles can distinguish G_1 and quiescent cells. Our results are consistent with reports on other organisms in which ncRNA expression is highly cell state-specific, including in plants, invertebrates, and humans (Akay et al., 2019; Kang & Liu, 2015; Seifuddin et al., 2020). Additionally, ncRNAs have emerged as promising biomarkers for several cancers, including liver, breast, and prostate cancer (Beylerli et al., 2022; Qian et al., 2020). Cumulatively, these results suggest that ncRNAs are markers for cell state across eukaryotes. ncRNAs tend to have poor sequence conservation (Szcześniak et al., 2021) and may be undergoing rapid evolution for cell state specific function.

Across species, a very small minority of ncRNAs have been functionally characterized. Since the discovery that eukaryotic genomes are pervasively transcribed, it has been an open question as to whether these transcription events are functional or simply a side-effect of cellular inefficiency, such as improper transcriptional initiation or termination (Dinger et al., 2009; Villa & Porrua, 2022). Since cellular energy is limited in quiescence, we expected to find that there was less inefficiency permitted, not more. Early in this work, we hypothesized that ncRNAs may play key regulatory roles for transcriptional repression in quiescent yeast cells, based on previous reports that ncRNAs can repress the transcription of overlapping mRNAs through the formation of repressive chromatin structures (Pelechano & Steinmetz, 2013). However, we unexpectedly found that antisense transcription is only weakly repressive in quiescence. We suspect this may be because chromatin is already in a highly repressive state in quiescence (Cucinotta et al., 2021; McKnight et al., 2015; Mews et al., 2014; Swygert et al., 2019; Young et al., 2017).

2.4.2 *Post-transcriptional regulation by the NNS-nuclear exosome in quiescence*

Comparisons of nascent and steady-state transcriptomes in quiescent and G_1 cells led to our unexpected finding that post-transcriptional regulation plays a larger role in quiescence. Our time-course experiments revealed that during quiescence entry, *RRP6* controls the abundance of distinct sets of genes with shared GO terms at distinct time points. It is possible that some of the *rrp6Δ* effects observed in quiescence are due in part to the impaired activity of Dis3, the essential exonuclease in the nuclear exosome (Januszyk & Lima, 2014; Kilchert et al., 2016) that exhibits decreased activity in the absence of Rrp6 *in vitro* (Wasmuth & Lima, 2012). Regardless, defects in mRNA abundance in *rrp6Δ* increase through quiescence entry, suggesting that as a

complex, the nuclear exosome has an expanded role in mRNA metabolism upon entry into quiescence. Further work is necessary to understand which nuclear exosome cofactors are relevant in quiescence as well as the extent to which the conclusions drawn from cycling cells are applicable in quiescence. Transcriptional and post-transcriptional control during quiescence entry is highly dynamic and complex, and we found that PCA is a method complementary to differential expression analyses that is highly informative during this period.

We also found that upstream of Rrp6, NNS is a crucial transcriptional silencer in quiescence. Such NNS activity has been described at telomeres and the rDNA region in actively diving cells (Vasiljeva, Kim, Terzi, et al., 2008), but our results demonstrated that NNS represses thousands of transcripts, both coding and non-coding, in quiescence. Previous reports have implicated the NNS-nuclear exosome in mRNA regulation upon rapid carbon source shift from glucose to ethanol/glycerol (Bresson et al., 2017). It is therefore possible that the NNS-nuclear exosome pathway targets mRNAs under different stress conditions and that the NNS-nuclear exosome pathway may have currently unknown targets under other stress conditions that have not yet been investigated. The only distinguishing features of mRNAs regulated by Nab3 upon quiescence entry were relatively short gene length and low levels of transcription. Since transcription is globally repressed by multiple chromatin-based mechanisms (McKnight et al., 2015; Miles et al., 2013; Swygert et al., 2019; Young et al., 2017), low-level mRNA transcription may behave more similarly to cryptic non-coding transcription in quiescence than in other cell states. However, it remains to be determined whether other features are required for NNS to target specific mRNAs in quiescence.

We wondered why a larger fraction of transcription resources are used for ncRNAs in quiescence despite the presence of active NNS complex. One possible underlying reason is that a

larger fraction of NNS is devoted to targeting lowly expressed mRNAs, leaving non-coding transcription comparatively unregulated. However, currently available gene overexpression systems meaningfully interfere with the quiescent state, and advances on this front are necessary to further address this question. This phenomenon may be enhanced by the sequestration of Nab3 into granules upon glucose deprivation (Loya et al., 2018). Consistent with this idea, the strains in which Nab3 is mostly sequestered into granules grow poorly on glycerol plates compared to strains with low-granule accumulation (Hutchinson et al., 2022), suggesting that an increased level of freely available NNS is beneficial to yeast in nutrient-poor environments.

Several RNA decay pathways other than the NNS-nuclear exosome pathway have been implicated in other physiologically relevant processes. The Ccr4-Not complex has been implicated in quiescence in mouse and human immune cells (Akiyama et al., 2021), and Tis11, another RNA-binding protein that promotes mRNA degradation, acts in *Drosophila* intestinal stem cell quiescence (McClelland et al., 2017). In budding yeast, selective RNA autophagy takes place in yeast upon treatment with rapamycin (Makino et al., 2021), and the RNA-binding protein Ssd1 extends the chronological lifespan of quiescent yeast (L. Li et al., 2009). In a human fibroblast model of quiescence, over ~500 transcripts were found to have altered RNA stability (Johnson et al., 2017). The altered regulation of RNA decay may be a hallmark of quiescence in eukaryotes, and thus more work is warranted to elucidate mechanisms and biological roles for RNA decay pathways across eukaryotic quiescent cells.

Collectively, our work identified a previously unknown key biological role for the nuclear exosome and NNS complex in mRNA regulation, and uncovered an additional layer of gene expression control in quiescence. Although quiescence entry defects caused by *RRP6* deletion and Nab3 depletion likely indirectly affect the transcriptome, changes under these

conditions are distinct from those caused by other mutations responsible for quiescence entry defects, such as *rpd3Δ* deletion (McKnight et al., 2015), condensin depletion (Swygert et al., 2019), and histone H4 N-terminal mutations (Swygert et al., 2021). The fact that *RRP6*- and *NAB3*-dependent genes have global overlaps also strongly supports our conclusion that the NNS-nuclear exosome pathway functions to decrease the abundance of a large number of transcripts in quiescence. Since the vast majority of studies on gene expression control have been done using actively dividing cells, important mechanisms for regulating other cell states could have been missed for many genes. Quiescent yeast can serve as a powerful model system to identify the currently unknown biological functions of well-characterized genes and novel non-coding features, and to better characterize the global changes in gene regulation that promote cellular dormancy.

2.5 DATA AVAILABILITY

Data have been deposited in the Gene Expression Omnibus (GEO) with accession GSE239568; previously published data are also available from ArrayExpress E-TABM-590 (Xu et al., 2009), NCBI SRA SRA030505 (van Dijk et al., 2011), GEO repository GSE74028 (Vera & Dowell, 2016), NCBI SRA SRP089706 (Venkatesh et al., 2016), and ArrayExpress E-MTAB-1766 (Schulz et al., 2013).

To review GEO accession GSE239568, go to https://www.ncbi.nlm.nih.gov/geo/query/acc.cgi?acc=GSE239568. Enter token "ovitcmoehtkdnit" into the box.

Source code and documentation for computational experiments and analyses, and copies of counts matrices, Gene Transfer Format (gtf), and Gene Feature Format (gff3) files, are available at github.com/kalavattam/2023_Greenlaw-et-al.

2.6 FUNDING

Funding provided by National Science Foundation GRFP fellowship DGE-1762114 to A. C. G. and National Institutes of Health R35 R35GM139429 to T. T.

2.7 AUTHOR CONTRIBUTIONS

A.C.G. and T.T. drafted the manuscript with edits and additions provided by K.G.A. A.C.G. and T.T. designed the study and bench experiments; A.C.G., K.G.A., and T.T. designed the computational experiments/analyses. A.C.G. conducted the wet-lab experiments; A.C.G. and K.G.A conducted the dry-lab experiments. A.C.G., K.G.A., and T.T. interpreted the results. A.C.G. and T.T. obtained resources. T.T. was the overall supervisor of this work.

2.8 ACKNOWLEDGEMENTS

We thank Dr. Brian Haas for advice on the operation and parameterization of Trinity. We thank Tsukiyama Lab members and Dr. Steve Hahn for feedback on the manuscript. We thank Matt Fitzgibbon for suggestions regarding bioinformatics involved in this study. We thank Dr. Jeremy Schofield for advice and feedback regarding 4tU labeling. We thank Dolores Covarrubias from the Fred Hutch Genomics Core for operating Illumina sequencers. We thank Andy Marty from the Fred Hutch Genomics Core for offering advice on library prep and quantification. We thank Jordan Gessaman for constructing

*rrp6*Δ strains and preliminary work. We thank Dr. Steve Hahn, Dr. Arvind (Rasi) Subramaniam, Dr. Edith Wang, and Dr. David Shechner for serving as the thesis committee for A.C.G.

2.9 CONFLICT OF INTEREST

None declared.

Chapter 3. MATERIALS AND METHODS

This chapter is adapted from "Post-transcriptional regulation shapes the transcriptome of quiescent budding yeast" which has been accepted for publication at *Nucleic Acids Research*. It has been adapted to collapse the Materials and Methods with the Supplemental Materials and Methods.

3.1 REAGENTS

Table 3.1 Reagents

Reagent	**Source**	**Identifier**
Antibodies		
Anti-HSV•Tag® Antibody, clone HSV 78 (mouse)	Millipore Sigma	MAC123
Anti-H2B (rabbit)	Active Motif	39238
IRDye® 680RD Goat anti-Rabbit IgG Secondary Antibody	LI-COR	926-32211
IRDye® 800CW Goat anti-Mouse IgG Secondary Antibody	LI-COR	926-32210
Chemicals		
4-Thiouracil 97%	Sigma Aldrich	440736-1G
3-Indoleacetic acid 98%	Sigma Aldrich	I3750-5G-A
Percoll PLUS density gradient media	Cytiva	17544501
MTSEA Biotin-XX	Biotium	90066
Dynabeads™ MyOne™ Streptavidin C1	Thermo Fisher	65001
OneTaq® Quick-Load® 2X Master Mix with Standard Buffer	NEB	M0486S
Transcriptor First Strand cDNA Synthesis Kit	Roche	4896866001
AMPure XP Reagent, 60 mL	Beckman Coulter	A63881
Intercept® (PBS) Blocking Buffer	LI-COR	927-70001
4–20% Mini-PROTEAN® TGX™ Precast Protein Gels, 15-well, 15 µl	Biorad	#4561096

SYTOX™ Green Nucleic Acid Stain	Thermo Fisher	S7020
Commercial Assays		
Ovation® SoLo® RNA-Seq library preparation kit and custom yeast rRNA depletion (AnyDeplete®)	Tecan	Contact Tecan Rep
Universal Plus™ Total RNA-Seq library preparation kit and custom yeast rRNA depletion (AnyDeplete®)	Tecan	Contact Tecan Rep
RiboPure™ RNA Purification Kit, yeast	Thermo Fisher	AM1926
miRNeasy Micro Kit	Qiagen	217084

Table 3.2 Primers

Name	**Purpose**	**Sequence**
FLC2-1	Check primer for 4tU and for DNA contamination for *S. cerevisiae* FLC2	CCTTTTAACGTGTTTCGTACTGTG
FLC2-2	Check primer for 4tU and for DNA contamination for *S. cerevisiae* FLC2	GGGGTAAAATTTCACATCAAAGAA
KL ACT1 F	Check primer for 4tU for *K. lactis* ACT1	GCTCCAATGAACCCAAAGAA
KL ACT1 R	Check primer for 4tU for *K. lactis* ACT1	AAGATAGCGTGAGGCAAGGA

3.2 Biological Resources

Due to requirements for quiescence entry, all experiments were conducted in the W303 RAD5+ prototrophic background. Additionally, this background is more sensitized to mutations in the

nuclear exosome pathway (Klauer & van Hoof, 2013). Using independently created strains, each experiment was performed in biological duplicate.

Table 3.3 Strains

Strain Number	Source	Complete Genotype
yTT5781	Tsukiyama Lab	*MATa RAD5+ can1-100*
yTT5782	Tsukiyama Lab	*MATa RAD5+ can1-100*
yTT7078	Tsukiyama Lab	*MATa RAD5+ can1-100 rrp6Δ::Nat*
yTT7079	Tsukiyama Lab	*MATa RAD5+ can1-100 rrp6Δ::Nat*
yTT6125	Tsukiyama Lab	*MATa RAD5+ can1-100 pMK200 (URA3 ADH1p-OsTIR[codon optimized])*
yTT6126	Tsukiyama Lab	*MATa RAD5+ can1-100 pMK200 (URA3 ADH1p-OsTIR[codon optimized])*
yTT7716	Tsukiyama Lab	*MATa RAD5+ can1-100 pMK200 (URA3 ADH1p-OsTIR[codon optimized]) NAB3-3HSV-AID-Hyg*
yTT7718	Tsukiyama Lab	*MATa RAD5+ can1-100 pMK200 (URA3 ADH1p-OsTIR[codon optimized]) NAB3-3HSV-AID-Hyg*
NRRL Y-1140	Nathan Clark Lab	*K. lactis spike-in strain*

3.3 Statistical Analyses

No statistical methods were used to predetermine sample sizes. No data were excluded from analyses. The experiments were not randomized, and investigators were not blinded to allocation during experiments and assessment. Where appropriate, the mean or median is reported as a measurement of central tendency, and the standard error of the mean or standard deviation is used as measures of precision. Statistical significance was thresholded at $\alpha = 0.05$. When multiple test correction was performed, $q < \alpha$ is considered significant; otherwise, $p < \alpha$ is considered significant. Where appropriate, numbers of sample and replicates are reported in

figure captions. Statistical analyses were performed using base R (version 4.2.2, 2022-10-31) and/or various software packages listed in the below subsections. Strategies for stratification, sampling, and enrichment are described in the below subsections.

3.4 Materials availability

Strains used in this study available from Toshio Tsukiyama (ttsukiya@fredhutch.org) upon request.

3.5 Growth and measurement of yeast cells

Quiescent cells were grown for 7 days to saturation in YEP with 2% glucose, except in *rrp6Δ* experiments, where both knockout and parental strains were grown for 8 days due to the slow cell division associated with *rrp6Δ* cells. All cells were cultured at 30 °C on a platform shaker at 180 revolutions per minute (RPM) in unbaffled flasks. To achieve appropriate aeration, we used a ratio of 1/10th volume YPD to the flask size. We estimated culture density by measuring optical density per mL at wavelength 660 (OD_{660} per mL). Briefly, yeast cultures were diluted to be within a linear range of the spectrophotometer, and then original-culture cell densities were back calculated to obtain measurements of OD_{660} per mL. Consistent numbers of total ODs were used for each experiment as described below. To evaluate Q entry, the saturated OD_{660} per mL of the original culture was measured along with the OD_{660} per mL of obtained Q cells.

3.6 Growth and purification of quiescent yeast cells

Quiescent yeast were purified using the Percoll (Cytiva) gradient method (Allen et al., 2006; M. M. Spain et al., 2018). Briefly, 12.5 mL of 9:1 Percoll and 1.5 M NaCl were mixed and spun in a gradient tube at 10,000 RPM (13,776 RCF) for 15 minutes at 4 °C in an Aventi J-E centrifuge

(Beckman Coulter). In parallel, yeast cells in 7- or 8-day cultures were spun down and suspended in 1 mL water. After creating the gradient, we carefully layered saturated yeast in water over the gradient tube. Yeast cells from 12.5 or 25 mL cultures were added to each gradient, with larger cultures split over several gradients to prevent the gradient from plugging. In most cases, only one gradient was needed to obtain 100 OD_{660}, with Nab3 depletion requiring two due to the reduced efficiency of Q entry. All strains in this study saturate at approximately 30 OD_{660} per mL. Loaded gradients were spun for 1 hour at 1,200 RPM (410 RCF) in an Aventi J-HC (Beckman Coulter). The lower quiescent fraction (approximately 5 mL) was separated, rinsed twice in sterile water, and then snap-frozen and stored at –80 °C. The non-quiescent fraction was discarded.

3.7 GROWTH OF DIAUXIC SHIFT YEAST

For diauxic shift (DS) experiments, glucose exhaustion was measured using glucose strips (Precision Laboratories). The diauxic shift was noted as the time that glucose dipped below detectable levels, at which time points after the DS were taken precisely. Cells were immediately spun out of the media and snap-frozen. The collection of samples at time points before the DS is particularly challenging, since the time of glucose exhaustion must be estimated prior to taking place. Thus, OD_{660} was monitored in the hours leading up to the DS to estimate the time point of DS–2 hours, which occurs at a reproducible but strain-dependent OD_{660}. YTT5781/5782 reach DS–2 at an OD_{660} per mL of approximately 4, whereas YTT7078/7089 reach DS–2 at an OD_{660} per mL of approximately 5. For each time point, 5 OD_{660} of cells were immediately spun out of the media and snap-frozen.

3.8 G_1 ARREST

G_1 arrest was achieved by adding α factor at a concentration of 5 µg/mL to early log-phase yeast (0.1 OD_{660} per mL). We evaluated the arrest via microscope and, if necessary, a second dose of α factor was added at 90 minutes. *rrp6Δ* cells arrested slowly due to slow cell division. Since α factor arrest lasts only 3 hours, WT and *rrp6Δ* cells were collected just prior to the 3-hour mark. Flow cytometry was used to confirm G_1 arrest (arrest profiles in Figure 3.1).

3.9 QUIESCENCE EXIT KINETICS

Quiescence cells in pure water were added at a concentration of 0.5 OD_{660} per mL to YPD. Exit was performed at room temperature (25 °C) to slow kinetics as previously described (Cucinotta et al., 2021). Samples were collected at 1 hour, 2 hours, and then every 30 minutes after for analysis by flow cytometry.

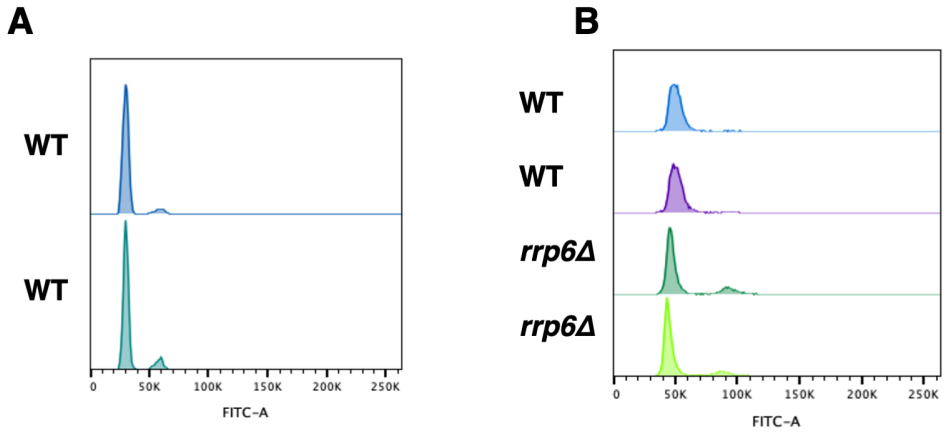

Figure 3.1 Profile of G_1 arrested cells.
(**A**) FACs profile of wildtype G_1 arrested cells used for Figure 2.3 and 2.8.
(**B**) FACs profile of wildtype and *rrp6Δ* G_1 arrested cells used for Figure 3 and 6.

3.10 FLOW CYTOMETRY

Flow cytometry was used to confirm G_1 arrest as well the kinetics of quiescence exit. Cells for flow cytometry were stored in approximately 70% EtOH at 4 °C prior to staining. Cells were treated with RNase A (2 mg/mL) for 4 hours at 37 °C, followed by Proteinase K (2 mg/mL) for 45 minutes at 50 °C. Afterward, the cells were incubated at 4 °C overnight. The cells were then sonicated and resuspended in 50 mM Tris pH 7.5 containing 1/5000 SYTOX Green (Invitrogen) for 1 hour at 4 °C. Flow cytometry was performed using a BD Bioscience FacsCanto II Flow Cytometer in the Fred Hutch Cancer Center Flow Cytometry Core facility. Data was analyzed with FlowJo (version 10; FlowJo, LLC).

3.11 THERMOTOLERANCE ASSAY

Quiescence cells in pure water were diluted to a concentration of 1 OD_{660} per mL. Early log cells (between 0.3–0.55 OD_{660} per mL) were spun down and resuspended in water to a concentration of 1 OD_{660} per mL to serve as a control for poor thermotolerance. Cells were heat-treated in a hot-water bath measuring 51 °C for 15 or 30 minutes as quiescent cells have been shown to be sensitive in this range (Allen et al., 2006; Klosinska et al., 2011). Cells were serially diluted 10-fold 4 times, and then 2 µL of all 5 concentrations were plated on YPD and grown at 25 °C. Plates were photographed using a Biorad Universal Hood II Gel Doc XR System with epi-white light. No image adjustments were performed.

3.12 NAB3 DEPLETION

3-indoleacetic acid (IAA) powder (98% purity, Sigma Aldrich) was added at a concentration of 1 mg/mL to both the tag strain and parental strain at exactly DS+6 hours (approximately 24 hours after inoculation). The addition of IAA later in Q entry results in poor depletion, while earlier

treatment results in inhibited quiescence entry. Depletion was confirmed by western blot analysis.

3.13 WESTERN BLOTTING

We obtained protein extracts via trichloroacetic acid (TCA) precipitation. Cell pellets corresponding to 10 OD_{660} units were bead-beaten in 200 µL of 20% TCA for 10 minutes. The lysates were precipitated on ice, followed by the addition of 400 µL of 5% TCA. We separated the lysate from the beads via the needle poking method and then pelleted the lysate at room temperature. The resulting pellet was washed and resuspended in a solution of 2 parts 0.5 M Tris pH 7.5 and 3 parts sample buffer. The extract was boiled at 95 °C for 5 minutes, then centrifuged at maximum speed for 10 minutes prior to loading an equal volume into a gradient gel (4–20% Mini-PROTEAN® TGX™, Biorad). The gel was transferred to a nitrocellulose membrane (pore size of 0.2 µm) at 100 V for 1 hour at room temperature using a wet transfer method (Bio-Rad Trans-Blot electrophoretic Transfer Cell). The transfer was visualized by Ponceau staining before blocking the membrane with 5% milk in PBS-Tween 20 (PBST; 0.1% Tween 20 in 1× PBS). Subsequently, the membranes were incubated with primary antibodies (1:1000 αHSV Millipore Sigma, 1:5000 αH2B Active Motif) in 5% milk PBST. We diluted secondary antibodies (LI-COR) 1:10,000 in 1:1 PBST and intercept blocking buffer prior to application. Finally, the blots were imaged using the Odyssey CLx system (LI-COR) and processed with ImageJ (Abramoff et al., 2004).

3.14 RNA-SEQ: SAMPLE PREPARATION, LIBRARY GENERATION, AND SEQUENCING

For RNA-seq, 5 OD_{660} of yeast were used. This is more than sufficient, producing ~50 µL with a concentration of 200–800 ng/µL depending on cell state. To provide a consistent spike in across

RNA-seq and 4tU-seq experiments, *K. lactis* cells were grown to mid-log and labeled with 5 mM 4-thiouracil for 6 minutes. These cells were snap frozen and stored at -80 °C. All spike-in cells were grown on a single day and labeled simultaneously to minimize variation between aliquots. 25 µL *K. lactis* cells at a concentration of 20 OD_{660} per mL were added to *S. cerevisiae*. Using the yeast RiboPure™ RNA Purification Kit (Invitrogen), we extracted RNA from this mixture, ethanol-precipitated overnight, washed, and then assessed for integrity using a TapeStation (Agilent). We tested the effectiveness of DNase treatment using PCR without reverse transcriptase. The RNA was prepared for Illumina sequencing using the Tecan Universal Plus™ Total RNA-Seq library preparation kit with NuQuant® and custom AnyDeplete® for *S. cerevisiae* rRNA; to enhance the accuracy of transcript quantification, the protocol incorporated Unique Molecular Identifiers (UMIs). The resulting libraries were paired-end sequenced on either a HiSeq 2500 (Illumina) or NextSeq 2000 (Illumina) in high-output runs with 100 cycles, 50 cycles for each end. The sequencing was performed at the Fred Hutch Cancer Center Genomics Core facility.

3.15 4TU-SEQ: SAMPLE PREPARATION, LIBRARY GENERATION, AND SEQUENCING

4tU-seq was performed as described (Cucinotta et al., 2021). In brief, cells were labeled with 5 mM 4-thiouracil (4tU; added as powder) for 6 minutes before being spun down and snap-frozen. For each sample, one tube of cells was labeled with 4tU, while another control tube was left unlabeled. We used 100 OD_{660} for quiescent yeast and 12.5 OD_{660} for G_1-arrested yeast. RNA was prepared as described in **RNA-seq: Sample preparation, library generation, and sequencing** except 50 µL *K. lactis* cells were added instead of 25 to account for the increased number of cells needed for 4tU-seq. Labeled and unlabeled control RNA was incubated with MTSEA-biotin-XX (Biotium) for 30 minutes. Subsequently, labeled and unlabeled RNA were

extracted, isopropanol-precipitated, and washed. RNA at this stage was referred to as "steady-state" in experiments where 4tU-seq was being performed.

To isolate nascent RNA, we combined RNA with Streptavidin Magnetic Beads (Thermo Fisher), which were blocked with glycogen for 1 hour at room temperature. RNA and beads were incubated at room temperature for 15 minutes, followed by 3 washes to remove unbound RNA. Bound RNA was eluted at 23 °C and concentrated using the miRNeasy Micro Kit (Qiagen). To assess pull-down efficiency, small volumes of labeled and unlabeled RNA eluted from beads were converted to cDNA using a Transcriptor First Strand cDNA Synthesis Kit (Roche), and RT-PCR was performed on labeled and unlabeled samples. For a list of primers, *see 2.3.1 Reagents.*

Both the pulled-down (nascent) and input (steady-state) labeled RNA were prepared for Illumina sequencing using either the Ovation® SoLo® RNA-Seq library preparation kit (for wild-type quiescent and G_1 data in Figures 2.3 and 2.8) or the Tecan Universal Plus™ Total RNA-Seq library preparation kit with NuQuant® (for all other samples); both protocols made use of custom AnyDeplete® for *S. cerevisiae* rRNA, and both incorporated UMIs. The libraries were paired-end sequenced on either a HiSeq 2500 (Illumina) or NextSeq 2000 (Illumina) in high-output runs with 100 cycles, 50 cycles for each end. The sequencing was performed at the Fred Hutch Cancer Center Genomics Core facility.

3.16 RNA-SEQ AND 4TU-SEQ READ QUALITY ASSESSMENT AND PRE-PROCESSING

Prior to alignment, we took the following sequential steps to assess, and process reads from paired-end sequencing of RNA-seq and 4tU-seq sample libraries:

1. We assessed the quality of sequenced paired-end reads (hereafter, "reads") with FastQC (version 0.11.8) (Simon Andrews, 2014) and MultiQC (version 1.14; data not shown) (Ewels et al., 2016).
2. We appended sequenced UMIs to fastq QNAMEs with the program UMI-tools (umi_tools extract; version 1.01) (T. Smith et al., 2017). After alignment (see below), we use this information to distinguish and filter out PCR amplification-based duplicate reads (i.e., "technical duplicates") while retaining duplicate reads that are biological in origin (i.e., "biological duplicates"). We assessed the absolute counts and proportions of technical and biological duplicates with UMI-tools and MultiQC (data not shown).
3. We performed read adapter and quality trimming with the program Atria (version 3.2.1) (Chuan et al., 2021) with default settings except for the switch --no-length-filtration.
4. Step #4 was performed only for those fastq files used to build wild-type quiescent and G_1 nascent transcriptome assemblies (see **Drafting nascent transcriptome assemblies**): To correct random sequencing errors in the reads, the presence of which adversely affect transcriptome assembly, we ran the k-mer-based adjustment method Rcorrector (version 1.0.5) (L. Song & Florea, 2015) with default settings. Then, we filtered adjusted fastq files to exclude read pairs identified as containing irreparable errors (which tend to be associated with low-complexity sequences).

3.17 RNA-SEQ AND 4TU-SEQ READ ALIGNMENT AND POST-PROCESSING

Using the splice-aware aligner STAR (version 2.7.10b) (Dobin et al., 2013), unadjusted and k-mer-adjusted reads were aligned to a concatenated multi-organism reference genome made from the *S. cerevisiae*, *K. lactis*, and 20S RNA narnavirus reference genomes. Using the utility Samtools (versions 1.16.1 or 1.17) (Danecek et al., 2021), non-k-mer-adjusted bam files were

indexed and filtered to retain only primary alignments; k-mer-adjusted bam files were indexed and filtered to retain both primary and secondary alignments. The non-k-mer-adjusted bams were deduplicated using UMI-tools (version 1.01).

3.18 Feature-level quantification of alignments

Using filtered, UMI-deduplicated bams from the alignment of non-k-mer-adjusted fastqs, we created "counts matrices" comprised of the numbers of sample-specific reads aligned to features in Gene Feature Format (gff3) or Gene Transfer Format (gtf) files. To this end, the utility htseq-count from the HTseq software package (version 2.0.2) (Anders et al., 2015; Putri et al., 2022) was used.

3.19 Principal component analysis

Principal component analysis (PCA) was performed with the R package PCAtools (version 2.10) (Kevin Blighe & Aaron Lun, 2022). Prior to performing PCA, counts matrices were filtered to remove rows containing all zeroes; then, matrix columns (samples) were normalized with the transcripts per million (TPM) calculation (Conesa et al., 2016; B. Li et al., 2010) and regularized through a $\log_2$ pseudocount transformation. To run PCA, the PCAtools function pca was called with default settings and parameters. To evaluate proportions of PC variance explained by metadata variables, we used the PCAtools function eigencorplot to calculate coefficients of determination (r^2; data not shown). To identify the top feature-wise positive and negative component loading vectors for PCs of interest, we sorted matrices of component loading vectors based on their sign and magnitude for the relevant PCs; then, we selected the top 750 positive and the top 750 negative loading vectors for features (Figure 2.8B).

3.20 DIFFERENTIAL FEATURE EXPRESSION ANALYSES

The software package DESeq2 (version 1.38.0) (Love et al., 2014) was used to perform differential feature expression analyses. Prior to running DESeq2, we filtered counts matrices to exclude low-count features (rows): For a given feature to be maintained, a minimum of four counts must have been observed in at least $n - 1$ samples (columns), where n is the total number of samples in each matrix; rows not meeting this requirement were discarded. Where appropriate (Figures 2.9, 2.13 and 2.17), spike-in normalizations were applied to *S. cerevisiae* sample counts by supplying *K. lactis* features and counts as "control genes" to the DESeq2 function estimateSizeFactors. When running DESeq2, we constructed Wald tests of significance for observed results against expected values under a null distribution in which the difference between two experimental groups was no larger than an effect size of 0.58 (i.e., a fold change of approximately 1.5). P-values were adjusted for the false discovery rate using the Benjamini-Hochberg method. Using the R package EnhancedVolcano (version 1.16) (Kevin Blighe et al., 2022), we visualized the results of differential feature expression analyses in volcano plots.

3.21 GENE ONTOLOGY ANALYSES

We performed Gene Ontology (Ashburner et al., 2000; Gene Ontology Consortium, 2021) term enrichment analyses using the YeastMine web application (version Jun-20-2023, GO-Release 2023-06-11) (Balakrishnan et al., 2012; Kalderimis et al., 2014; R. N. Smith et al., 2012); default settings were used, and the full gene set for each category was used as the background set. P-values were obtained from hypergeometric distributions and adjusted for the false discovery rate with Benjamini-Hochberg corrections.

3.22 Estimation of steady-state mRNA abundance between G_1 and quiescent yeast cells

We aimed to estimate the steady-state RNA levels across wild-type G_1 and quiescent samples, adapting a method previously developed in the Tsukiyama lab (McKnight et al., 2015). The significantly lower expression in quiescent compared to G_1 requires the use of a larger number of quiescent cells in RNA/4tU-seq library preparation—a discrepancy that leads to a higher quiescent cell-to-spike-in ratio versus the G_1 cell-to-spike-in ratio. To enable inter-sample transcript abundance estimation, this necessitates an adjustment for the increased ratio as described in the following steps:

1. We began with a counts matrix derived from steady-state 4tU-seq data, comprising wild-type G_1 and quiescent alignments to both *S. cerevisiae* and *K. lactis* ORFs (*see* **RNA-seq and 4tU-seq read alignment** and **post-processing and Feature-level quantification of alignments**). We applied a filtering criterion to exclude any ORFs (rows) that had fewer than 10 counts observed across all but one sample (column), ensuring a baseline level of count abundance.
2. To adjust for the effects of gene length and sequencing depth, each sample underwent a TPM normalization. To stabilize the variance and prepare for linear modeling, we log2-regularized the TPM values.
3. For each ORF, we computed the geometric mean of TPM values for both quiescent and G_1 cells by evaluating the mean log2(TPM) values for each cell state. This method ensured a balanced representation of quiescent and G_1 expression levels for each ORF while minimizing the influence of extreme values.

4. To explore the transcriptional relationship between quiescent and G_1 cells, we used the geometric mean values derived from *K. lactis* spike-in controls to fit a linear regression model. In this model, G_1 geometric means were designated as the dependent variable (DV), and quiescent geometric means as the independent variable (IV).
5. We applied the same method of calculating geometric means and fitting a linear regression model to the quiescent and G_1 S. *cerevisiae* data.
6. We adjusted the *K. lactis* joint distribution to align with the line of equation x = y. This alignment was achieved by modifying the dependent variable (DVKL, representing G_1 values). Each DVKL value was first reduced by the parameter β0KL of the original *K. lactis* linear equation and then divided by the parameter β1KL: Adjusted DVKL = (DVKL – β0KL) ÷ β1KL. By refitting the joint distribution to conform to a 1:1 relationship, we approximated a scenario where the amount of *K. lactis* spike-in was uniformly represented across both cell states.
7. We adjusted the *S. cerevisiae* values to align with the recalibrated *K. lactis* values. To refit the *S. cerevisiae* joint distribution, we applied the *K. lactis* parameters, β0KL and β1KL, by adjusting the S. *cerevisiae* dependent-variable (i.e., G_1) values (DVSC): Adjusted DVSC = (DVSC – β0KL) ÷ β1KL.
8. We aimed to address the variations in cell-to-spike-in ratios between G_1 and quiescent cells by estimating a scaling coefficient based on *S. cerevisiae* ODs used in library generation. The OD for quiescent cells was 100, while the OD for G_1 cells was 12.5 (*see* **4tU-seq: Sample preparation, library generation, and sequencing**). To obtain the coefficient, we divided the quiescent value by the G_1 value: scaling coefficient = 100 / 12.5 = 8.

9. To equilibrate the quiescent and G_1 cell-to-spike-in ratios, we reverted the Adjusted DVSC values to a linear scale by squaring them. We then multiplied these values by the scaling coefficient derived in step #8. This resulted in the G_1 ratio being the same as the quiescent ratio.
10. Finally, we calculated the arithmetic means of the adjusted, scaled G_1 TPM values (derived from Steps #7–9) and the quiescent TPM values. This allowed us to estimate the fold-change difference in mean S. cerevisiae transcript abundances: fold change estimate = mean adjusted G_1 values ÷ mean adjusted quiescent values.

3.23 NORMALIZING AND PLOTTING COVERAGE

To normalize and plot coverage for the wild-type G_1 and quiescent nascent and steady-state samples (Figures 2.3 and 2.8), we input non-k-mer-adjusted bam files to the deepTools (Ramírez et al., 2014) utility bamCoverage with the bins per million mapped reads (BPM) normalization method (--normalizeUsing BPM); the bin size was set to 1 base pair (--binSize 1), and we excluded all rRNA and tRNA regions from the calculation (--blackListFileName "Greenlaw-et-al.R64-1-1_blacklist_rRNA-tRNA.gtf"). To normalize and plot coverage for the other samples analyzed in this study (Figures 2.9, 2.13 and 2.17), we calculated library size estimates with the DESeq2 function estimateSizeFactors (Anders & Huber, 2010; Love et al., 2014); the *K. lactis* features within counts matrices (*see* **Feature-level quantification of alignments**) were used as input to estimateSizeFactors. We took the reciprocal of the library size estimates and applied them to samples with deepTools bamCoverage; the bin size was set to 1 base pair. Coverage metaplots were drawn using the deepTools utility plotProfile (Figure 2.13D). The *MEP2* locus was excluded from metaplots due to a sequencing artifact within 500 bp of a stop codon.

3.24 INVESTIGATING RELATIONSHIPS BETWEEN INDEPENDENT AND DEPENDENT VARIABLES

To assess the relationships between independent and dependent variable distributions, we performed linear regression analyses, Pearson correlation calculations, and Mann-Whitney U (MWU) tests (Figures 2.8, 2.9, 2.13 and 2.17). Using the R (version 4.2.2, 2022-10-31) function lm, we formulated the model $DV = \beta_0 + (\beta_1 \times IV) + \varepsilon$, where DV represents the dependent variable; IV represents the independent variable; β_0 and β_1 are the model coefficients representing, respectively, the intercept and slope; and ε denotes the error term. The significance of the regression coefficients was determined using two-tailed Student's t-tests (data not shown). To quantify the proportion of variance in DV explained by IV, we calculated coefficients of determination (r^2). To determine the extent to which DV and IV linearly associated, we calculated Pearson correlation coefficients (r). To assess significant differences in DV and IV distributions, we employed MWU tests; in Figure 2.8C, row 3, we performed MWU tests to assign significance to differences in distributions predicted by linear regressions.

3.25 TWO-STEP CLUSTERING OF GENES REPRESSED BY RRP6 IN QUIESCENCE

Using the R package pheatmap (version 1.0.12) (Raivo Kolde, 2019), we performed two-step clustering of genes repressed by *RRP6* in quiescence as follows: (**1**) We performed k-means clustering of *rrp6*Δ and wild-type control samples at the G_1, DS minus 2 hours (DS–2), DS plus 2 hours (DS+2), DS plus 24 hours (DS+24), DS plus 48 hours (DS+48), and Q states; we set k to 3. (**2**) We assigned each gene (feature) to the cluster with which it showed the highest association. (**3**) For each cluster of samples, we performed hierarchical clustering on the associated genes to identify substructures and patterns within that cluster. To evaluate the sample-specific expression of cluster-associated genes, we plotted distributions of TPM-

normalized, $\log_2$ pseudocount-regularized counts. We assigned statistical significance to experiment-control pairs with Kolmogorov-Smirnov tests; p-values were adjusted with the Benjamini-Hochberg method.

3.26 DRAFTING AND PROCESSING NASCENT TRANSCRIPTOME ASSEMBLIES

To assemble nascent transcriptomes, we ran the program Trinity (version 2.14) (Grabherr et al., 2011; Haas et al., 2013) in genome-guided mode using bams comprised of both primary and secondary alignments (*see* **4tU-seq read alignment and post-processing**); genome-guided mode uses the genome to partition reads associated with primary and secondary alignments into loci-based clusters prior to k-mer-ization and *de novo* graph-based assembly.. Prior to running Trinity, we used Samtools to filter out alignments associated with the *K. lactis* or 20S RNA narnavirus genomes; then, biological replicates were merged with samtools merge. Trinity was called as follows:

```
❯ Trinity \
>     --verbose \
>     --max_memory "${j_mem}" \
>     --CPU "${j_cor}" \
>     --SS_lib_type FR \
>     --genome_guided_bam "${bam}" \
>     --genome_guided_max_intron 1002 \
>     --jaccard_clip \
>     --output "${out}" \
>     --full_cleanup \
```

```
> --min_kmer_cov 4 \
> --min_iso_ratio .05 \
> --min_glue 2 \
> --glue_factor .05 \
> --max_reads_per_graph 2000 \
> --normalize_max_read_cov 200 \
> --group_pairs_distance 700 \
> --min_contig_length 200
```

where variable "${j_mem}" was set to "50G" (i.e., 50 GB max memory allocation), "${j_cor}" was set to 6, "${bam}" was set to a specific sample bam (i.e., that for either G_1 or quiescent nascent transcription), and "${out}" represent an output file directory for the given sample.

Trinity outputs fastas made up of putative transcripts/transcript fragments. Using the aligner GMAP (T. D. Wu & Watanabe, 2005), we aligned Trinity fastas to the sacCer3 R64-1-1 reference genome; GMAP was called with default settings except for argument --format="gff3_gene", which outputs alignments in the gff3 format. The information in these files constituted draft G_1 and quiescent nascent transcriptome assemblies. To increase the levels of certainty in our transcript estimates, we filtered the draft assemblies to retain only those transcript loci at or above the first quartile of raw count depth.

3.27 CONTEXTUALIZING AND CLASSIFYING THE NASCENT TRANSCRIPTOME ASSEMBLIES

To contextualize and classify transcripts in nascent transcriptome assemblies, we created a representation of the *S. cerevisiae* reference genome in which each base was associated with

relevant annotations. Then, transcripts were classified based on their overlaps with specific "feature" and "region" categories, assessing properties such as "mixedness," "repetitiveness," and "completeness" to assign formal classifications to the transcripts. The final classifications included "coding," "TE" (transposable elements), "ambiguous," "coding: multiple," "coding: partial," "non-coding: R64" (associated with known R64 non-coding annotations), and "non-coding: not R64" (not associated with known R64 features). Further classification was done for "non-coding: not R64" transcripts based on their sense and antisense associations with "region" and "feature" categories, respectively, and the novelty of "non-coding: not R64" transcripts was evaluated by assessing overlaps with previously annotated ncRNA features from different studies (*see* **Processing R64-1-1 and previously annotated ncRNA transcriptome assemblies**).

3.28 PROCESSING R64-1-1 AND PREVIOUSLY ANNOTATED NCRNA (PA-NCRNA) TRANSCRIPTOME ASSEMBLIES

To categorize alignments with respect to coding and non-coding features in the *S. cerevisiae* genome, publicly available transcriptome assemblies were obtained and processed. For the assessment of alignments with respect to official Ensembl R64-1-1 feature annotations, the R64-1-1 gff3 file was filtered to retain the labels "gene", "pseudogene", "snRNA", "snoRNA", and "TE" ("transposable element"). To classify alignments with respect to pa-ncRNAs, the following assembly files were obtained, processed, and merged: CUT and SUT features (Xu et al., 2009, p. 200); CUT_4x and CUT_2016 features (Vera & Dowell, 2016); NUT features (Schulz et al., 2013); R64-1-1 ncRNA features (*Saccharomyces Cerevisiae S288C Genome Assembly R64*, n.d.); SRAT features (Venkatesh et al., 2016); XUT features (van Dijk et al., 2011). When necessary, coordinate conversion between genome assemblies was performed using UCSC liftOver (version 377) (Hinrichs et al., 2006).

3.29 BOOTSTRAPPING ENRICHMENT RATIOS

BEDTools (version 2.30.0) (Quinlan & Hall, 2010) shuffle was run on BED files comprised of Nab3-regulated mRNAs 105 times. Then, BED files were converted to fasta files using getfasta (FASTX-Toolkit; version 0.0.14) (G. J. Hannon, 2010). Simple enrichment analysis from MEME Suite (version 5.5.1) (T. L. Bailey et al., 2009) was run on a fasta comprised of Nab3-regulated mRNAs using the 105 shuffled fastas as controls. Meme values were taken from Schulz et al. 2013 (Schulz et al., 2013) and manually converted to meme format using the utility iupac2meme from MEME Suite. Simple enrichment analysis was run as follows: sea --p mRNAs_nab3_rna.fasta --n ${file} --m Nab3_3013.meme --o nab3_${file%.fasta}. Data from each run was collated and visualized.

3.30 GENE OVERLAP ANALYSES

Gene names were extracted from an Excel file provided in the supplement of Bresson et al. 2017 (Bresson et al., 2017). Names were imported into R and matched with official names from SGD (Cherry et al., 2012). To evaluate overlaps, a merge operation was performed between the Bresson et al. genes and those we identified as regulated by Nab3 or Rrp6 in Q. Venn diagrams were constructed to have proportional sizes using the R package venneuler (version 1.1-3) (Lee Wilkinson, 2022) and then imported into Affinity Designer (version 1.10.6).

3.31 FIGURE PREPARATION

Plots were generated with, alone or in combination, base R (version 4.2.2, 2022-10-31), the R software package ggplot2 (version 3.4.2), Prism (version 9.4.1, GraphPad), and various plotting programs employed by the other software packages used in this study. Affinity Designer (version 1.10.6, Affinity) was used for composing figures.

Chapter 4. DISCUSSION

4.1 EXPANDED KNOWLEDGE AND REMAINING QUESTIONS REGARDING THE QUIESCENT TRANSCRIPTOME

Since the Tsukiyama lab began working on quiescence in yeast, RNA sequencing experiments have suggested that non-coding transcription is highly prevalent in the quiescent transcriptome. As part of understanding the role of non-coding transcription (discussed in detail in 4.3), I sought to systematically characterize the nascent quiescent transcriptome, which had not previously been done. By annotating the quiescence transcriptome, we identified 241 unique non-coding transcripts in quiescence (Figure 2.3). This work was an important step in understanding what distinguishes the quiescent transcriptome from that of G_1-arrested cells. This annotation can serve as a resource to future work on how regulation of the genome supports quiescence. Some questions remain which will require further study with expanded approaches.

4.1.1 *Why are snoRNAs and snRNAs so abundant in Q?*

One observation from characterizing the quiescent transcriptome is that small nucleolar RNAs (snoRNAs) and small nuclear RNAs (snRNAs) are a larger fraction of the quiescent transcriptome than in G_1-arrested cells. Together these two RNA types make up an average of 17% of the steady state *S. cerevisiae* reads in quiescence (rRNA and tRNA were excluded for technical reasons) (Figure 2.3). These same RNA types make up only ~4% in G_1. Yeast cells encode 76 snoRNAs (Piekna-Przybylska et al., 2007), and 5 snRNAs (Mitrovich & Guthrie, 2007). These transcripts are of high relative abundance in quiescence, but what biological function that they may serve in this state is unknown.

SnoRNAs are known to function in rRNA processing. The primary described function of snoRNAs is during ribosome biogenesis, however they have also been suggested to function in additional RNA processes such as alternate splicing and regulating mRNA abundance (Bratkovič et al., 2020). snoRNAs come in two major classes depending on their structure and the associated rRNA modification; C/D box snoRNAs direct 2′-O-methylation modifications while H/ACA box snoRNAs are responsible for pseudouridylation (Bratkovič & Rogelj, 2014; Dupuis-Sandoval et al., 2015). These modifications are typically described as constitutive (Ge & Yu, 2013). However, emerging research in cancer (Z. Huang et al., 2022) suggests snoRNAs play a role in cell fate, and that they may be more dynamic regulators than previously imagined.

snRNAs are the RNA component of the spliceosome (Mitrovich & Guthrie, 2007). Most yeast RNAs are not spliced, with only ~280 yeast genes containing introns. Nevertheless, splicing is essential for viability in *Saccharomyces cerevisiae* (Parenteau et al., 2008). A large portion of spliced RNAs are ribosomal proteins (Parenteau et al., 2011), which are reduced in abundance during quiescence entry (Figure 2.20), suggesting reduced splicing in quiescence. Alternative splicing is a well described method of gene regulation in metazoans (Blencowe, 2006; Kelemen et al., 2013; Marasco & Kornblihtt, 2023) and to a lesser extent yeast (Hurtig et al., 2020; Juneau et al., 2009). We did not attempt to annotate alternative splicing in quiescence, as it was not readily apparent by eye. However, given high snRNA expression, further study may reveal splicing a regulator of quiescence in yeast.

Altered snoRNA and snRNA relative abundance in quiescence has not been previously described. The question remains why these small RNAs are prevalent. One possibility is that rRNA processing and splicing require this level in quiescence. However, since transcription (McKnight et al., 2015; Young et al., 2017) and translation (Ashe et al., 2000; L. M. Dickson & Brown, 1998;

Fuge et al., 1994) are globally repressed, the need for these factors at these levels may be during the exit from quiescence rather than during quiescence itself. Another possibility is that these highly structured RNAs support the formation of liquid phase separated bodies which are known to form under stress conditions (Kroschwald et al., 2015; Wallace et al., 2015). Understanding why snoRNAs and snRNAs are high relative abundance in quiescence may reveal novel biology.

4.1.2 *5′ and 3′ ends remain uncharacterized in quiescence*

One observation I made during this work is that transcription initiation and termination in wild-type quiescent cells appears to be occurring at distinct locations at some genes. To perform transcriptome annotation, we used Trinity, a well maintained and highly cited software (Grabherr et al., 2011; Haas et al., 2013). I found that Trinity was most successful at generating reasonable assemblies in the gene dense yeast genome compared to other transcriptome assembly programs I tried such as Cufflinks (Trapnell et al., 2012) and Stringtie (Pertea et al., 2015). However, because Trinity relies on assembling transcripts from read fragments, it selects the longest transcript at a given loci, not necessary the most abundant isoform. As a result, we refrained from further characterizing these changes in transcription start and termination site since we would need to perform robust 3′ and 5′ end sequencing to do so.

Short read 5′ end sequencing relies on recognizing the 5′ end m^7Gppp cap structure present on mRNA (Policastro & Zentner, 2021). These approaches can require high input or have low strand-specificity (Adiconis et al., 2018), making them non-ideal for studying quiescent cells. Future approaches to 5′ end sequencing would benefit from thinking beyond cap recognition. Uncapped mRNAs were once thought to be rapidly degraded by cytoplasmic exonuclease Xrn1; however the discovery of cytoplasmic recapping enzymes changed that paradigm (Trotman & Schoenberg, 2019). Additionally, a non-canonical RNA cap made with NAD has been found in

prokaryotes and eukaryotes, including yeast, though the function of these caps is not well characterized (Julius & Yuzenkova, 2019; Kiledjian, 2018). In exponentially growing yeast, these NAD caps are actively removed from most RNAs and then to be restricted to 3′ truncated RNAs (Y. Zhang et al., 2020). Altogether, evidence is building that the 5′ cap is not as ubiquitous as once believed and may not be restricted to polymerase start sites.

While 5′ end mapping is equated with mapping transcription initiation sites, this practice ignores these underlying RNA dynamic processes which potentially obscure the true initiation site. A high-resolution 5′ end sequencing technique which does not rely on the canonical cap would benefit researchers studying multiple areas of gene regulation. This might also help in the interpretation of results obtained using these methods. In yeast, alternative start sites have been observed in stress conditions (Lu & Lin, 2019) and meiosis (Chia et al., 2021) but not across nutrient conditions when growth rate was held constant (Börlin et al., 2018). 5′ end mapping in quiescence would be of interest, but because the extent and efficiency of capping in quiescence has not been studied, these results would be hard to interpret. Cap recognition factor eIF4E was found to be dispensable for starvation survival while another translation initiation factor, eIF4A, was not (Paz & Choder, 2001). Additionally, internal ribosome entry sites have been shown to be crucial for translation during nitrogen starvation (Gilbert et al., 2007). These results suggest cap recognition is not necessary for the low levels of translation occurring in nutrient poor environments (Ashe et al., 2000; L. M. Dickson & Brown, 1998; Fuge et al., 1994). It remains to be determined if the canonical cap structure is lower abundance in these conditions.

On the other hand, commonly used 3′ end sequencing methods rely on the assumptions that 3′ ends of mRNA transcripts are polyadenylated (W. Chen et al., 2017). Polyadenylation length has been shown to be altered by media and temperature (Tudek et al., 2021) but has not

been characterized in quiescent cells. My work suggests the possibility that mRNA polyadenylation levels may be altered in quiescence. A major finding of this work is that NNS regulates many mRNAs in quiescence (Figure 2.13). Such NNS-regulated transcripts would likely be polyadenylated by the polyadenylation complex known as TRAMP (Arigo, Eyler, et al., 2006; LaCava et al., 2005; Wyers et al., 2005). TRAMP has relatively low processivity and produces shorter poly(A) tails than the canonical polyadenylation and cleavage pathway (Jia et al., 2011, 2012). Our work found mRNA abundance decreased by 14-fold in quiescence compared to G_1 arrest, while work in McKnight et al. 2015 found a 30-fold decrease between quiescence and logarithmic growth (McKnight et al., 2015). One explanation for these different numbers is that McKnight et al. used poly(A) selection while I used rRNA depletion; if mRNAs have different length or extent of poly (A) tailing in quiescence these methodological differences would alter the results. Whether mRNAs are always polyadenylated has not been the subject of much study since this stretch of A's is thought to be crucial for mRNA stability (C.-Y. A. Chen & Shyu, 2011; J. Liu et al., 2022). However, several studies in human cell lines found a greater extent of non-polyadenylated mRNA than would be expected (Cheng et al., 2005; Yang et al., 2011), and in one case those mRNAs were enriched for transcription factors and cell cycle genes (Yang et al., 2011). To my knowledge, no similar work has been performed in yeast or across cell states. Therefore, the consensus that most mRNAs are polyadenylated may not hold in quiescence.

Work around the diauxic shift has shown that transcripts termination occurs closer to the stop codon than in cycling cells (Yague-Sanz et al., 2020). Mechanistically, evidence suggest that transcription termination is highly dependent upon the kinetics of transcription (Geisberg et al., 2020; Hazelbaker et al., 2013; Turner et al., 2021), and that in low nutrient environments Pol II speed might function to sense nutritional status of the cell (Yague-Sanz et al., 2020). These works

suggest the faster the speed of polymerase, the longer it can transcribe before termination occurs. Interestingly in quiescence, I observed that by eye some transcripts have extended, rather than truncated 3′ ends. Since chromatin is globally compacted (McKnight et al., 2015; Swygert et al., 2019, 2021; Young et al., 2017), it is hard to believe that polymerase moves more quickly under these conditions. Instead, termination factors may be more limited, allowing polymerase to move further before the nascent transcript is recognized. Alternatively, the compacted chromatin environment may influence transcription termination, as nucleosome placement has been shown to rescue transcription termination defects in cycling cells (Hildreth et al., 2020).

Characterization of the 3′ and 5′ ends may reveal interesting biology about the regulation of cellular quiescence. Both transcription and RNA metabolism are distinct in quiescence as described in this work and others (L. Li et al., 2009; McKnight et al., 2015). Current short read sequencing approaches to capture 3′ or 5′ ends have drawbacks and bias in answering how differently RNA related processes may occur in quiescence. Direct long read sequencing RNA, although currently error-prone, has already been leveraged to analyze poly(A) tail length (Jain et al., 2022; Tudek et al., 2021). Further technical advances in long read technology with likely play a key role in understanding 3′ and 5′ end modifications across biological systems in the coming years without the biases introduced by currently available short read technologies.

4.2 NNS-NUCLEAR EXOSOME – TRANSCRIPTION TERMINATION AND RNA DECAY

4.2.1 *How is NNS/Rrp6 retargeted in quiescence?*

A major conclusion of my thesis work is that NNS and the nuclear exosome regulate mRNA abundance in quiescence. During this work, I was unable to find a reason why some mRNAs had increased transcription in the absence of Nab3 in quiescence while others did not. The strongest trend was that these mRNAs tend to be lowly expressed (Figure 2.17). This low

level of transcription may result in a chromatin structure more like that at non-coding loci in quiescence, suggesting this might serve to regulate NNS targeting. However, using Deseq2, we did not find a strong set of genes which we could say with statistical confidence were not affected by Nab3. As a result, we didn't have a set of control genes to compare how chromatin might influence NNS specificity. Future work on this question would be of interest, as histone methylation has been implicated in regulating NNS activity (K. Y. Lee et al., 2018; Terzi et al., 2011) and histone methylation is altered in quiescence (Mews et al., 2014; Young et al., 2017).

Using an RNA IP method which captures RNA/protein interactions between Nab3 and its target RNAs might have a lower background noise and reduce the number of any indirectly affected transcripts in the data set. Additionally, many RNA-IP techniques are better able to identify RNA sequence motifs. One possibility is that NNS has an expanded or altered set of RNA sequence motifs in quiescence. However, Nrd1 has been suggested to be only partially sequence specific (Bacikova et al., 2014) and NNS and polyadenylation and cleavage have overlapping recognition motifs (Porrua et al., 2012) so such motifs might not exist or be highly degenerate. Alternatively, another non-sequence feature of these RNA targets may be more relevant. RNA secondary structure and RNA modifications have been shown to influence RNA/protein interactions (C. J. T. Lewis et al., 2017) and may play a role in determining specificity in quiescence.

Another possibility is NNS altered in some way during quiescence entry to affect its specificity. All three subunits of the NNS complex are methylated in logarithmic growth, and further study of one of the methylated residues on Nab3 showed this modification is crucial for Nab3's RNA binding affinity (K. Y. Lee et al., 2020). Histone post-translational modifications have been shown to be crucial for quiescence (McKnight et al., 2015; Swygert et al., 2019;

Young et al., 2017), and proteins are often post-translationally modified to regulate cell fate (Tarazona & Pourquié, 2020). One or more NNS subunits may be post-translationally modified to shift its target specificity in quiescence.

It is also possible that specificity is determined more by RNA polymerase itself than by any modification in NNS or the composition of the RNA target. Transcription speed has been demonstrated to be a key determinant of termination site selection (Geisberg et al., 2020; Turner et al., 2021), and what speed polymerase achieves in quiescence and with what consistency is unknown. Dense chromatin structure at repressed loci may function not through any specific modification, but instead slow RNA polymerase down, giving time for NNS to recognize the nascent transcript. Using a fast elongation polymerase allele, NNS transcription termination was shown to be have increased readthrough transcription when polymerase speed was increased (Hazelbaker et al., 2013).

Alternatively, modifications of the c-terminal domain (CTD) of RNA polymerase II in quiescence may explain altered NNS targeting. Nrd1 is known to interact with the phosphorylated Ser5 (Kubicek et al., 2012; Mayer et al., 2012; Vasiljeva, Kim, Mutschler, et al., 2008), which peaks early in transcription. By the time polymerase reaches the 3′ end of the gene, Ser5 phosphorylation is removed and Ser2 is instead phosphorylated. (Dias et al., 2015; Mayer et al., 2012; N. Singh et al., 2022; Tietjen et al., 2010; Zaborowska et al., 2016) This interaction with Ser5 is suggested as a reason NNS preferentially interacts with short transcripts (Gudipati et al., 2008). By western blot, Ser2 phosphorylation is not observable in quiescence cells while Ser5 phosphorylation is still detectable (Cucinotta et al., 2021). It is possible that Ser5 phosphorylation is differently distributed or more long lived on the polymerase CTD in quiescence than in other cell states. Understanding which of these potential mechanisms of NNS

retargeting is relevant in quiescence would improve our understanding not just of this complex and cell state, but also of the general principles of regulating transcription termination.

4.2.2 *Quiescence entry vs. rapid nutrient shift*

We found that the mRNAs regulated by Nab3 in quiescence were distinct from those identified on rapid shift from glucose to ethanol (Bresson et al., 2017) (Figure 2.19). One possibility is that technical differences altered the RNAs identified; Bresson et al. used the RNA IP technique CRAC while we evaluated changes in nascent transcripts. This raises the question of whether NNS may have multiple roles in regulating responses to nutritional changes. Nab3 has been shown to regulate nitrogen metabolism genes (Merran & Corden, 2017), further supporting this possibility. Since Nab3 was depleted six hours after the diauxic shift, it is possible that depletion earlier in quiescence entry would result in more overlap between our two studies.

Supporting this, Rrp6 acts in at least two distinct phases, one around the diauxic shift and one later in quiescence entry (Figure 2.20). Interestingly, genes effected by *RRP6* deletion around the diauxic shift are enriched for ribosome proteins. A large portion of spliced RNAs are ribosomal proteins (Parenteau et al., 2011), and Rrp6 has been shown to function in quality control of spliced mRNAs (P. Singh et al., 2021; Steinmetz & Brow, 1998). Around the diauxic shift, splicing efficiency may be decreased to promote degradation of these RNAs. If NNS behaves similarly, this first retargeting event would be missed because I depleted Nab3 after the diauxic shift.

Using time points through quiescence entry allowed me to identify three distinct gene clusters, with distinct timing and gene ontology terms. This experiment was logistically challenging to perform, and it is clear why investigators prefer rapid nutrient shift experiments

for their relative ease. However, fluctuations in nutrient availability in nature often occur over much longer time spans (Nguyen et al., 2021). Yeast enter quiescence by sensing changes in nutrient availability, thus preparing for starvation, rather than waiting for nutrients to be exhausted (Lillie & Pringle, 1980; Miles et al., 2013). As a result, rapid nutrient downshift does not confer longevity (L. Li et al., 2009). Though onerous, the identification of relevant time points during physiologically relevant changes in nutrient availability are key to building an understanding of how gene expression is coordinately regulated to change cell state.

4.3 CHALLENGES TO UNDERSTANDING NON-CODING TRANSCRIPTION

Since the discovery of cryptic pervasive transcription, there has been a question of what functions, if any, it possesses (Dinger et al., 2009; Villa & Porrua, 2022). One of my goals at the beginning of my time in the Tsukiyama lab was to understand what functions abundant non-coding transcription in quiescence might play (Figure 2.3). My thesis work found antisense transcription to be weakly repressive genome-wide, but only found 20 induced antisense transcripts with their associate mRNAs reduced by 1.5-fold or more on Nab3 depletion. Since over 4000 antisense transcripts were induced, less than 0.5% of antisense transcripts have evidence for strong repressive function at their given loci in quiescence. This is in sharp contrast to two studies performed in log-phase growth. The first study found 114 antisense transcripts associated with repressed mRNAs, and 828 at loci that were not repressive (Schulz et al., 2013). In this case, approximately 12% of antisense transcripts show evidence for strong repressive function by their criteria. A second study found 217 antisense transcripts with “sense repression” and 469 antisense transcripts at non-responsive genes (Gill et al., 2020). This would suggest ~31% of antisense transcripts are potentially repressive in log.

One explanation for this discrepancy is that antisense transcripts behave differently in quiescence than in log. Chromatin structure is globally repressive in quiescence (McKnight et al., 2015; Swygert et al., 2019; Young et al., 2017), and antisense transcripts have been suggested to function via the formation of repressive chromatin structures (Gill et al., 2020; Houseley et al., 2008). If the chromatin is already in a strongly repressive state, the addition of antisense transcription may cause only minor changes or none. However, given several meaningful technical differences between my thesis work and the work done by others, it is possible that these differences are not due to cell state.

4.3.1 *Potential confounding factors in NNS depletion work*

Both Gill et al. 2020 and Schulz et al. 2013 used Nrd1, rather than Nab3 as the NNS protein they manipulated. I attempted to deplete Nrd1 using the auxin inducible degron system but found that protein levels did not dramatically change in quiescence (data not shown). This is likely at least in part due to Nrd1's ability to regulate its own RNA levels (Arigo, Carroll, et al., 2006). However, because Nrd1 and Nab3 form a heterodimer (Chaves-Arquero et al., 2022), depletion of one is likely to have an effect on the other.

Additional technical differences include the depletion system, and the strain backgrounds used. Gill et al. and Schulz et al. used anchor away, which relies on rapamycin to remove the tagged factor from the nucleus. To use this system, *TOR1* is mutated to *tor1-1* and *FPR1* is deleted to make cells insensitive to rapamycin. Additionally, the human gene FKBP12 is fused to a yeast gene to serve as the "anchor". The protein of interest is then tagged with the FKBP12-rapamycin-binding domain of human mTOR. Upon addition of rapamycin, the tagged protein is exported from the nucleus via the rapamycin dependent interaction between target and anchor proteins (Haruki et al., 2008). This system is incompatible with cellular quiescence, as TOR is a crucial

signaling pathway to responding to nutrient limitation (Breeden & Tsukiyama, 2022; Saxton & Sabatini, 2017). Instead, we used an auxin inducible degron system, where the protein of interest is tagged, and the *Oryza sativa* (rice) protein TIR1 (OsTIR) is introduced into the background. Upon addition of auxin, the tagged protein interacts with the E3 ubiquitin ligase complex made up by OsTIR and endogenous yeast protein Skp1, and is subsequently degraded by the proteosome (Nishimura et al., 2009; Nishimura & Kanemaki, 2014). Both these depletion systems have major drawbacks. Anchor away relies on mutating an essential signaling pathway. Alternatively, TOR is a target of IAA (Nicastro et al., 2021) and we find that yeast produce more quiescent cells in the presence of auxin (Figure 2.18). It is not outside of the realm of possibility that one or both of these systems meaningfully changes the "wild type" response to depleting a protein and obscures its typical function. We were pleased to see *rrp6Δ* and Nab3-AID depletion systems affected similar transcripts in quiescence (Figure 2.13), suggesting that at least in this case that the depletion behaves similarly to a related constitutive null within the same established pathway. As costs of sequencing continue to decrease and further depletion systems are developed, using multiple parallel systems of depletion to interrogate protein function in gene expression will become increasingly feasible, thus reducing this as source of variability in the future.

Even without these sources of variability, one major difference remains: normalization. For this work we relied on spike-in normalization to compares steady-state and nascent RNA levels between cell states, and to compare between mutant and wild-type. How normalization should be performed at the bench or at the computer is not standardized in the field. This is a major concern, with field-wide implications. Both Gill et al. 2020 and Schulz et al. 2013 performed RNAseq or 4tUseq without any spike-in normalization. This is a major short-coming of both papers.

Using a spike-in correctly makes it possible to understand if the total amount of RNA or transcription is altered between two conditions. In the absence of a spike-in, the assumption is that total levels are unaltered. In many cases, especially when depleting proteins with strongly activating or repressive effects, this assumption is inappropriate. In the absence of a spike-in, the "highest hits" will remain the same, however the distribution will be shifted. In the case of antisense transcription this is especially crucial.

4.3.2 *Normalization in the analysis of antisense transcripts*

To demonstrate the change a spike-in can make when analyzing antisense transcripts, I have reanalyzed my Nab3-AID depletion nascent transcription data without considering spike-in. When spike-in is considered, 1417 mRNAs and 4011 antisense transcripts are increased by greater than 1.5 fold with a q value <.05 (Figure 4.1A). As a default, Deseq2 provides a read depth-based normalization, and assumes that total transcripts are the same between states. With this read-depth normalization, only 278 mRNAs and 1968 antisense transcripts are increased by greater than 1.5 fold with a q value <.05 (Figure 4.1B). In addition to the dramatic decrease in over-expressed mRNAs with read depth normalization, 674 mRNAs have decreased expression by 1.5 fold or more with a q value <.05, compared to only 27 when spike-in normalization is used. Comparing antisense with significantly increased expression to mRNAs with significantly decreased expression is where the potential for repressive antisense transcripts exists. When spike-in normalization is used, 20 out of 4011 antisense transcripts are predicted to be repressive, compared to 354 out of 1968 when only read depth normalization is used (Figure 4.1C). Simply by shifting the distribution, the percent of predicted repressive antisense transcripts goes from .5% to 18%. This single change brings our result much closer to Gill et al. 2020 and Schulz et al. 2013.

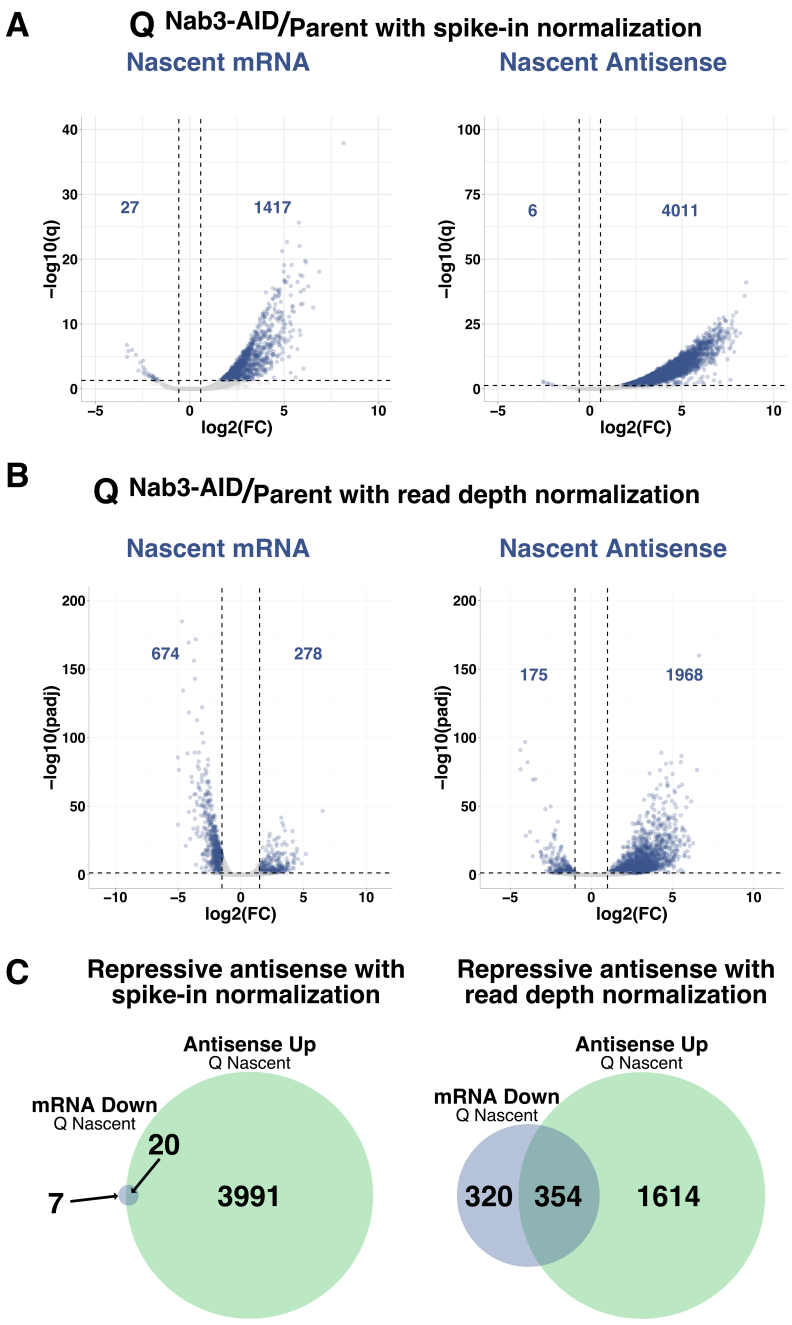

Figure 4.1 Analysis of antisense transcript repressive activity with spike-in versus read depth normalization.

(**A**) Volcano plots showing *NAB3*-dependent changes in transcript levels (*NAB3-AID*/parent). Analyses were performed using DESeq2 (Love et al., 2014), and panels show the magnitudes of *NAB3-AID/*parent $\log_2$ fold change (x-axis) versus significance ($-\log_{10}$ q value, y-axis) for nascent mRNA (left) and antisense transcripts (right) in quiescence. Significant differences were defined as $q < 0.05$ and absolute log2 fold change > 0.58. q values were obtained from Wald

tests with Benjamini-Hochberg corrections. Spike-in *K. lactis* reads were used for normalization with *K. lactis* genes set as control genes in DESeq2.
(**B**) Volcano plots showing *NAB3*-dependent changes in transcript levels (*NAB3-AID*/parent). Analyses were performed using DESeq2 (Love et al., 2014) , and panels show the magnitudes of *NAB3-AID/*parent $\log_2$ fold change (x-axis) versus significance ($-\log_{10}$ q value, y-axis) for nascent (left) and steady-state (right) pa-ncRNA and mRNA in quiescence. Significant differences were defined as $q < 0.05$ and absolute log2 fold change > 0.58. q values were obtained from Wald tests with Benjamini-Hochberg corrections. Deseq2 estimated size factors based on one matrix of sense and antisense counts.
(**C**) Venn diagrams of mRNAs significantly down on Nab3 depletion (green) and antisense significantly up on Nab3 depletion (blue). The intersection of these represent loci were antisense is up and mRNA is down. On the left, spike-in calculated gene numbers are used (Figure 4.1A) and on the right read depth calculated gene numbers are used (Figure 4.1B).

Based on this analysis, meaningfully comparing the results here to those preformed without spike-in normalization is not possible. The issue of normalization is not limited to studying non-coding transcripts and is a matter of field-wide concern for scientists studying gene expression (K. Chen et al., 2016; Evans et al., 2018). Even when spike-ins are used they may be used inappropriately either at the bench or in subsequent computational analyses. Authors often do not report the details of how spike-in normalization was performed, making it harder to review if the spike-in was handled correctly. In some cases, spike-ins do not behave linearly, distorting the distribution (B. M. Dickson et al., 2020; Locati et al., 2015). This problem is especially concerning in cases where incorrect normalization leads to incorrect biological conclusions about the processes being studied.

4.3.3 *Why is non-coding RNA so prevalent in quiescence?*

This work found very few non-coding transcripts with evidence of the canonical repressive effect of antisense transcripts. It is possible that they possess this activity, but our assay was insufficient to detect it. This might be the case if Nab3 is required for the normal function of

antisense transcripts, or if the wild-type expression level provides a maximum repressive effect that over-expression of these transcripts does not alter.

It is also possible that non-coding transcripts provide other, yet undescribed, benefits to the cell. In quiescence, there may be benefits to keeping transcription above a certain threshold without transcribing additional mRNA. Hyper-transcription upon quiescence exit (Cucinotta et al., 2021) may be more efficient if a certain amount of transcription is maintained during quiescence. Non-coding transcription during quiescence may help the cell recognize DNA damage through transcription guided repair (Kamarthapu & Nudler, 2015). Another possibility is that these non-coding RNAs encode functional, translated short-ORFs (Orr et al., 2020; J. E. Smith et al., 2014; Yagoub et al., 2015) or have functions as an RNA product (Kyriakou et al., 2016). Finally, the possibility remains that these transcription units and their associated transcripts are inert and functionless, or potentially even harmful to overall cellular fitness.

Further study and new approaches are required to answer these questions. A recent paper by Hegazy et al., suggests that genetic systems bias our understanding of antisense transcription. By deleting the gene encoding RNA helicase *DBP2*, they found that change in antisense and sense transcription was positively correlated between wild-type and *dbp2Δ* (Hegazy et al., 2023). This is a very different relationship than I observed when depleting Nab3 or when Nrd1 was depleted by others (Gill et al., 2020; Schulz et al., 2013), demonstrating that which genetic system is used directly influences results. Single locus experiments have been instrumental in building our understanding of the mechanisms and functions of antisense transcripts (Hongay et al., 2006; Lenstra et al., 2015; Nevers et al., 2018). These experiments are time-consuming, technically challenging, and hard to control for off target effects that occur due to editing at the locus. They are also prone to similar normalization issues as global genomic experiments, as commonly used

reference genes such as *ACT1* do not always behave as expected (Teste et al., 2009). Editing at the locus has the potential to interfere with gene looping, as well as the 3´UTR of the mRNA (Hegazy et al., 2023). CRISPR approaches have been leveraged to avoid editing the locus of interest (Lenstra et al., 2015; Novačić et al., 2022), however, strand-specificity remains imperfect (Howe et al., 2017). Finally, a wealth of negative data may remain unpublished. Since papers which conclusively find an effect or mechanism are much more likely to be published (Hopewell et al., 2009; Møller & Jennions, 2001), the scientific literature may be biased towards results suggesting that antisense transcripts have repressive functions, regardless of if that is usually the case.

4.4 CONCLUSIONS

In conclusion, my thesis work characterized the quiescent transcriptome in detail, and demonstrated extensive post-transcriptional regulation on both coding and non-coding transcripts in this cell state. This work also annotated several hundred novel non-coding transcripts in quiescence, enabling future further study of their function. Finally, I discovered a novel role for the nuclear exosome-NNS pathway in the regulation of mRNA in quiescence and quiescence entry. Together, these finding expand our knowledge of gene regulation in quiescence and presents many future avenues for investigation.

REFERENCES

Abramoff, M. D., Magalhães, P. J., & Ram, S. J. (2004). Image processing with ImageJ. *Biophotonics International*, *11*(7), 36–42.

Adiconis, X., Haber, A. L., Simmons, S. K., Levy Moonshine, A., Ji, Z., Busby, M. A., Shi, X., Jacques, J., Lancaster, M. A., Pan, J. Q., Regev, A., & Levin, J. Z. (2018). Comprehensive comparative analysis of 5′-end RNA-sequencing methods. *Nature Methods*, *15*(7), Article 7. https://doi.org/10.1038/s41592-018-0014-2

Ahn, S. H., Kim, M., & Buratowski, S. (2004). Phosphorylation of serine 2 within the RNA polymerase II C-terminal domain couples transcription and 3' end processing. *Molecular Cell*, *13*(1), 67–76. https://doi.org/10.1016/s1097-2765(03)00492-1

Akay, A., Jordan, D., Navarro, I. C., Wrzesinski, T., Ponting, C. P., Miska, E. A., & Haerty, W. (2019). Identification of functional long non-coding RNAs in C. elegans. *BMC Biology*, *17*(1), 14. https://doi.org/10.1186/s12915-019-0635-7

Akiyama, T., Suzuki, T., & Yamamoto, T. (2021). RNA decay machinery safeguards immune cell development and immunological responses. *Trends in Immunology*, *42*(5), 447–460. https://doi.org/10.1016/j.it.2021.03.008

Akiyama, T., & Yamamoto, T. (2021). Regulation of Early Lymphocyte Development via mRNA Decay Catalyzed by the CCR4-NOT Complex. *Frontiers in Immunology*, *12*. https://www.frontiersin.org/articles/10.3389/fimmu.2021.715675

Alcid, E. A., & Tsukiyama, T. (2016). Expansion of antisense lncRNA transcriptomes in budding yeast species since the loss of RNAi. *Nature Structural & Molecular Biology*, *23*(5), 450–455. https://doi.org/10.1038/nsmb.3192

Alexander, R. P., Fang, G., Rozowsky, J., Snyder, M., & Gerstein, M. B. (2010). Annotating non-coding regions of the genome. *Nature Reviews Genetics*, *11*(8), Article 8. https://doi.org/10.1038/nrg2814

Allen, C., Büttner, S., Aragon, A. D., Thomas, J. A., Meirelles, O., Jaetao, J. E., Benn, D., Ruby, S. W., Veenhuis, M., Madeo, F., & Werner-Washburne, M. (2006). Isolation of quiescent and nonquiescent cells from yeast stationary-phase cultures. *The Journal of Cell Biology*, *174*(1), 89–100. https://doi.org/10.1083/jcb.200604072

Allmang, C., Mitchell, P., Petfalski, E., & Tollervey, D. (2000). Degradation of ribosomal RNA precursors by the exosome. *Nucleic Acids Research*, *28*(8), 1684–1691. https://doi.org/10.1093/nar/28.8.1684

Allmang, C., Petfalski, E., Podtelejnikov, A., Mann, M., Tollervey, D., & Mitchell, P. (1999). The yeast exosome and human PM–Scl are related complexes of 3′ → 5′ exonucleases. *Genes & Development*, *13*(16), 2148–2158.

Anders, S., & Huber, W. (2010). Differential expression analysis for sequence count data. *Genome Biology*, *11*(10), R106. https://doi.org/10.1186/gb-2010-11-10-r106

Anders, S., Pyl, P. T., & Huber, W. (2015). HTSeq—A Python framework to work with high-throughput sequencing data. *Bioinformatics (Oxford, England)*, *31*(2), 166–169. https://doi.org/10.1093/bioinformatics/btu638

Aragon, A. D., Quiñones, G. A., Thomas, E. V., Roy, S., & Werner-Washburne, M. (2006). Release of extraction-resistant mRNA in stationary phase Saccharomyces cerevisiae produces a massive increase in transcript abundance in response to stress. *Genome Biology*, *7*(2), R9. https://doi.org/10.1186/gb-2006-7-2-r9

Aragon, A. D., Rodriguez, A. L., Meirelles, O., Roy, S., Davidson, G. S., Tapia, P. H., Allen, C., Joe, R., Benn, D., & Werner-Washburne, M. (2008). Characterization of Differentiated Quiescent and Nonquiescent Cells in Yeast Stationary-Phase Cultures. *Molecular Biology of the Cell*, *19*(3), 1271–1280. https://doi.org/10.1091/mbc.e07-07-0666

Arigo, J. T., Carroll, K. L., Ames, J. M., & Corden, J. L. (2006). Regulation of Yeast NRD1 Expression by Premature Transcription Termination. *Molecular Cell*, *21*(5), 641–651. https://doi.org/10.1016/j.molcel.2006.02.005

Arigo, J. T., Eyler, D. E., Carroll, K. L., & Corden, J. L. (2006). Termination of Cryptic Unstable Transcripts Is Directed by Yeast RNA-Binding Proteins Nrd1 and Nab3. *Molecular Cell*, *23*(6), 841–851. https://doi.org/10.1016/j.molcel.2006.07.024

Arndt, K. M., & Reines, D. (2015). Termination of Transcription of Short Noncoding RNAs by RNA Polymerase II. *Annual Review of Biochemistry*, *84*, 381–404. https://doi.org/10.1146/annurev-biochem-060614-034457

Ashburner, M., Ball, C. A., Blake, J. A., Botstein, D., Butler, H., Cherry, J. M., Davis, A. P., Dolinski, K., Dwight, S. S., Eppig, J. T., Harris, M. A., Hill, D. P., Issel-Tarver, L., Kasarskis, A., Lewis, S., Matese, J. C., Richardson, J. E., Ringwald, M., Rubin, G. M., & Sherlock, G. (2000). Gene Ontology: Tool for the unification of biology. *Nature Genetics*, *25*(1), Article 1. https://doi.org/10.1038/75556

Ashe, M. P., De Long, S. K., & Sachs, A. B. (2000). Glucose Depletion Rapidly Inhibits Translation Initiation in Yeast. *Molecular Biology of the Cell*, *11*(3), 833–848.

Bacikova, V., Pasulka, J., Kubicek, K., & Stefl, R. (2014). Structure and semi-sequence-specific RNA binding of Nrd1. *Nucleic Acids Research*, *42*(12), 8024–8038. https://doi.org/10.1093/nar/gku446

Bailey, T. B., Whitty, P. A., Selker, E. U., McKnight, J. N., & McKnight, L. E. (2022). Tup1 is critical for transcriptional repression in Quiescence in S. cerevisiae. *PLOS Genetics*, *18*(12), e1010559. https://doi.org/10.1371/journal.pgen.1010559

Bailey, T. L., Boden, M., Buske, F. A., Frith, M., Grant, C. E., Clementi, L., Ren, J., Li, W. W., & Noble, W. S. (2009). MEME SUITE: Tools for motif discovery and searching. *Nucleic Acids Research*, *37*(Web Server issue), W202-208. https://doi.org/10.1093/nar/gkp335

Balakrishnan, R., Park, J., Karra, K., Hitz, B. C., Binkley, G., Hong, E. L., Sullivan, J., Micklem, G., & Michael Cherry, J. (2012). YeastMine—An integrated data warehouse for Saccharomyces cerevisiae data as a multipurpose tool-kit. *Database*, *2012*, bar062. https://doi.org/10.1093/database/bar062

Barrass, J. D., Reid, J. E. A., Huang, Y., Hector, R. D., Sanguinetti, G., Beggs, J. D., & Granneman, S. (2015). Transcriptome-wide RNA processing kinetics revealed using extremely short 4tU labeling. *Genome Biology*, *16*(1), 282. https://doi.org/10.1186/s13059-015-0848-1

Barski, A., Cuddapah, S., Cui, K., Roh, T.-Y., Schones, D. E., Wang, Z., Wei, G., Chepelev, I., & Zhao, K. (2007). High-Resolution Profiling of Histone Methylations in the Human Genome. *Cell*, *129*(4), 823–837. https://doi.org/10.1016/j.cell.2007.05.009

Beylerli, O., Gareev, I., Sufianov, A., Ilyasova, T., & Guang, Y. (2022). Long noncoding RNAs as promising biomarkers in cancer. *Non-Coding RNA Research*, *7*(2), 66–70. https://doi.org/10.1016/j.ncrna.2022.02.004

Blencowe, B. J. (2006). Alternative Splicing: New Insights from Global Analyses. *Cell*, *126*(1), 37–47. https://doi.org/10.1016/j.cell.2006.06.023

Boer, V. M., Amini, S., & Botstein, D. (2008). Influence of genotype and nutrition on survival and metabolism of starving yeast. *Proceedings of the National Academy of Sciences*, *105*(19), 6930–6935. https://doi.org/10.1073/pnas.0802601105

Boer, V. M., Crutchfield, C. A., Bradley, P. H., Botstein, D., & Rabinowitz, J. D. (2010). Growth-limiting Intracellular Metabolites in Yeast Growing under Diverse Nutrient Limitations. *Molecular Biology of the Cell*, *21*(1), 198–211. https://doi.org/10.1091/mbc.e09-07-0597

Bojsen, R., Regenberg, B., & Folkesson, A. (2014). Saccharomyces cerevisiae biofilm tolerance towards systemic antifungals depends on growth phase. *BMC Microbiology*, *14*(1), 305. https://doi.org/10.1186/s12866-014-0305-4

Börlin, C. S., Cvetesic, N., Holland, P., Bergenholm, D., Siewers, V., Lenhard, B., & Nielsen, J. (2018). Saccharomyces cerevisiae displays a stable transcription start site landscape in multiple conditions. *FEMS Yeast Research*, *19*(2), foy128. https://doi.org/10.1093/femsyr/foy128

Bratkovič, T., Božič, J., & Rogelj, B. (2020). Functional diversity of small nucleolar RNAs. *Nucleic Acids Research*, *48*(4), 1627–1651. https://doi.org/10.1093/nar/gkz1140

Bratkovič, T., & Rogelj, B. (2014). The many faces of small nucleolar RNAs. *Biochimica et Biophysica Acta (BBA) - Gene Regulatory Mechanisms*, *1839*(6), 438–443. https://doi.org/10.1016/j.bbagrm.2014.04.009

Breeden, L. L., & Tsukiyama, T. (2022). Quiescence in Saccharomyces cerevisiae. *Annual Review of Genetics*, *56*, 253–278. https://doi.org/10.1146/annurev-genet-080320-023632

Bresson, S., & Tollervey, D. (2018). Surveillance-ready transcription: Nuclear RNA decay as a default fate. *Open Biology*, *8*(3), 170270. https://doi.org/10.1098/rsob.170270

Bresson, S., Tuck, A., Staneva, D., & Tollervey, D. (2017). Nuclear RNA Decay Pathways Aid Rapid Remodeling of Gene Expression in Yeast. *Molecular Cell*, *65*(5), 787-800.e5. https://doi.org/10.1016/j.molcel.2017.01.005

Brown, G. D., Denning, D. W., Gow, N. A. R., Levitz, S. M., Netea, M. G., & White, T. C. (2012). Hidden Killers: Human Fungal Infections. *Science Translational Medicine*, *4*(165), 165rv13-165rv13. https://doi.org/10.1126/scitranslmed.3004404

Bruschini, S., Ciliberto, G., & Mancini, R. (2020). The emerging role of cancer cell plasticity and cell-cycle quiescence in immune escape. *Cell Death & Disease*, *11*(6), Article 6. https://doi.org/10.1038/s41419-020-2669-8

Bumgarner, S. L., Dowell, R. D., Grisafi, P., Gifford, D. K., & Fink, G. R. (2009). Toggle involving cis-interfering noncoding RNAs controls variegated gene expression in yeast. *Proceedings of the National Academy of Sciences*, *106*(43), 18321–18326. https://doi.org/10.1073/pnas.0909641106

Bumgarner, S. L., Neuert, G., Voight, B. F., Symbor-Nagrabska, A., Grisafi, P., van Oudenaarden, A., & Fink, G. R. (2012). Single-cell analysis reveals that noncoding RNAs contribute to clonal heterogeneity by modulating transcription factor recruitment. *Molecular Cell*, *45*(4), 470–482. https://doi.org/10.1016/j.molcel.2011.11.029

Burtner, C. R., Murakami, C. J., Kennedy, B. K., & Kaeberlein, M. (2009). A molecular mechanism of chronological aging in yeast. *Cell Cycle (Georgetown, Tex.)*, *8*(8), 1256–1270.

Camblong, J., Beyrouthy, N., Guffanti, E., Schlaepfer, G., Steinmetz, L. M., & Stutz, F. (2009). Trans-acting antisense RNAs mediate transcriptional gene cosuppression in S. cerevisiae. *Genes & Development*, *23*(13), 1534–1545. https://doi.org/10.1101/gad.522509

Camblong, J., Iglesias, N., Fickentscher, C., Dieppois, G., & Stutz, F. (2007). Antisense RNA stabilization induces transcriptional gene silencing via histone deacetylation in S. cerevisiae. *Cell*, *131*(4), 706–717. https://doi.org/10.1016/j.cell.2007.09.014

Carroll, K. L., Ghirlando, R., Ames, J. M., & Corden, J. L. (2007). Interaction of yeast RNA-binding proteins Nrd1 and Nab3 with RNA polymerase II terminator elements. *RNA*, *13*(3), 361–373. https://doi.org/10.1261/rna.338407

Carroll, K. L., Pradhan, D. A., Granek, J. A., Clarke, N. D., & Corden, J. L. (2004). Identification of cis elements directing termination of yeast nonpolyadenylated snoRNA transcripts. *Molecular and Cellular Biology*, *24*(14), 6241–6252. https://doi.org/10.1128/MCB.24.14.6241-6252.2004

Castelnuovo, M., Rahman, S., Guffanti, E., Infantino, V., Stutz, F., & Zenklusen, D. (2013). Bimodal expression of PHO84 is modulated by early termination of antisense transcription. *Nature Structural & Molecular Biology*, *20*(7), 851–858. https://doi.org/10.1038/nsmb.2598

Chapman, N. M., Boothby, M. R., & Chi, H. (2020). Metabolic coordination of T cell quiescence and activation. *Nature Reviews Immunology*, *20*(1), Article 1. https://doi.org/10.1038/s41577-019-0203-y

Chaves-Arquero, B., Martínez-Lumbreras, S., Camero, S., Santiveri, C. M., Mirassou, Y., Campos-Olivas, R., Jiménez, M. Á., Calvo, O., & Pérez-Cañadillas, J. M. (2022). Structural basis of Nrd1-Nab3 heterodimerization. *Life Science Alliance*, *5*(4), e202101252. https://doi.org/10.26508/lsa.202101252

Chen, C.-Y. A., & Shyu, A.-B. (2011). Mechanisms of deadenylation-dependent decay. *WIREs RNA*, *2*(2), 167–183. https://doi.org/10.1002/wrna.40

Chen, K., Hu, Z., Xia, Z., Zhao, D., Li, W., & Tyler, J. K. (2016). The Overlooked Fact: Fundamental Need for Spike-In Control for Virtually All Genome-Wide Analyses. *Molecular and Cellular Biology*, *36*(5), 662–667. https://doi.org/10.1128/MCB.00970-14

Chen, W., Dong, J., Haiech, J., Kilhoffer, M.-C., & Zeniou, M. (2016, June 21). *Cancer Stem Cell Quiescence and Plasticity as Major Challenges in Cancer Therapy* [Review Article]. Stem Cells International; Hindawi. https://doi.org/10.1155/2016/1740936

Chen, W., Jia, Q., Song, Y., Fu, H., Wei, G., & Ni, T. (2017). Alternative Polyadenylation: Methods, Findings, and Impacts. *Genomics, Proteomics & Bioinformatics*, *15*(5), 287–300. https://doi.org/10.1016/j.gpb.2017.06.001

Cheng, J., Kapranov, P., Drenkow, J., Dike, S., Brubaker, S., Patel, S., Long, J., Stern, D., Tammana, H., Helt, G., Sementchenko, V., Piccolboni, A., Bekiranov, S., Bailey, D. K., Ganesh, M., Ghosh, S., Bell, I., Gerhard, D. S., & Gingeras, T. R. (2005). Transcriptional Maps of 10 Human Chromosomes at 5-Nucleotide Resolution. *Science*, *308*(5725), 1149–1154. https://doi.org/10.1126/science.1108625

Cherry, J. M., Hong, E. L., Amundsen, C., Balakrishnan, R., Binkley, G., Chan, E. T., Christie, K. R., Costanzo, M. C., Dwight, S. S., Engel, S. R., Fisk, D. G., Hirschman, J. E., Hitz, B. C., Karra, K., Krieger, C. J., Miyasato, S. R., Nash, R. S., Park, J., Skrzypek, M. S., … Wong, E. D. (2012). Saccharomyces Genome Database: The genomics resource of budding yeast. *Nucleic Acids Research*, *40*(Database issue), D700–D705. https://doi.org/10.1093/nar/gkr1029

Cheung, T. H., & Rando, T. A. (2013). Molecular regulation of stem cell quiescence. *Nature Reviews. Molecular Cell Biology*, *14*(6), 329–340. https://doi.org/10.1038/nrm3591

Chia, M., Li, C., Marques, S., Pelechano, V., Luscombe, N. M., & van Werven, F. J. (2021). High-resolution analysis of cell-state transitions in yeast suggests widespread transcriptional tuning by alternative starts. *Genome Biology*, *22*(1), 34. https://doi.org/10.1186/s13059-020-02245-3

Chuan, J., Zhou, A., Hale, L. R., He, M., & Li, X. (2021). Atria: An ultra-fast and accurate trimmer for adapter and quality trimming. *GigaByte*, *2021*, gigabyte31. https://doi.org/10.46471/gigabyte.31

Cohen, S., Puget, N., Lin, Y.-L., Clouaire, T., Aguirrebengoa, M., Rocher, V., Pasero, P., Canitrot, Y., & Legube, G. (2018). Senataxin resolves RNA:DNA hybrids forming at DNA double-strand breaks to prevent translocations. *Nature Communications*, *9*(1), Article 1. https://doi.org/10.1038/s41467-018-02894-w

Collin, P., Jeronimo, C., Poitras, C., & Robert, F. (2019). RNA Polymerase II CTD Tyrosine 1 Is Required for Efficient Termination by the Nrd1-Nab3-Sen1 Pathway. *Molecular Cell*, *73*(4), 655-669.e7. https://doi.org/10.1016/j.molcel.2018.12.002

Conesa, A., Madrigal, P., Tarazona, S., Gomez-Cabrero, D., Cervera, A., McPherson, A., Szcześniak, M. W., Gaffney, D. J., Elo, L. L., Zhang, X., & Mortazavi, A. (2016). A survey of best practices for RNA-seq data analysis. *Genome Biology*, *17*(1), 13. https://doi.org/10.1186/s13059-016-0881-8

Cucinotta, C. E., Dell, R. H., Braceros, K. C., & Tsukiyama, T. (2021). RSC primes the quiescent genome for hypertranscription upon cell-cycle re-entry. *eLife*, *10*, e67033. https://doi.org/10.7554/eLife.67033

Danecek, P., Bonfield, J. K., Liddle, J., Marshall, J., Ohan, V., Pollard, M. O., Whitwham, A., Keane, T., McCarthy, S. A., Davies, R. M., & Li, H. (2021). Twelve years of SAMtools and BCFtools. *GigaScience*, *10*(2), giab008. https://doi.org/10.1093/gigascience/giab008

David, L., Huber, W., Granovskaia, M., Toedling, J., Palm, C. J., Bofkin, L., Jones, T., Davis, R. W., & Steinmetz, L. M. (2006). A high-resolution map of transcription in the yeast genome. *Proceedings of the National Academy of Sciences*, *103*(14), 5320–5325. https://doi.org/10.1073/pnas.0601091103

Davidson, L., Muniz, L., & West, S. (2014). 3′ end formation of pre-mRNA and phosphorylation of Ser2 on the RNA polymerase II CTD are reciprocally coupled in human cells. *Genes & Development*, *28*(4), 342–356. https://doi.org/10.1101/gad.231274.113

de Morree, A., & Rando, T. A. (2023). Regulation of adult stem cell quiescence and its functions in the maintenance of tissue integrity. *Nature Reviews Molecular Cell Biology*, *24*(5), Article 5. https://doi.org/10.1038/s41580-022-00568-6

De Virgilio, C. (2012). The essence of yeast quiescence. *FEMS Microbiology Reviews*, *36*(2), 306–339. https://doi.org/10.1111/j.1574-6976.2011.00287.x

Descostes, N., Heidemann, M., Spinelli, L., Schüller, R., Maqbool, M. A., Fenouil, R., Koch, F., Innocenti, C., Gut, M., Gut, I., Eick, D., & Andrau, J.-C. (2014). Tyrosine phosphorylation of RNA polymerase II CTD is associated with antisense promoter transcription and active enhancers in mammalian cells. *eLife*, *3*, e02105. https://doi.org/10.7554/eLife.02105

Dhawan, J., & Laxman, S. (2015). Decoding the stem cell quiescence cycle – lessons from yeast for regenerative biology. *Journal of Cell Science*, *128*(24), 4467–4474. https://doi.org/10.1242/jcs.177758

Dias, J. D., Rito, T., Torlai Triglia, E., Kukalev, A., Ferrai, C., Chotalia, M., Brookes, E., Kimura, H., & Pombo, A. (2015). Methylation of RNA polymerase II non-consensus Lysine residues marks early transcription in mammalian cells. *eLife*, *4*, e11215. https://doi.org/10.7554/eLife.11215

Dickson, B. M., Tiedemann, R. L., Chomiak, A. A., Cornett, E. M., Vaughan, R. M., & Rothbart, S. B. (2020). A physical basis for quantitative ChIP-sequencing. *The Journal of Biological Chemistry*, *295*(47), 15826–15837. https://doi.org/10.1074/jbc.RA120.015353

Dickson, L. M., & Brown, A. J. P. (1998). mRNA translation in yeast during entry into stationary phase. *Molecular and General Genetics MGG*, *259*(3), 282–293. https://doi.org/10.1007/s004380050814

Dinger, M. E., Amaral, P. P., Mercer, T. R., & Mattick, J. S. (2009). Pervasive transcription of the eukaryotic genome: Functional indices and conceptual implications. *Briefings in Functional Genomics*, *8*(6), 407–423. https://doi.org/10.1093/bfgp/elp038

Dobin, A., Davis, C. A., Schlesinger, F., Drenkow, J., Zaleski, C., Jha, S., Batut, P., Chaisson, M., & Gingeras, T. R. (2013). STAR: Ultrafast universal RNA-seq aligner. *Bioinformatics*, *29*(1), 15–21. https://doi.org/10.1093/bioinformatics/bts635

Drebot, M. A., Johnston, G. C., & Singer, R. A. (1987). A yeast mutant conditionally defective only for reentry into the mitotic cell cycle from stationary phase. *Proceedings of the National Academy of Sciences*, *84*(22), 7948–7952. https://doi.org/10.1073/pnas.84.22.7948

Drinnenberg, I. A., Fink, G. R., & Bartel, D. P. (2011). Compatibility with Killer Explains the Rise of RNAi-Deficient Fungi. *Science*, *333*(6049), 1592–1592. https://doi.org/10.1126/science.1209575

Drinnenberg, I. A., Weinberg, D. E., Xie, K. T., Mower, J. P., Wolfe, K. H., Fink, G. R., & Bartel, D. P. (2009). RNAi in Budding Yeast. *Science*, *326*(5952), 544–550. https://doi.org/10.1126/science.1176945

Duffy, E. E., Schofield, J. A., & Simon, M. D. (2019). Gaining insight into transcriptome-wide RNA population dynamics through the chemistry of 4-thiouridine. *WIREs RNA*, *10*(1), e1513. https://doi.org/10.1002/wrna.1513

Dupuis-Sandoval, F., Poirier, M., & Scott, M. S. (2015). The emerging landscape of small nucleolar RNAs in cell biology. *WIREs RNA*, *6*(4), 381–397. https://doi.org/10.1002/wrna.1284

Dworkin, J., & Harwood, C. S. (2022). Metabolic Reprogramming and Longevity in Quiescence. *Annual Review of Microbiology*, *76*(1), 91–111. https://doi.org/10.1146/annurev-micro-041320-111014

Escalante, L. E., & Gasch, A. P. (2021). The role of stress-activated RNA–protein granules in surviving adversity. *RNA*, *27*(7), 753–762. https://doi.org/10.1261/rna.078738.121

Evans, C., Hardin, J., & Stoebel, D. M. (2018). Selecting between-sample RNA-Seq normalization methods from the perspective of their assumptions. *Briefings in Bioinformatics*, *19*(5), 776–792. https://doi.org/10.1093/bib/bbx008

Ewels, P., Magnusson, M., Lundin, S., & Käller, M. (2016). MultiQC: Summarize analysis results for multiple tools and samples in a single report. *Bioinformatics*, *32*(19), 3047–3048. https://doi.org/10.1093/bioinformatics/btw354

Fabian, M. R., Frank, F., Rouya, C., Siddiqui, N., Lai, W. S., Karetnikov, A., Blackshear, P. J., Nagar, B., & Sonenberg, N. (2013). Structural basis for the recruitment of the human

CCR4–NOT deadenylase complex by tristetraprolin. *Nature Structural & Molecular Biology*, *20*(6), Article 6. https://doi.org/10.1038/nsmb.2572

Fox, M. J., Gao, H., Smith-Kinnaman, W. R., Liu, Y., & Mosley, A. L. (2015). The Exosome Component Rrp6 Is Required for RNA Polymerase II Termination at Specific Targets of the Nrd1-Nab3 Pathway. *PLOS Genetics*, *11*(2), e1004999. https://doi.org/10.1371/journal.pgen.1004999

Fuge, E. K., Braun, E. L., & Werner-Washburne, M. (1994). Protein synthesis in long-term stationary-phase cultures of Saccharomyces cerevisiae. *Journal of Bacteriology*, *176*(18), 5802–5813. https://doi.org/10.1128/JB.176.18.5802-5813.1994

G. J. Hannon. (2010). *FASTX-Toolkit* (0.0.14) [Computer software]. http://hannonlab.cshl.edu/fastx_toolkit.

Galloway, A., Saveliev, A., Łukasiak, S., Hodson, D. J., Bolland, D., Balmanno, K., Ahlfors, H., Monzón-Casanova, E., Mannurita, S. C., Bell, L. S., Andrews, S., Díaz-Muñoz, M. D., Cook, S. J., Corcoran, A., & Turner, M. (2016). RNA-binding proteins ZFP36L1 and ZFP36L2 promote cell quiescence. *Science*, *352*(6284), 453–459. https://doi.org/10.1126/science.aad5978

Garmendia-Torres, C., Skupin, A., Michael, S. A., Ruusuvuori, P., Kuwada, N. J., Falconnet, D., Cary, G. A., Hansen, C., Wiggins, P. A., & Dudley, A. M. (2014). Unidirectional P-Body Transport during the Yeast Cell Cycle. *PLOS ONE*, *9*(6), e99428. https://doi.org/10.1371/journal.pone.0099428

Ge, J., & Yu, Y.-T. (2013). RNA pseudouridylation: New insights into an old modification. *Trends in Biochemical Sciences*, *38*(4), 210–218. https://doi.org/10.1016/j.tibs.2013.01.002

Geisberg, J. V., Moqtaderi, Z., & Struhl, K. (2020). The transcriptional elongation rate regulates alternative polyadenylation in yeast. *eLife*, *9*, e59810. https://doi.org/10.7554/eLife.59810

Gelfand, B., Mead, J., Bruning, A., Apostolopoulos, N., Tadigotla, V., Nagaraj, V., Sengupta, A. M., & Vershon, A. K. (2011). Regulated Antisense Transcription Controls Expression of Cell-Type-Specific Genes in Yeast ▿ . *Molecular and Cellular Biology*, *31*(8), 1701–1709. https://doi.org/10.1128/MCB.01071-10

Gene Ontology Consortium. (2021). The Gene Ontology resource: Enriching a GOld mine. *Nucleic Acids Research*, *49*(D1), D325–D334. https://doi.org/10.1093/nar/gkaa1113

Gil, N., & Ulitsky, I. (2020). Regulation of gene expression by cis-acting long non-coding RNAs. *Nature Reviews Genetics*, *21*(2), Article 2. https://doi.org/10.1038/s41576-019-0184-5

Gilbert, W. V., Zhou, K., Butler, T. K., & Doudna, J. A. (2007). Cap-Independent Translation Is Required for Starvation-Induced Differentiation in Yeast. *Science*, *317*(5842), 1224–1227. https://doi.org/10.1126/science.1144467

Gill, J. K., Maffioletti, A., García-Molinero, V., Stutz, F., & Soudet, J. (2020). Fine Chromatin-Driven Mechanism of Transcription Interference by Antisense Noncoding Transcription. *Cell Reports*, *31*(5). https://doi.org/10.1016/j.celrep.2020.107612

Goddard, M. R. (2008). Quantifying the complexities of Saccharomyces cerevisiae's ecosystem engineering via fermentation. *Ecology*, *89*(8), 2077–2082. https://doi.org/10.1890/07-2060.1

Goddard, M. R., & Greig, D. (2015). Saccharomyces cerevisiae: A nomadic yeast with no niche? *FEMS Yeast Research*, *15*(3), fov009. https://doi.org/10.1093/femsyr/fov009

Grabherr, M. G., Haas, B. J., Yassour, M., Levin, J. Z., Thompson, D. A., Amit, I., Adiconis, X., Fan, L., Raychowdhury, R., Zeng, Q., Chen, Z., Mauceli, E., Hacohen, N., Gnirke, A., Rhind, N., di Palma, F., Birren, B. W., Nusbaum, C., Lindblad-Toh, K., … Regev, A. (2011). Trinity: Reconstructing a full-length transcriptome without a genome from RNA-Seq data. *Nature Biotechnology*, *29*(7), 644–652. https://doi.org/10.1038/nbt.1883

Gray, J. V., Petsko, G. A., Johnston, G. C., Ringe, D., Singer, R. A., & Werner-Washburne, M. (2004). "Sleeping Beauty": Quiescence in Saccharomyces cerevisiae. *Microbiology and Molecular Biology Reviews*, *68*(2), 187–206. https://doi.org/10.1128/mmbr.68.2.187-206.2004

Gudipati, R. K., Villa, T., Boulay, J., & Libri, D. (2008). Phosphorylation of the RNA polymerase II C-terminal domain dictates transcription termination choice. *Nature Structural & Molecular Biology*, *15*(8), Article 8. https://doi.org/10.1038/nsmb.1460

Haas, B. J., Papanicolaou, A., Yassour, M., Grabherr, M., Blood, P. D., Bowden, J., Couger, M. B., Eccles, D., Li, B., Lieber, M., MacManes, M. D., Ott, M., Orvis, J., Pochet, N., Strozzi, F., Weeks, N., Westerman, R., William, T., Dewey, C. N., … Regev, A. (2013). De novo transcript sequence reconstruction from RNA-seq using the Trinity platform for reference generation and analysis. *Nature Protocols*, *8*(8), Article 8. https://doi.org/10.1038/nprot.2013.084

Hainer, S. J., Pruneski, J. A., Mitchell, R. D., Monteverde, R. M., & Martens, J. A. (2011). Intergenic transcription causes repression by directing nucleosome assembly. *Genes & Development*, *25*(1), 29–40. https://doi.org/10.1101/gad.1975011

Han, Z., Jasnovidova, O., Haidara, N., Tudek, A., Kubicek, K., Libri, D., Stefl, R., & Porrua, O. (2020). Termination of non-coding transcription in yeast relies on both an RNA Pol II

CTD interaction domain and a CTD-mimicking region in Sen1. *The EMBO Journal*, *39*(7), e101548. https://doi.org/10.15252/embj.2019101548

Han, Z., Libri, D., & Porrua, O. (2017). Biochemical characterization of the helicase Sen1 provides new insights into the mechanisms of non-coding transcription termination. *Nucleic Acids Research*, *45*(3), 1355–1370. https://doi.org/10.1093/nar/gkw1230

Hanahan, D., & Weinberg, R. A. (2011). Hallmarks of cancer: The next generation. *Cell*, *144*(5), 646–674. https://doi.org/10.1016/j.cell.2011.02.013

Hartwell, L. H., Culotti, J., Pringle, J. R., & Reid, B. J. (1974). Genetic Control of the Cell Division Cycle in Yeast: A model to account for the order of cell cycle events is deduced from the phenotypes of yeast mutants. *Science*, *183*(4120), 46–51. https://doi.org/10.1126/science.183.4120.46

Haruki, H., Nishikawa, J., & Laemmli, U. K. (2008). The anchor-away technique: Rapid, conditional establishment of yeast mutant phenotypes. *Molecular Cell*, *31*(6), 925–932. https://doi.org/10.1016/j.molcel.2008.07.020

Hasanova, Z., Klapstova, V., Porrua, O., Stefl, R., & Sebesta, M. (2023). Human senataxin is a bona fide R-loop resolving enzyme and transcription termination factor. *Nucleic Acids Research*, *51*(6), 2818–2837. https://doi.org/10.1093/nar/gkad092

Hazelbaker, D. Z., Marquardt, S., Wlotzka, W., & Buratowski, S. (2013). Kinetic Competition between RNA Polymerase II and Sen1-Dependent Transcription Termination. *Molecular Cell*, *49*(1), 55–66. https://doi.org/10.1016/j.molcel.2012.10.014

Hegazy, Y. A., Cloutier, S. C., Utturkar, S. M., Das, S., & Tran, E. J. (2023). The genomic region of the 3′ untranslated region (3′UTR) of PHO84, rather than the antisense RNA,

promotes gene repression. *Nucleic Acids Research*, *51*(15), 7900–7913. https://doi.org/10.1093/nar/gkad579

Heo, D., Yoo, I., Kong, J., Lidschreiber, M., Mayer, A., Choi, B.-Y., Hahn, Y., Cramer, P., Buratowski, S., & Kim, M. (2013). The RNA Polymerase II C-terminal Domain-interacting Domain of Yeast Nrd1 Contributes to the Choice of Termination Pathway and Couples to RNA Processing by the Nuclear Exosome *. *Journal of Biological Chemistry*, *288*(51), 36676–36690. https://doi.org/10.1074/jbc.M113.508267

Herskowitz, I. (1988). Life cycle of the budding yeast Saccharomyces cerevisiae. *Microbiological Reviews*, *52*(4), 536. https://doi.org/10.1128/mr.52.4.536-553.1988

Hildreth, A. E., Ellison, M. A., Francette, A. M., Seraly, J. M., Lotka, L. M., & Arndt, K. M. (2020). The nucleosome DNA entry-exit site is important for transcription termination and prevention of pervasive transcription. *eLife*, *9*, e57757. https://doi.org/10.7554/eLife.57757

Hinrichs, A. S., Karolchik, D., Baertsch, R., Barber, G. P., Bejerano, G., Clawson, H., Diekhans, M., Furey, T. S., Harte, R. A., Hsu, F., Hillman-Jackson, J., Kuhn, R. M., Pedersen, J. S., Pohl, A., Raney, B. J., Rosenbloom, K. R., Siepel, A., Smith, K. E., Sugnet, C. W., … Kent, W. J. (2006). The UCSC Genome Browser Database: Update 2006. *Nucleic Acids Research*, *34*(Database issue), D590-598. https://doi.org/10.1093/nar/gkj144

Hongay, C. F., Grisafi, P. L., Galitski, T., & Fink, G. R. (2006). Antisense transcription controls cell fate in Saccharomyces cerevisiae. *Cell*, *127*(4), 735–745. https://doi.org/10.1016/j.cell.2006.09.038

Honorine, R., Mosrin-Huaman, C., Hervouet-Coste, N., Libri, D., & Rahmouni, A. R. (2011). Nuclear mRNA quality control in yeast is mediated by Nrd1 co-transcriptional

recruitment, as revealed by the targeting of Rho-induced aberrant transcripts. *Nucleic Acids Research*, *39*(7), 2809–2820. https://doi.org/10.1093/nar/gkq1192

Hook, B. A., Goldstrohm, A. C., Seay, D. J., & Wickens, M. (2007). Two Yeast PUF Proteins Negatively Regulate a Single mRNA*. *Journal of Biological Chemistry*, *282*(21), 15430–15438. https://doi.org/10.1074/jbc.M611253200

Hopewell, S., Loudon, K., Clarke, M. J., Oxman, A. D., & Dickersin, K. (2009). Publication bias in clinical trials due to statistical significance or direction of trial results. *The Cochrane Database of Systematic Reviews*, *2009*(1), MR000006. https://doi.org/10.1002/14651858.MR000006.pub3

Houseley, J., Rubbi, L., Grunstein, M., Tollervey, D., & Vogelauer, M. (2008). A ncRNA Modulates Histone Modification and mRNA Induction in the Yeast GAL Gene Cluster. *Molecular Cell*, *32*(5), 685–695. https://doi.org/10.1016/j.molcel.2008.09.027

Howe, F. S., Russell, A., Lamstaes, A. R., El-Sagheer, A., Nair, A., Brown, T., & Mellor, J. (2017). CRISPRi is not strand-specific at all loci and redefines the transcriptional landscape. *eLife*, *6*, e29878. https://doi.org/10.7554/eLife.29878

Huang, H., Kawamata, T., Horie, T., Tsugawa, H., Nakayama, Y., Ohsumi, Y., & Fukusaki, E. (2015). Bulk RNA degradation by nitrogen starvation-induced autophagy in yeast. *The EMBO Journal*, *34*(2), 154–168. https://doi.org/10.15252/embj.201489083

Huang, Z., Du, Y., Wen, J., Lu, B., & Zhao, Y. (2022). snoRNAs: Functions and mechanisms in biological processes, and roles in tumor pathophysiology. *Cell Death Discovery*, *8*(1), Article 1. https://doi.org/10.1038/s41420-022-01056-8

Huber, F., Bunina, D., Gupta, I., Khmelinskii, A., Meurer, M., Theer, P., Steinmetz, L. M., & Knop, M. (2016). Protein Abundance Control by Non-coding Antisense Transcription. *Cell Reports*, *15*(12), 2625–2636. https://doi.org/10.1016/j.celrep.2016.05.043

Hurowitz, E. H., & Brown, P. O. (2004). Genome-wide analysis of mRNA lengths in Saccharomyces cerevisiae. *Genome Biology*, *5*(1), R2.

Hurtig, J. E., Kim, M., Orlando-Coronel, L. J., Ewan, J., Foreman, M., Notice, L.-A., Steiger, M. A., & van Hoof, A. (2020). Origin, conservation, and loss of alternative splicing events that diversify the proteome in Saccharomycotina budding yeasts. *RNA*, *26*(10), 1464–1480. https://doi.org/10.1261/rna.075655.120

Hutchinson, K. M., Hunn, J. C., & Reines, D. (2022). Nab3 nuclear granule accumulation is driven by respiratory capacity. *Current Genetics*, *68*(5–6), 581–591. https://doi.org/10.1007/s00294-022-01248-w

Iida, H., & Yahara, I. (1984). Durable synthesis of high molecular weight heat shock proteins in G0 cells of the yeast and other eucaryotes. *Journal of Cell Biology*, *99*(1), 199–207. https://doi.org/10.1083/jcb.99.1.199

International Human Genome Sequencing Consortium. (2004). Finishing the euchromatic sequence of the human genome. *Nature*, *431*(7011), Article 7011. https://doi.org/10.1038/nature03001

Jain, M., Abu-Shumays, R., Olsen, H. E., & Akeson, M. (2022). Advances in nanopore direct RNA sequencing. *Nature Methods*, *19*(10), Article 10. https://doi.org/10.1038/s41592-022-01633-w

Januszyk, K., & Lima, C. D. (2014). The eukaryotic RNA exosome. *Current Opinion in Structural Biology*, *24*, 132–140. https://doi.org/10.1016/j.sbi.2014.01.011

Jia, H., Wang, X., Anderson, J. T., & Jankowsky, E. (2012). RNA unwinding by the Trf4/Air2/Mtr4 polyadenylation (TRAMP) complex. *Proceedings of the National Academy of Sciences*, *109*(19), 7292–7297. https://doi.org/10.1073/pnas.1201085109

Jia, H., Wang, X., Liu, F., Guenther, U.-P., Srinivasan, S., Anderson, J. T., & Jankowsky, E. (2011). The RNA Helicase Mtr4p Modulates Polyadenylation in the TRAMP Complex. *Cell*, *145*(6), 890–901. https://doi.org/10.1016/j.cell.2011.05.010

Johnson, E. L., Robinson, D. G., & Coller, H. A. (2017). Widespread changes in mRNA stability contribute to quiescence-specific gene expression patterns in a fibroblast model of quiescence. *BMC Genomics*, *18*(1), 123. https://doi.org/10.1186/s12864-017-3521-0

Julius, C., & Yuzenkova, Y. (2019). Noncanonical RNA-capping: Discovery, mechanism, and physiological role debate. *WIREs RNA*, *10*(2), e1512. https://doi.org/10.1002/wrna.1512

Juneau, K., Nislow, C., & Davis, R. W. (2009). Alternative splicing of PTC7 in Saccharomyces cerevisiae determines protein localization. *Genetics*, *183*(1), 185–194. https://doi.org/10.1534/genetics.109.105155

Kaczmarek Michaels, K., Mohd Mostafa, S., Ruiz Capella, J., & Moore, C. L. (2020). Regulation of alternative polyadenylation in the yeast Saccharomyces cerevisiae by histone H3K4 and H3K36 methyltransferases. *Nucleic Acids Research*, *48*(10), 5407–5425. https://doi.org/10.1093/nar/gkaa292

Kadaba, S., Krueger, A., Trice, T., Krecic, A. M., Hinnebusch, A. G., & Anderson, J. (2004). Nuclear surveillance and degradation of hypomodified initiator tRNAMet in S. cerevisiae. *Genes & Development*, *18*(11), 1227–1240. https://doi.org/10.1101/gad.1183804

Kadaba, S., Wang, X., & Anderson, J. T. (2006). Nuclear RNA surveillance in Saccharomyces cerevisiae: Trf4p-dependent polyadenylation of nascent hypomethylated tRNA and an aberrant form of 5S rRNA. *RNA*, *12*(3), 508–521. https://doi.org/10.1261/rna.2305406

Kalderimis, A., Lyne, R., Butano, D., Contrino, S., Lyne, M., Heimbach, J., Hu, F., Smith, R., Stěpán, R., Sullivan, J., & Micklem, G. (2014). InterMine: Extensive web services for modern biology. *Nucleic Acids Research*, *42*(Web Server issue), W468-472. https://doi.org/10.1093/nar/gku301

Kamarthapu, V., & Nudler, E. (2015). Rethinking Transcription Coupled DNA Repair. *Current Opinion in Microbiology*, *24*, 15–20. https://doi.org/10.1016/j.mib.2014.12.005

Kang, C., & Liu, Z. (2015). Global identification and analysis of long non-coding RNAs in diploid strawberry Fragaria vesca during flower and fruit development. *BMC Genomics*, *16*(1), 815. https://doi.org/10.1186/s12864-015-2014-2

Kelemen, O., Convertini, P., Zhang, Z., Wen, Y., Shen, M., Falaleeva, M., & Stamm, S. (2013). Function of alternative splicing. *Gene*, *514*(1), 1–30. https://doi.org/10.1016/j.gene.2012.07.083

Kevin Blighe & Aaron Lun. (2022). *PCAtools: PCAtools: Everything Principal Components Analysis* (R package version 2.10.0) [Computer software]. https://github.com/kevinblighe/PCAtools

Kevin Blighe, Sharmila Rana, & Myles Lewis. (2022). *EnhancedVolcano: Publication-ready volcano plots with enhanced colouring and labeling* (R package version 1.16) [Computer software]. https://github.com/kevinblighe/EnhancedVolcano

Khaladkar, M., Smyda, M., & Hannenhalli, S. (2011). Epigenomic and RNA structural correlates of polyadenylation. *RNA Biology*, *8*(3), 529–537. https://doi.org/10.4161/rna.8.3.15194

Kilchert, C., Wittmann, S., & Vasiljeva, L. (2016). The regulation and functions of the nuclear RNA exosome complex. *Nature Reviews Molecular Cell Biology*, *17*(4), Article 4. https://doi.org/10.1038/nrm.2015.15

Kiledjian, M. (2018). Eukaryotic RNA 5′-end NAD+ Capping and deNADding. *Trends in Cell Biology*, *28*(6), 454–464. https://doi.org/10.1016/j.tcb.2018.02.005

Kim, H.-D., Choe, J., & Seo, Y.-S. (1999). The sen1+ Gene of Schizosaccharomyces pombe, a Homologue of Budding Yeast SEN1, Encodes an RNA and DNA Helicase. *Biochemistry*, *38*(44), 14697–14710. https://doi.org/10.1021/bi991470c

Klauer, A. A., & van Hoof, A. (2013). Genetic interactions suggest multiple distinct roles of the arch and core helicase domains of Mtr4 in Rrp6 and exosome function. *Nucleic Acids Research*, *41*(1), 533–541. https://doi.org/10.1093/nar/gks1013

Klosinska, M. M., Crutchfield, C. A., Bradley, P. H., Rabinowitz, J. D., & Broach, J. R. (2011). Yeast cells can access distinct quiescent states. *Genes & Development*, *25*(4), 336–349. https://doi.org/10.1101/gad.2011311

Komarnitsky, P., Cho, E. J., & Buratowski, S. (2000). Different phosphorylated forms of RNA polymerase II and associated mRNA processing factors during transcription. *Genes & Development*, *14*(19), 2452–2460. https://doi.org/10.1101/gad.824700

Kroschwald, S., Maharana, S., Mateju, D., Malinovska, L., Nüske, E., Poser, I., Richter, D., & Alberti, S. (2015). Promiscuous interactions and protein disaggregases determine the material state of stress-inducible RNP granules. *eLife*, *4*, e06807. https://doi.org/10.7554/eLife.06807

Kubicek, K., Cerna, H., Holub, P., Pasulka, J., Hrossova, D., Loehr, F., Hofr, C., Vanacova, S., & Stefl, R. (2012). Serine phosphorylation and proline isomerization in RNAP II CTD

control recruitment of Nrd1. *Genes & Development*, *26*(17), 1891–1896. https://doi.org/10.1101/gad.192781.112

Kuehner, J. N., & Brow, D. A. (2008). Regulation of a Eukaryotic Gene by GTP-Dependent Start Site Selection and Transcription Attenuation. *Molecular Cell*, *31*(2), 201–211. https://doi.org/10.1016/j.molcel.2008.05.018

Kumar, A., Clerici, M., Muckenfuss, L. M., Passmore, L. A., & Jinek, M. (2019). Mechanistic insights into mRNA 3′-end processing. *Current Opinion in Structural Biology*, *59*, 143–150. https://doi.org/10.1016/j.sbi.2019.08.001

Kyriakou, D., Stavrou, E., Demosthenous, P., Angelidou, G., San Luis, B.-J., Boone, C., Promponas, V. J., & Kirmizis, A. (2016). Functional characterisation of long intergenic non-coding RNAs through genetic interaction profiling in Saccharomyces cerevisiae. *BMC Biology*, *14*(1), 106. https://doi.org/10.1186/s12915-016-0325-7

LaCava, J., Houseley, J., Saveanu, C., Petfalski, E., Thompson, E., Jacquier, A., & Tollervey, D. (2005). RNA Degradation by the Exosome Is Promoted by a Nuclear Polyadenylation Complex. *Cell*, *121*(5), 713–724. https://doi.org/10.1016/j.cell.2005.04.029

Lafontaine, D. L. J., Riback, J. A., Bascetin, R., & Brangwynne, C. P. (2021). The nucleolus as a multiphase liquid condensate. *Nature Reviews Molecular Cell Biology*, *22*(3), Article 3. https://doi.org/10.1038/s41580-020-0272-6

Lajtha, L. G. (1963). On the Concept of the Cell Cycle. *Journal of Cellular and Comparative Physiology*, *62*(SUPPL1), 143–145.

Lee, C., & Chen, L. (2013). Alternative polyadenylation sites reveal distinct chromatin accessibility and histone modification in human cell lines. *Bioinformatics*, *29*(14), 1713–1717. https://doi.org/10.1093/bioinformatics/btt288

Lee, K. Y., Chen, Z., Jiang, R., & Meneghini, M. D. (2018). H3K4 Methylation Dependent and Independent Chromatin Regulation by JHD2 and SET1 in Budding Yeast. *G3 Genes|Genomes|Genetics*, *8*(5), 1829–1839. https://doi.org/10.1534/g3.118.200151

Lee, K. Y., Chopra, A., Burke, G. L., Chen, Z., Greenblatt, J. F., Biggar, K. K., & Meneghini, M. D. (2020). A crucial RNA-binding lysine residue in the Nab3 RRM domain undergoes SET1 and SET3-responsive methylation. *Nucleic Acids Research*, *48*(6), 2897–2911. https://doi.org/10.1093/nar/gkaa029

Lee, P., Kim, M. S., Paik, S.-M., Choi, S.-H., Cho, B.-R., & Hahn, J.-S. (2013). Rim15-dependent activation of Hsf1 and Msn2/4 transcription factors by direct phosphorylation in Saccharomyces cerevisiae. *FEBS Letters*, *587*(22), 3648–3655. https://doi.org/10.1016/j.febslet.2013.10.004

Lee Wilkinson. (2022). *venneuler: Venn and Euler Diagrams* (R package version 1.1-3) [Computer software]. https://cran.r-project.org/web/packages/venneuler/index.html

Lemieux, C., Marguerat, S., Lafontaine, J., Barbezier, N., Bähler, J., & Bachand, F. (2011). A Pre-mRNA degradation pathway that selectively targets intron-containing genes requires the nuclear poly(A)-binding protein. *Molecular Cell*, *44*(1), 108–119. https://doi.org/10.1016/j.molcel.2011.06.035

Lenstra, T. L., Coulon, A., Chow, C. C., & Larson, D. R. (2015). Single-Molecule Imaging Reveals a Switch between Spurious and Functional ncRNA Transcription. *Molecular Cell*, *60*(4), 597–610. https://doi.org/10.1016/j.molcel.2015.09.028

Lewis, C. J. T., Pan, T., & Kalsotra, A. (2017). RNA modifications and structures cooperate to guide RNA–protein interactions. *Nature Reviews Molecular Cell Biology*, *18*(3), Article 3. https://doi.org/10.1038/nrm.2016.163

Lewis, D., & Gattie, D. (1991). The ecology of quiescent microbes. *ASM News*, *57*(1), 27–32.

Li, B., Ruotti, V., Stewart, R. M., Thomson, J. A., & Dewey, C. N. (2010). RNA-Seq gene expression estimation with read mapping uncertainty. *Bioinformatics*, *26*(4), 493–500. https://doi.org/10.1093/bioinformatics/btp692

Li, J., Liu, X., Yin, Z., Hu, Z., & Zhang, K.-Q. (2021). An Overview on Identification and Regulatory Mechanisms of Long Non-coding RNAs in Fungi. *Frontiers in Microbiology*, *12*. https://www.frontiersin.org/articles/10.3389/fmicb.2021.638617

Li, L., Lu, Y., Qin, L.-X., Bar-Joseph, Z., Werner-Washburne, M., & Breeden, L. L. (2009). Budding Yeast SSD1-V Regulates Transcript Levels of Many Longevity Genes and Extends Chronological Life Span in Purified Quiescent Cells. *Molecular Biology of the Cell*, *20*(17), 3851–3864. https://doi.org/10.1091/mbc.e09-04-0347

Li, L., Miles, S., Melville, Z., Prasad, A., Bradley, G., & Breeden, L. L. (2013). Key events during the transition from rapid growth to quiescence in budding yeast require posttranscriptional regulators. *Molecular Biology of the Cell*, *24*(23), 3697–3709. https://doi.org/10.1091/mbc.e13-05-0241

Lillie, S. H., & Pringle, J. R. (1980). Reserve carbohydrate metabolism in Saccharomyces cerevisiae: Responses to nutrient limitation. *Journal of Bacteriology*, *143*(3), 1384–1394.

Liu, C. L., Kaplan, T., Kim, M., Buratowski, S., Schreiber, S. L., Friedman, N., & Rando, O. J. (2005). Single-Nucleosome Mapping of Histone Modifications in S. cerevisiae. *PLOS Biology*, *3*(10), e328. https://doi.org/10.1371/journal.pbio.0030328

Liu, J., Lu, X., Zhang, S., Yuan, L., & Sun, Y. (2022). Molecular Insights into mRNA Polyadenylation and Deadenylation. *International Journal of Molecular Sciences*, *23*(19), Article 19. https://doi.org/10.3390/ijms231910985

Liu, P., Kenney, J. M., Stiller, J. W., & Greenleaf, A. L. (2010). Genetic Organization, Length Conservation, and Evolution of RNA Polymerase II Carboxyl-Terminal Domain. *Molecular Biology and Evolution*, *27*(11), 2628–2641. https://doi.org/10.1093/molbev/msq151

Locati, M. D., Terpstra, I., de Leeuw, W. C., Kuzak, M., Rauwerda, H., Ensink, W. A., van Leeuwen, S., Nehrdich, U., Spaink, H. P., Jonker, M. J., Breit, T. M., & Dekker, R. J. (2015). Improving small RNA-seq by using a synthetic spike-in set for size-range quality control together with a set for data normalization. *Nucleic Acids Research*, *43*(14), e89. https://doi.org/10.1093/nar/gkv303

Love, M. I., Huber, W., & Anders, S. (2014). Moderated estimation of fold change and dispersion for RNA-seq data with DESeq2. *Genome Biology*, *15*(12), 550. https://doi.org/10.1186/s13059-014-0550-8

Loya, T. J., O'Rourke, T. W., Simke, W. C., Kelley, J. B., & Reines, D. (2018). Nab3's localization to a nuclear granule in response to nutrient deprivation is determined by its essential prion-like domain. *PLOS ONE*, *13*(12), e0209195. https://doi.org/10.1371/journal.pone.0209195

Lu, Z., & Lin, Z. (2019). Pervasive and dynamic transcription initiation in Saccharomyces cerevisiae. *Genome Research*, *29*(7), 1198–1210. https://doi.org/10.1101/gr.245456.118

Maharana, S., Wang, J., Papadopoulos, D. K., Richter, D., Pozniakovsky, A., Poser, I., Bickle, M., Rizk, S., Guillén-Boixet, J., Franzmann, T. M., Jahnel, M., Marrone, L., Chang, Y.-T., Sterneckert, J., Tomancak, P., Hyman, A. A., & Alberti, S. (2018). RNA buffers the phase separation behavior of prion-like RNA binding proteins. *Science*, *360*(6391), 918–921. https://doi.org/10.1126/science.aar7366

Makino, S., Kawamata, T., Iwasaki, S., & Ohsumi, Y. (2021). Selectivity of mRNA degradation by autophagy in yeast. *Nature Communications*, *12*(1), Article 1. https://doi.org/10.1038/s41467-021-22574-6

Marasco, L. E., & Kornblihtt, A. R. (2023). The physiology of alternative splicing. *Nature Reviews Molecular Cell Biology*, *24*(4), Article 4. https://doi.org/10.1038/s41580-022-00545-z

Mayer, A., Heidemann, M., Lidschreiber, M., Schreieck, A., Sun, M., Hintermair, C., Kremmer, E., Eick, D., & Cramer, P. (2012). CTD Tyrosine Phosphorylation Impairs Termination Factor Recruitment to RNA Polymerase II. *Science*, *336*(6089), 1723–1725. https://doi.org/10.1126/science.1219651

McClelland, L., Jasper, H., & Biteau, B. (2017). Tis11 mediated mRNA decay promotes the reacquisition of Drosophila intestinal stem cell quiescence. *Developmental Biology*, *426*(1), 8–16. https://doi.org/10.1016/j.ydbio.2017.04.013

McKnight, J. N., Boerma, J. W., Breeden, L. L., & Tsukiyama, T. (2015). Global Promoter Targeting of a Conserved Lysine Deacetylase for Transcriptional Shutoff during Quiescence Entry. *Molecular Cell*, *59*(5), 732–743. https://doi.org/10.1016/j.molcel.2015.07.014

Merran, J., & Corden, J. L. (2017). Yeast RNA-Binding Protein Nab3 Regulates Genes Involved in Nitrogen Metabolism. *Molecular and Cellular Biology*, *37*(18). https://doi.org/10.1128/MCB.00154-17

Mews, P., Zee, B. M., Liu, S., Donahue, G., Garcia, B. A., & Berger, S. L. (2014). Histone Methylation Has Dynamics Distinct from Those of Histone Acetylation in Cell Cycle

Reentry from Quiescence. *Molecular and Cellular Biology*, *34*(21), 3968–3980. https://doi.org/10.1128/MCB.00763-14

Miles, S., Lee, C., & Breeden, L. (2023). BY4741 cannot enter quiescence from rich medium. *microPublication Biology*. https://doi.org/10.17912/micropub.biology.000742

Miles, S., Li, L., Davison, J., & Breeden, L. L. (2013). Xbp1 Directs Global Repression of Budding Yeast Transcription during the Transition to Quiescence and Is Important for the Longevity and Reversibility of the Quiescent State. *PLOS Genetics*, *9*(10), e1003854. https://doi.org/10.1371/journal.pgen.1003854

Miles, S., Li, L. H., Melville, Z., & Breeden, L. L. (2019). Ssd1 and the cell wall integrity pathway promote entry, maintenance, and recovery from quiescence in budding yeast. *Molecular Biology of the Cell*, *30*(17), 2205–2217. https://doi.org/10.1091/mbc.E19-04-0190

Mitrovich, Q. M., & Guthrie, C. (2007). Evolution of small nuclear RNAs in S. cerevisiae, C. albicans, and other hemiascomycetous yeasts. *RNA*, *13*(12), 2066–2080. https://doi.org/10.1261/rna.766607

Møller, A. P., & Jennions, M. D. (2001). Testing and adjusting for publication bias. *Trends in Ecology & Evolution*, *16*(10), 580–586. https://doi.org/10.1016/S0169-5347(01)02235-2

Moore, J. L., Bhaskar, D., Gao, F., Matte-Martone, C., Du, S., Lathrop, E., Ganesan, S., Shao, L., Norris, R., Campamà Sanz, N., Annusver, K., Kasper, M., Cox, A., Hendry, C., Rieck, B., Krishnaswamy, S., & Greco, V. (2023). Cell cycle controls long-range calcium signaling in the regenerating epidermis. *Journal of Cell Biology*, *222*(7), e202302095. https://doi.org/10.1083/jcb.202302095

Moreau, K., Le Dantec, A., Mosrin-Huaman, C., Bigot, Y., Piégu, B., & Rahmouni, A. R. (2019). Perturbation of mRNP biogenesis reveals a dynamic landscape of the Rrp6-dependent surveillance machinery trafficking along the yeast genome. *RNA Biology*, *16*(7), 879–889. https://doi.org/10.1080/15476286.2019.1593745

Moretto, F., Wood, N. E., Chia, M., Li, C., Luscombe, N. M., & Werven, F. J. van. (2021). Transcription levels of a noncoding RNA orchestrate opposing regulatory and cell fate outcomes in yeast. *Cell Reports*, *34*(3). https://doi.org/10.1016/j.celrep.2020.108643

Munder, M. C., Midtvedt, D., Franzmann, T., Nüske, E., Otto, O., Herbig, M., Ulbricht, E., Müller, P., Taubenberger, A., Maharana, S., Malinovska, L., Richter, D., Guck, J., Zaburdaev, V., & Alberti, S. (2016). A pH-driven transition of the cytoplasm from a fluid- to a solid-like state promotes entry into dormancy. *eLife*, *5*, e09347. https://doi.org/10.7554/eLife.09347

Murakami, C. J., Wall, V., Basisty, N., & Kaeberlein, M. (2011). Composition and Acidification of the Culture Medium Influences Chronological Aging Similarly in Vineyard and Laboratory Yeast. *PLOS ONE*, *6*(9), e24530. https://doi.org/10.1371/journal.pone.0024530

Nadal-Ribelles, M., Solé, C., Xu, Z., Steinmetz, L. M., de Nadal, E., & Posas, F. (2014). Control of Cdc28 CDK1 by a Stress-Induced lncRNA. *Molecular Cell*, *53*(4), 549–561. https://doi.org/10.1016/j.molcel.2014.01.006

Narendranath, N. V., & Power, R. (2005). Relationship between pH and Medium Dissolved Solids in Terms of Growth and Metabolism of Lactobacilli and Saccharomyces cerevisiae during Ethanol Production. *Applied and Environmental Microbiology*, *71*(5), 2239–2243. https://doi.org/10.1128/AEM.71.5.2239-2243.2005

Nevers, A., Doyen, A., Malabat, C., Néron, B., Kergrohen, T., Jacquier, A., & Badis, G. (2018). Antisense transcriptional interference mediates condition-specific gene repression in budding yeast. *Nucleic Acids Research*, *46*(12), 6009–6025. https://doi.org/10.1093/nar/gky342

Nguyen, J., Lara-Gutiérrez, J., & Stocker, R. (2021). Environmental fluctuations and their effects on microbial communities, populations and individuals. *FEMS Microbiology Reviews*, *45*(4), fuaa068. https://doi.org/10.1093/femsre/fuaa068

Nicastro, R., Raucci, S., Michel, A. H., Stumpe, M., Garcia Osuna, G. M., Jaquenoud, M., Kornmann, B., & De Virgilio, C. (2021). Indole-3-acetic acid is a physiological inhibitor of TORC1 in yeast. *PLoS Genetics*, *17*(3), e1009414. https://doi.org/10.1371/journal.pgen.1009414

Nik Nabil, W. N., Xi, Z., Song, Z., Jin, L., Zhang, X. D., Zhou, H., De Souza, P., Dong, Q., & Xu, H. (2021). Towards a Framework for Better Understanding of Quiescent Cancer Cells. *Cells*, *10*(3), Article 3. https://doi.org/10.3390/cells10030562

Nishimura, K., Fukagawa, T., Takisawa, H., Kakimoto, T., & Kanemaki, M. (2009). An auxin-based degron system for the rapid depletion of proteins in nonplant cells. *Nature Methods*, *6*(12), 917–922. https://doi.org/10.1038/nmeth.1401

Nishimura, K., & Kanemaki, M. T. (2014). Rapid Depletion of Budding Yeast Proteins via the Fusion of an Auxin-Inducible Degron (AID). *Current Protocols in Cell Biology*, *64*(1), 20.9.1-20.9.16. https://doi.org/10.1002/0471143030.cb2009s64

Novačić, A., Menéndez, D., Ljubas, J., Barbarić, S., Stutz, F., Soudet, J., & Stuparević, I. (2022). Antisense non-coding transcription represses the PHO5 model gene at the level of

promoter chromatin structure. *PLOS Genetics*, *18*(10), e1010432. https://doi.org/10.1371/journal.pgen.1010432

Ogami, K., Chen, Y., & Manley, J. L. (2018). RNA Surveillance by the Nuclear RNA Exosome: Mechanisms and Significance. *Non-Coding RNA*, *4*(1), 8. https://doi.org/10.3390/ncrna4010008

Orr, M. W., Mao, Y., Storz, G., & Qian, S.-B. (2020). Alternative ORFs and small ORFs: Shedding light on the dark proteome. *Nucleic Acids Research*, *48*(3), 1029–1042. https://doi.org/10.1093/nar/gkz734

Otsuki, L., & Brand, A. H. (2018). Cell cycle heterogeneity directs the timing of neural stem cell activation from quiescence. *Science*, *360*(6384), 99–102. https://doi.org/10.1126/science.aan8795

Palková, Z., & Váchová, L. (2016). Yeast cell differentiation: Lessons from pathogenic and non-pathogenic yeasts. *Seminars in Cell & Developmental Biology*, *57*, 110–119. https://doi.org/10.1016/j.semcdb.2016.04.006

Pardee, A. B. (1974). A Restriction Point for Control of Normal Animal Cell Proliferation. *Proceedings of the National Academy of Sciences of the United States of America*, *71*(4), 1286–1290.

Pardee, A. B. (1989). G1 events and regulation of cell proliferation. *Science (New York, N.Y.)*, *246*(4930), 603–608. https://doi.org/10.1126/science.2683075

Parenteau, J., Durand, M., Morin, G., Gagnon, J., Lucier, J.-F., Wellinger, R. J., Chabot, B., & Abou Elela, S. (2011). Introns within Ribosomal Protein Genes Regulate the Production and Function of Yeast Ribosomes. *Cell*, *147*(2), 320–331. https://doi.org/10.1016/j.cell.2011.08.044

Parenteau, J., Durand, M., Véronneau, S., Lacombe, A.-A., Morin, G., Guérin, V., Cecez, B., Gervais-Bird, J., Koh, C.-S., Brunelle, D., Wellinger, R. J., Chabot, B., & Abou Elela, S. (2008). Deletion of Many Yeast Introns Reveals a Minority of Genes that Require Splicing for Function. *Molecular Biology of the Cell*, *19*(5), 1932–1941. https://doi.org/10.1091/mbc.e07-12-1254

Parker, D. M., Winkenbach, L. P., & Osborne Nishimura, E. (2022). It's Just a Phase: Exploring the Relationship Between mRNA, Biomolecular Condensates, and Translational Control. *Frontiers in Genetics*, *13*. https://www.frontiersin.org/articles/10.3389/fgene.2022.931220

Paz, I., Abramovitz, L., & Choder, M. (1999). Starved Saccharomyces cerevisiae Cells Have the Capacity to Support Internal Initiation of Translation *. *Journal of Biological Chemistry*, *274*(31), 21741–21745. https://doi.org/10.1074/jbc.274.31.21741

Paz, I., & Choder, M. (2001). Eukaryotic translation initiation factor 4E-dependent translation is not essential for survival of starved yeast cells. *Journal of Bacteriology*, *183*(15), 4477–4483. https://doi.org/10.1128/JB.183.15.4477-4483.2001

Pelechano, V., & Steinmetz, L. M. (2013). Gene regulation by antisense transcription. *Nature Reviews Genetics*, *14*(12), Article 12. https://doi.org/10.1038/nrg3594

Peña, A., Sánchez, N. S., Álvarez, H., Calahorra, M., & Ramírez, J. (2015). Effects of high medium pH on growth, metabolism and transport in Saccharomyces cerevisiae. *FEMS Yeast Research*, *15*(2), fou005. https://doi.org/10.1093/femsyr/fou005

Pertea, M. (2012). The Human Transcriptome: An Unfinished Story. *Genes*, *3*(3), 344. https://doi.org/10.3390/genes3030344

Pertea, M., Pertea, G. M., Antonescu, C. M., Chang, T.-C., Mendell, J. T., & Salzberg, S. L. (2015). StringTie enables improved reconstruction of a transcriptome from RNA-seq reads. *Nature Biotechnology*, *33*(3), Article 3. https://doi.org/10.1038/nbt.3122

Pfeiffer, T., & Morley, A. (2014). An evolutionary perspective on the Crabtree effect. *Frontiers in Molecular Biosciences*, *1*. https://www.frontiersin.org/articles/10.3389/fmolb.2014.00017

Pfeiffer, T., Schuster, S., & Bonhoeffer, S. (2001). Cooperation and Competition in the Evolution of ATP-Producing Pathways. *Science*, *292*(5516), 504–507. https://doi.org/10.1126/science.1058079

Piekna-Przybylska, D., Decatur, W. A., & Fournier, M. J. (2007). New bioinformatic tools for analysis of nucleotide modifications in eukaryotic rRNA. *RNA*, *13*(3), 305–312. https://doi.org/10.1261/rna.373107

Piñon, R. (1978). Folded chromosomes in non-cycling yeast cells: Evidence for a characteristic g0 form. *Chromosoma*, *67*(3), 263–274. https://doi.org/10.1007/BF02569039

Pinto, P. A. B., Henriques, T., Freitas, M. O., Martins, T., Domingues, R. G., Wyrzykowska, P. S., Coelho, P. A., Carmo, A. M., Sunkel, C. E., Proudfoot, N. J., & Moreira, A. (2011). RNA polymerase II kinetics in polo polyadenylation signal selection. *The EMBO Journal*, *30*(12), 2431–2444. https://doi.org/10.1038/emboj.2011.156

Policastro, R. A., & Zentner, G. E. (2021). Global approaches for profiling transcription initiation. *Cell Reports Methods*, *1*(5), 100081. https://doi.org/10.1016/j.crmeth.2021.100081

Poon, P. P., Nothwehr, S. F., Singer, R. A., & Johnston, G. C. (2001). The Gcs1 and Age2 ArfGAP proteins provide overlapping essential function for transport from the yeast

trans-Golgi network. *Journal of Cell Biology*, *155*(7), 1239–1250. https://doi.org/10.1083/jcb.200108075

Porrua, O., Boudvillain, M., & Libri, D. (2016). Transcription Termination: Variations on Common Themes. *Trends in Genetics*, *32*(8), 508–522. https://doi.org/10.1016/j.tig.2016.05.007

Porrua, O., Hobor, F., Boulay, J., Kubicek, K., D'Aubenton-Carafa, Y., Gudipati, R. K., Stefl, R., & Libri, D. (2012). In vivo SELEX reveals novel sequence and structural determinants of Nrd1-Nab3-Sen1-dependent transcription termination. *The EMBO Journal*, *31*(19), 3935–3948. https://doi.org/10.1038/emboj.2012.237

Proudfoot, N. J. (2011). Ending the message: Poly(A) signals then and now. *Genes & Development*, *25*(17), 1770–1782. https://doi.org/10.1101/gad.17268411

Putnam, A., Thomas, L., & Seydoux, G. (2023). RNA granules: Functional compartments or incidental condensates? *Genes & Development*, *37*(9–10), 354–376. https://doi.org/10.1101/gad.350518.123

Putri, G. H., Anders, S., Pyl, P. T., Pimanda, J. E., & Zanini, F. (2022). Analysing high-throughput sequencing data in Python with HTSeq 2.0. *Bioinformatics (Oxford, England)*, *38*(10), 2943–2945. https://doi.org/10.1093/bioinformatics/btac166

Qian, Y., Shi, L., & Luo, Z. (2020). Long Non-coding RNAs in Cancer: Implications for Diagnosis, Prognosis, and Therapy. *Frontiers in Medicine*, *7*, 612393. https://doi.org/10.3389/fmed.2020.612393

Quinlan, A. R., & Hall, I. M. (2010). BEDTools: A flexible suite of utilities for comparing genomic features. *Bioinformatics*, *26*(6), 841–842. https://doi.org/10.1093/bioinformatics/btq033

Raivo Kolde. (2019). *pheatmap: Pretty Heatmaps* (R package version 1.0.12) [Computer software]. https://CRAN.R-project.org/package=pheatmap

Ramírez, F., Dündar, F., Diehl, S., Grüning, B. A., & Manke, T. (2014). deepTools: A flexible platform for exploring deep-sequencing data. *Nucleic Acids Research*, *42*(Web Server issue), W187–W191. https://doi.org/10.1093/nar/gku365

Reggiori, F., & Klionsky, D. J. (2013). Autophagic Processes in Yeast: Mechanism, Machinery and Regulation. *Genetics*, *194*(2), 341. https://doi.org/10.1534/genetics.112.149013

Rhind, N., Chen, Z., Yassour, M., Thompson, D. A., Haas, B. J., Habib, N., Wapinski, I., Roy, S., Lin, M. F., Heiman, D. I., Young, S. K., Furuya, K., Guo, Y., Pidoux, A., Chen, H. M., Robbertse, B., Goldberg, J. M., Aoki, K., Bayne, E. H., … Nusbaum, C. (2011). Comparative Functional Genomics of the Fission Yeasts. *Science*, *332*(6032), 930–936. https://doi.org/10.1126/science.1203357

Rittershaus, E. S. C., Baek, S.-H., & Sassetti, C. M. (2013). The Normalcy of Dormancy: Common Themes in Microbial Quiescence. *Cell Host & Microbe*, *13*(6), 643–651. https://doi.org/10.1016/j.chom.2013.05.012

Saccharomyces cerevisiae S288C genome assembly R64. (n.d.). NCBI. Retrieved July 19, 2023, from https://www.ncbi.nlm.nih.gov/data-hub/assembly/GCF_000146045.2/

Sarantopoulou, D., Tang, S. Y., Ricciotti, E., Lahens, N. F., Lekkas, D., Schug, J., Guo, X. S., Paschos, G. K., FitzGerald, G. A., Pack, A. I., & Grant, G. R. (2019). Comparative evaluation of RNA-Seq library preparation methods for strand-specificity and low input. *Scientific Reports*, *9*(1), Article 1. https://doi.org/10.1038/s41598-019-49889-1

Saxton, R. A., & Sabatini, D. M. (2017). mTOR Signaling in Growth, Metabolism, and Disease. *Cell*, *168*(6), 960–976. https://doi.org/10.1016/j.cell.2017.02.004

Schaughency, P., Merran, J., & Corden, J. L. (2014). Genome-Wide Mapping of Yeast RNA Polymerase II Termination. *PLOS Genetics*, *10*(10), e1004632. https://doi.org/10.1371/journal.pgen.1004632

Schmitt, M. J., & Breinig, F. (2006). Yeast viral killer toxins: Lethality and self-protection. *Nature Reviews Microbiology*, *4*(3), Article 3. https://doi.org/10.1038/nrmicro1347

Schneider, C., Kudla, G., Wlotzka, W., Tuck, A., & Tollervey, D. (2012). Transcriptome-wide Analysis of Exosome Targets. *Molecular Cell*, *48*(3–3), 422–433. https://doi.org/10.1016/j.molcel.2012.08.013

Schulz, D., Schwalb, B., Kiesel, A., Baejen, C., Torkler, P., Gagneur, J., Soeding, J., & Cramer, P. (2013). Transcriptome Surveillance by Selective Termination of Noncoding RNA Synthesis. *Cell*, *155*(5), 1075–1087. https://doi.org/10.1016/j.cell.2013.10.024

Seifuddin, F., Singh, K., Suresh, A., Judy, J. T., Chen, Y.-C., Chaitankar, V., Tunc, I., Ruan, X., Li, P., Chen, Y., Cao, H., Lee, R. S., Goes, F. S., Zandi, P. P., Jafri, M. S., & Pirooznia, M. (2020). lncRNAKB, a knowledgebase of tissue-specific functional annotation and trait association of long noncoding RNA. *Scientific Data*, *7*(1), Article 1. https://doi.org/10.1038/s41597-020-00659-z

Shi, L., Sutter, B. M., Ye, X., & Tu, B. P. (2010). Trehalose Is a Key Determinant of the Quiescent Metabolic State That Fuels Cell Cycle Progression upon Return to Growth. *Molecular Biology of the Cell*, *21*(12), 1982–1990. https://doi.org/10.1091/mbc.e10-01-0056

Shimoi, H., Kitagaki, H., Ohmori, H., Iimura, Y., & Ito, K. (1998). Sed1p Is a Major Cell Wall Protein ofSaccharomyces cerevisiae in the Stationary Phase and Is Involved in Lytic

Enzyme Resistance. *Journal of Bacteriology*, *180*(13), 3381–3387. https://doi.org/10.1128/jb.180.13.3381-3387.1998

Simon Andrews. (2014). *FastQC A Quality Control tool for High Throughput Sequence Data* (0.0.14) [Computer software]. https://www.bioinformatics.babraham.ac.uk/projects/fastqc/

Singh, N., Asalam, Mohd., Ansari, M. O., Gerasimova, N. S., Studitsky, V. M., & Akhtar, Md. S. (2022). Transcription by RNA polymerase II and the CTD-chromatin crosstalk. *Biochemical and Biophysical Research Communications*, *599*, 81–86. https://doi.org/10.1016/j.bbrc.2022.02.039

Singh, P., Chaudhuri, A., Banerjea, M., Marathe, N., & Das, B. (2021). Nrd1p identifies aberrant and natural exosomal target messages during the nuclear mRNA surveillance in Saccharomyces cerevisiae. *Nucleic Acids Research*, *49*(20), 11512–11536. https://doi.org/10.1093/nar/gkab930

Smith, J. E., Alvarez-Dominguez, J. R., Kline, N., Huynh, N. J., Geisler, S., Hu, W., Coller, J., & Baker, K. E. (2014). Translation of Small Open Reading Frames within Unannotated RNA Transcripts in Saccharomyces cerevisiae. *Cell Reports*, *7*(6), 1858–1866. https://doi.org/10.1016/j.celrep.2014.05.023

Smith, R. N., Aleksic, J., Butano, D., Carr, A., Contrino, S., Hu, F., Lyne, M., Lyne, R., Kalderimis, A., Rutherford, K., Stepan, R., Sullivan, J., Wakeling, M., Watkins, X., & Micklem, G. (2012). InterMine: A flexible data warehouse system for the integration and analysis of heterogeneous biological data. *Bioinformatics*, *28*(23), 3163–3165. https://doi.org/10.1093/bioinformatics/bts577

Smith, T., Heger, A., & Sudbery, I. (2017). UMI-tools: Modeling sequencing errors in Unique Molecular Identifiers to improve quantification accuracy. *Genome Research*, *27*(3), 491–499. https://doi.org/10.1101/gr.209601.116

Sohrabi-Jahromi, S., Hofmann, K. B., Boltendahl, A., Roth, C., Gressel, S., Baejen, C., Soeding, J., & Cramer, P. (2019). Transcriptome maps of general eukaryotic RNA degradation factors. *eLife*, *8*, e47040. https://doi.org/10.7554/eLife.47040

Song, L., & Florea, L. (2015). Rcorrector: Efficient and accurate error correction for Illumina RNA-seq reads. *GigaScience*, *4*(1), 48. https://doi.org/10.1186/s13742-015-0089-y

Song, Y., Milon, B., Ott, S., Zhao, X., Sadzewicz, L., Shetty, A., Boger, E. T., Tallon, L. J., Morell, R. J., Mahurkar, A., & Hertzano, R. (2018). A comparative analysis of library prep approaches for sequencing low input translatome samples. *BMC Genomics*, *19*(1), 696. https://doi.org/10.1186/s12864-018-5066-2

Spain, M., Keean C. A. Braceros, & Toshio Tsukiyama. (2018). *SWI/SNF coordinates transcriptional activation through Rpd3-mediated histone hypoacetylation during quiescence entry*. bioRxiv. https://doi.org/doi: https://doi.org/10.1101/426288

Spain, M. M., Swygert, S. G., & Tsukiyama, T. (2018). Preparation and Analysis of Saccharomyces cerevisiae Quiescent Cells. In H. D. Lacorazza (Ed.), *Cellular Quiescence: Methods and Protocols* (pp. 125–135). Springer. https://doi.org/10.1007/978-1-4939-7371-2_9

Spies, N., Nielsen, C. B., Padgett, R. A., & Burge, C. B. (2009). Biased chromatin signatures around polyadenylation sites and exons. *Molecular Cell*, *36*(2), 245–254. https://doi.org/10.1016/j.molcel.2009.10.008

Stead, J. A., Costello, J. L., Livingstone, M. J., & Mitchell, P. (2007). The PMC2NT domain of the catalytic exosome subunit Rrp6p provides the interface for binding with its cofactor Rrp47p, a nucleic acid-binding protein. *Nucleic Acids Research*, *35*(16), 5556–5567. https://doi.org/10.1093/nar/gkm614

Steinmetz, E. J., & Brow, D. A. (1998). Control of pre-mRNA accumulation by the essential yeast protein Nrd1 requires high-affinity transcript binding and a domain implicated in RNA polymerase II association. *Proceedings of the National Academy of Sciences*, *95*(12), 6699–6704. https://doi.org/10.1073/pnas.95.12.6699

Steinmetz, E. J., Conrad, N. K., Brow, D. A., & Corden, J. L. (2001). RNA-binding protein Nrd1 directs poly(A)-independent 3′-end formation of RNA polymerase II transcripts. *Nature*, *413*(6853), Article 6853. https://doi.org/10.1038/35095090

Sun, M., Schwalb, B., Pirkl, N., Maier, K. C., Schenk, A., Failmezger, H., Tresch, A., & Cramer, P. (2013). Global Analysis of Eukaryotic mRNA Degradation Reveals Xrn1-Dependent Buffering of Transcript Levels. *Molecular Cell*, *52*(1), 52–62. https://doi.org/10.1016/j.molcel.2013.09.010

Swygert, S. G., Kim, S., Wu, X., Fu, T., Hsieh, T.-H., Rando, O. J., Eisenman, R. N., Shendure, J., McKnight, J. N., & Tsukiyama, T. (2019). Condensin-Dependent Chromatin Compaction Represses Transcription Globally during Quiescence. *Molecular Cell*, *73*(3), 533-546.e4. https://doi.org/10.1016/j.molcel.2018.11.020

Swygert, S. G., Lin, D., Portillo-Ledesma, S., Lin, P.-Y., Hunt, D. R., Kao, C.-F., Schlick, T., Noble, W. S., & Tsukiyama, T. (2021). Local chromatin fiber folding represses transcription and loop extrusion in quiescent cells. *eLife*, *10*, e72062. https://doi.org/10.7554/eLife.72062

Szcześniak, M. W., Kubiak, M. R., Wanowska, E., & Makałowska, I. (2021). Comparative genomics in the search for conserved long noncoding RNAs. *Essays in Biochemistry*, *65*(4), 741–749. https://doi.org/10.1042/EBC20200069

Tarazona, O. A., & Pourquié, O. (2020). Exploring the Influence of Cell Metabolism on Cell Fate through Protein Post-translational Modifications. *Developmental Cell*, *54*(2), 282–292. https://doi.org/10.1016/j.devcel.2020.06.035

Terzi, N., Churchman, L. S., Vasiljeva, L., Weissman, J., & Buratowski, S. (2011). H3K4 Trimethylation by Set1 Promotes Efficient Termination by the Nrd1-Nab3-Sen1 Pathway. *Molecular and Cellular Biology*, *31*(17), 3569–3583. https://doi.org/10.1128/MCB.05590-11

Teste, M.-A., Duquenne, M., François, J. M., & Parrou, J.-L. (2009). Validation of reference genes for quantitative expression analysis by real-time RT-PCR in Saccharomyces cerevisiae. *BMC Molecular Biology*, *10*, 99. https://doi.org/10.1186/1471-2199-10-99

Tian, B., & Graber, J. H. (2012). Signals for pre-mRNA cleavage and polyadenylation. *Wiley Interdisciplinary Reviews. RNA*, *3*(3), 385–396. https://doi.org/10.1002/wrna.116

Tian, S., Curnutte, H. A., & Trcek, T. (2020). RNA Granules: A View from the RNA Perspective. *Molecules*, *25*(14), Article 14. https://doi.org/10.3390/molecules25143130

Tietjen, J. R., Zhang, D. W., Rodríguez-Molina, J. B., White, B. E., Akhtar, M. S., Heidemann, M., Li, X., Chapman, R. D., Shokat, K., Keles, S., Eick, D., & Ansari, A. Z. (2010). Chemical-genomic dissection of the CTD code. *Nature Structural & Molecular Biology*, *17*(9), Article 9. https://doi.org/10.1038/nsmb.1900

Till, P., Mach, R. L., & Mach-Aigner, A. R. (2018). A current view on long noncoding RNAs in yeast and filamentous fungi. *Applied Microbiology and Biotechnology*, *102*(17), 7319–7331. https://doi.org/10.1007/s00253-018-9187-y

Tomasin, R., & Bruni-Cardoso, A. (2022). The role of cellular quiescence in cancer – beyond a quiet passenger. *Journal of Cell Science*, *135*(15), jcs259676. https://doi.org/10.1242/jcs.259676

Trapnell, C., Roberts, A., Goff, L., Pertea, G., Kim, D., Kelley, D. R., Pimentel, H., Salzberg, S. L., Rinn, J. L., & Pachter, L. (2012). Differential gene and transcript expression analysis of RNA-seq experiments with TopHat and Cufflinks. *Nature Protocols*, *7*(3), 562–578. https://doi.org/10.1038/nprot.2012.016

Trotman, J. B., & Schoenberg, D. R. (2019). A recap of RNA recapping. *WIREs RNA*, *10*(1), e1504. https://doi.org/10.1002/wrna.1504

Tudek, A., Krawczyk, P. S., Mroczek, S., Tomecki, R., Turtola, M., Matylla-Kulińska, K., Jensen, T. H., & Dziembowski, A. (2021). Global view on the metabolism of RNA poly(A) tails in yeast Saccharomyces cerevisiae. *Nature Communications*, *12*(1), Article 1. https://doi.org/10.1038/s41467-021-25251-w

Tudek, A., Porrua, O., Kabzinski, T., Lidschreiber, M., Kubicek, K., Fortova, A., Lacroute, F., Vanacova, S., Cramer, P., Stefl, R., & Libri, D. (2014). Molecular Basis for Coordinating Transcription Termination with Noncoding RNA Degradation. *Molecular Cell*, *55*(3), 467–481. https://doi.org/10.1016/j.molcel.2014.05.031

Turner, R. E., Harrison, P. F., Swaminathan, A., Kraupner-Taylor, C. A., Goldie, B. J., See, M., Peterson, A. L., Schittenhelm, R. B., Powell, D. R., Creek, D. J., Dichtl, B., & Beilharz,

T. H. (2021). Genetic and pharmacological evidence for kinetic competition between alternative poly(A) sites in yeast. *eLife*, *10*, e65331. https://doi.org/10.7554/eLife.65331

van Dijk, E. L., Chen, C. L., d'Aubenton-Carafa, Y., Gourvennec, S., Kwapisz, M., Roche, V., Bertrand, C., Silvain, M., Legoix-Né, P., Loeillet, S., Nicolas, A., Thermes, C., & Morillon, A. (2011). XUTs are a class of Xrn1-sensitive antisense regulatory non-coding RNA in yeast. *Nature*, *475*(7354), 114–117. https://doi.org/10.1038/nature10118

van Nues, R., Schweikert, G., de Leau, E., Selega, A., Langford, A., Franklin, R., Iosub, I., Wadsworth, P., Sanguinetti, G., & Granneman, S. (2017). Kinetic CRAC uncovers a role for Nab3 in determining gene expression profiles during stress. *Nature Communications*, *8*(1), Article 1. https://doi.org/10.1038/s41467-017-00025-5

Vasiljeva, L., & Buratowski, S. (2006). Nrd1 interacts with the nuclear exosome for 3' processing of RNA polymerase II transcripts. *Molecular Cell*, *21*(2), 239–248. https://doi.org/10.1016/j.molcel.2005.11.028

Vasiljeva, L., Kim, M., Mutschler, H., Buratowski, S., & Meinhart, A. (2008). The Nrd1-Nab3-Sen1 termination complex interacts with the Ser5-phosphorylated RNA polymerase II C-terminal domain. *Nature Structural & Molecular Biology*, *15*(8), 795–804. https://doi.org/10.1038/nsmb.1468

Vasiljeva, L., Kim, M., Terzi, N., Soares, L. M., & Buratowski, S. (2008). Transcription Termination and RNA Degradation Contribute to Silencing of RNA Polymerase II Transcription within Heterochromatin. *Molecular Cell*, *29*(3), 313–323. https://doi.org/10.1016/j.molcel.2008.01.011

Venkatesh, S., Li, H., Gogol, M. M., & Workman, J. L. (2016). Selective suppression of antisense transcription by Set2-mediated H3K36 methylation. *Nature Communications*, *7*, 13610. https://doi.org/10.1038/ncomms13610

Vera, J. M., & Dowell, R. D. (2016). Survey of cryptic unstable transcripts in yeast. *BMC Genomics*, *17*(1), 305. https://doi.org/10.1186/s12864-016-2622-5

Villa, T., Barucco, M., Martin-Niclos, M.-J., Jacquier, A., & Libri, D. (2020). Degradation of Non-coding RNAs Promotes Recycling of Termination Factors at Sites of Transcription. *Cell Reports*, *32*(3), 107942. https://doi.org/10.1016/j.celrep.2020.107942

Villa, T., & Porrua, O. (2022). Pervasive transcription: A controlled risk. *The FEBS Journal*. https://doi.org/10.1111/febs.16530

Wallace, E. W. J., Kear-Scott, J. L., Pilipenko, E. V., Schwartz, M. H., Laskowski, P. R., Rojek, A. E., Katanski, C. D., Riback, J. A., Dion, M. F., Franks, A. M., Airoldi, E. M., Pan, T., Budnik, B. A., & Drummond, D. A. (2015). Reversible, Specific, Active Aggregates of Endogenous Proteins Assemble upon Heat Stress. *Cell*, *162*(6), 1286–1298. https://doi.org/10.1016/j.cell.2015.08.041

Wang, C., Schmich, F., Srivatsa, S., Weidner, J., Beerenwinkel, N., & Spang, A. (2018). Context-dependent deposition and regulation of mRNAs in P-bodies. *eLife*, *7*, e29815. https://doi.org/10.7554/eLife.29815

Wang, S., Han, Z., Libri, D., Porrua, O., & Strick, T. R. (2019). Single-molecule characterization of extrinsic transcription termination by Sen1 helicase. *Nature Communications*, *10*(1), Article 1. https://doi.org/10.1038/s41467-019-09560-9

Wasmuth, E. V., & Lima, C. D. (2012). Exo- and endoribonucleolytic activities of yeast cytoplasmic and nuclear RNA exosomes are dependent on the noncatalytic core and

central channel. *Molecular Cell*, *48*(1), 133–144. https://doi.org/10.1016/j.molcel.2012.07.012

Webb, S., Hector, R. D., Kudla, G., & Granneman, S. (2014). PAR-CLIP data indicate that Nrd1-Nab3-dependent transcription termination regulates expression of hundreds of protein coding genes in yeast. *Genome Biology*, *15*(1), R8. https://doi.org/10.1186/gb-2014-15-1-r8

Werner-Washburne, M., Braun, E., Johnston, G. C., & Singer, R. A. (1993). Stationary phase in the yeast Saccharomyces cerevisiae. *Microbiological Reviews*, *57*(2), 383–401.

Wickner, R. B., Fujimura, T., & Esteban, R. (2013). Viruses and prions of Saccharomyces cerevisiae. *Advances in Virus Research*, *86*, 1–36. https://doi.org/10.1016/B978-0-12-394315-6.00001-5

Wiedner, H. J., & Giudice, J. (2021). It's not just a phase: Function and characteristics of RNA-binding proteins in phase separation. *Nature Structural & Molecular Biology*, *28*(6), Article 6. https://doi.org/10.1038/s41594-021-00601-w

Wlotzka, W., Kudla, G., Granneman, S., & Tollervey, D. (2011). The nuclear RNA polymerase II surveillance system targets polymerase III transcripts. *The EMBO Journal*, *30*(9), 1790–1803. https://doi.org/10.1038/emboj.2011.97

Wu, J., Zhang, N., Hayes, A., Panoutsopoulou, K., & Oliver, S. G. (2004). Global analysis of nutrient control of gene expression in Saccharomyces cerevisiae during growth and starvation. *Proceedings of the National Academy of Sciences*, *101*(9), 3148–3153. https://doi.org/10.1073/pnas.0308321100

Wu, T. D., & Watanabe, C. K. (2005). GMAP: A genomic mapping and alignment program for mRNA and EST sequences. *Bioinformatics*, *21*(9), 1859–1875. https://doi.org/10.1093/bioinformatics/bti310

Wyers, F., Rougemaille, M., Badis, G., Rousselle, J.-C., Dufour, M.-E., Boulay, J., Régnault, B., Devaux, F., Namane, A., Séraphin, B., Libri, D., & Jacquier, A. (2005). Cryptic pol II transcripts are degraded by a nuclear quality control pathway involving a new poly(A) polymerase. *Cell*, *121*(5), 725–737. https://doi.org/10.1016/j.cell.2005.04.030

Xu, Z., Wei, W., Gagneur, J., Perocchi, F., Clauder-Münster, S., Camblong, J., Guffanti, E., Stutz, F., Huber, W., & Steinmetz, L. M. (2009). Bidirectional promoters generate pervasive transcription in yeast. *Nature*, *457*(7232), Article 7232. https://doi.org/10.1038/nature07728

Yagoub, D., Tay, A. P., Chen, Z., Hamey, J. J., Cai, C., Chia, S. Z., Hart-Smith, G., & Wilkins, M. R. (2015). Proteogenomic Discovery of a Small, Novel Protein in Yeast Reveals a Strategy for the Detection of Unannotated Short Open Reading Frames. *Journal of Proteome Research*, *14*(12), 5038–5047. https://doi.org/10.1021/acs.jproteome.5b00734

Yague-Sanz, C., Vanrobaeys, Y., Fernandez, R., Duval, M., Larochelle, M., Beaudoin, J., Berro, J., Labbé, S., Jacques, P.-É., & Bachand, F. (2020). Nutrient-dependent control of RNA polymerase II elongation rate regulates specific gene expression programs by alternative polyadenylation. *Genes & Development*, *34*(13–14), 883. https://doi.org/10.1101/gad.337212.120

Yalcin, S. K., & Yesim Ozbas, Z. (2008). Effects of pH and temperature on growth and glycerol production kinetics of two indigenous wine strains of Saccharomyces cerevisiae from

Turkey. *Brazilian Journal of Microbiology: [Publication of the Brazilian Society for Microbiology]*, *39*(2), 325–332. https://doi.org/10.1590/S1517-838220080002000024

Yamashita, A., Shichino, Y., & Yamamoto, M. (2016). The long non-coding RNA world in yeasts. *Biochimica et Biophysica Acta (BBA) - Gene Regulatory Mechanisms*, *1859*(1), 147–154. https://doi.org/10.1016/j.bbagrm.2015.08.003

Yang, L., Duff, M. O., Graveley, B. R., Carmichael, G. G., & Chen, L.-L. (2011). Genomewide characterization of non-polyadenylated RNAs. *Genome Biology*, *12*(2), R16. https://doi.org/10.1186/gb-2011-12-2-r16

Yassour, M., Pfiffner, J., Levin, J. Z., Adiconis, X., Gnirke, A., Nusbaum, C., Thompson, D.-A., Friedman, N., & Regev, A. (2010). Strand-specific RNA sequencing reveals extensive regulated long antisense transcripts that are conserved across yeast species. *Genome Biology*, *11*(8), R87. https://doi.org/10.1186/gb-2010-11-8-r87

Young, C. P., Hillyer, C., Hokamp, K., Fitzpatrick, D. J., Konstantinov, N. K., Welty, J. S., Ness, S. A., Werner-Washburne, M., Fleming, A. B., & Osley, M. A. (2017). Distinct histone methylation and transcription profiles are established during the development of cellular quiescence in yeast. *BMC Genomics*, *18*. https://doi.org/10.1186/s12864-017-3509-9

YPD media. (2010). *Cold Spring Harbor Protocols*, *2010*(9), pdb.rec12315. https://doi.org/10.1101/pdb.rec12315

Yüce, Ö., & West, S. C. (2013). Senataxin, Defective in the Neurodegenerative Disorder Ataxia with Oculomotor Apraxia 2, Lies at the Interface of Transcription and the DNA Damage Response. *Molecular and Cellular Biology*, *33*(2), 406–417. https://doi.org/10.1128/MCB.01195-12

Zaborowska, J., Egloff, S., & Murphy, S. (2016). The pol II CTD: New twists in the tail. *Nature Structural & Molecular Biology*, *23*(9), Article 9. https://doi.org/10.1038/nsmb.3285

Zetterberg, A., & Larsson, O. (1985). Kinetic analysis of regulatory events in G1 leading to proliferation or quiescence of Swiss 3T3 cells. *Proceedings of the National Academy of Sciences of the United States of America*, *82*(16), 5365–5369.

Zhang, J., Si, J., Gan, L., Di, C., Xie, Y., Sun, C., Li, H., Guo, M., & Zhang, H. (2019). Research progress on therapeutic targeting of quiescent cancer cells. *Artificial Cells, Nanomedicine, and Biotechnology*, *47*(1), 2810–2819. https://doi.org/10.1080/21691401.2019.1638793

Zhang, Y., Kuster, D., Schmidt, T., Kirrmaier, D., Nübel, G., Ibberson, D., Benes, V., Hombauer, H., Knop, M., & Jäschke, A. (2020). Extensive 5′-surveillance guards against non-canonical NAD-caps of nuclear mRNAs in yeast. *Nature Communications*, *11*(1), Article 1. https://doi.org/10.1038/s41467-020-19326-3

APPENDIX A: ACIDIC PH PROMOTES QUIESENCE ENTRY IN W303 *SACCHAROMYCES CEREVISIAE*

This appendix is composed of draft of a manuscript which will be submitted to microPublication Biology with authors A. C. Greenlaw and T. Tsukiyama.

Abstract

Quiescence is a conserved cellular state wherein cells cease proliferation and remain poised to re-enter the cell cycle when conditions are appropriate. Budding yeast has emerged as powerful tool for studying cellular quiescence. In this work, we demonstrate that the pH of the YPD media affects quiescence entry efficiency in *Saccharomyces cerevisiae*. Many more quiescent cells are produced in acidic pH YPD than in basic pH YPD. Thermotolerance of the produced quiescence yeast are similar, suggesting the starting media pH influences the quantity of quiescent cells more than quality of quiescence reached.

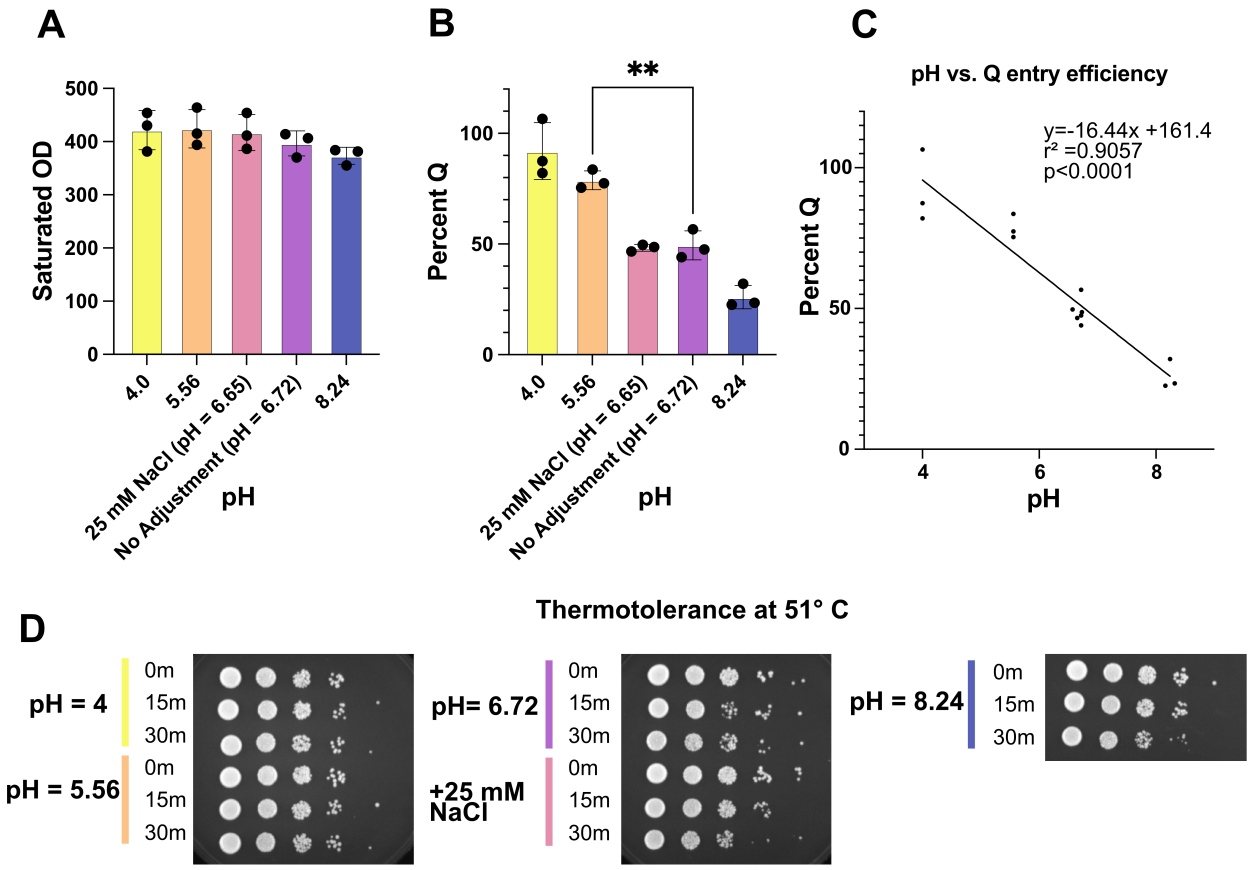

Figure 1 Acidic pH promotes quiescence entry.
(**A**) Bar graph showing total saturated OD_{660} of yeast produced by each media condition. Points represent each replicate and bars are standard deviation. Using pair t-test, difference is not significant.
(**B**) Bar graph showing percent quiescent cells produced by each media condition. Points represent each replicate and bars are standard deviation. Using pair t-test, difference between 5.56 and 6.72 is significant (** = $p < 0.001$).
(**C**) Scatter plot comparing media pH to percent quiescent. Linear regression analysis performed using Prism.
(**D**) Spot test of quiescent cell thermotolerance at 51 °C.

Description

Quiescence is conserved exit from the mitotic cell cycle, essential for long term survival in eukaryotes. *Saccharomyces cerevisiae* (hereafter yeast) have been leveraged as effective system

to study quiescence, since large quantities of quiescent cells can be readily purified (Allen et al., 2006). When quiescent cells are purified using the percoll gradient method, a quiescent and non-quiescent fraction are separated, and the percent of cells which enter quiescence can be measured.

We have found that quiescence entry yield of for the same yeast strain is variable over time, especially dependent upon the batch of YPD used. This was a frustrating logistical hurdle, as strains with low quiescence entry efficiency had to be grown and purified at large scale to ensure sufficient quiescent cell yield for genomic experiments. One aspect of the media that was uncontrolled in our laboratory was the pH. Standard recipes for liquid YPD do not generally mention media pH ("YPD Media," 2010). However, acidic pH has been demonstrated to increase glycerol production (Yalcin & Yesim Ozbas, 2008), and basic pH has been shown to inhibit fermentation and respiration (Peña et al., 2015). pH 5.5 has been reported as the optimal pH for ethanol production (Narendranath & Power, 2005). We wondered if media pH might influence quiescence entry yield.

To test this possibility, I grew three strains in in five different pH-adjusted YPD media. Four pH measurements were used; 4.0, 5.56, 6.72 (no adjustment) and 8.24. Since acetic acid is toxic to yeast and promotes aging (Burtner et al., 2009; Murakami et al., 2011), I used an inorganic acid (hydrochloric acid) and base (sodium hydroxide) to test the effect of media pH on quiescence entry. As an additional control, I added low concentration sodium chloride to the 5th YPD, to distinguish if the pH, or the chloride or sodium was responsible for changes to quiescence entry.

Yeast grown in all five batches of media saturated around 30 OD_{660} per mL, producing approximately 400 total OD_{660} (Figure 1A). Saturated density is essentially equivalent for all five media, with a slight but insignificant dip for the basic pH media. In contrast, pH dramatically changes the fraction of cells which are quiescent (Figure 1B). pH 4.0 results in in approximately

90% quiescence entry efficiency, compared to approximately 25% efficiency at pH 8.24. The additional of 25 mM NaCl did not significantly change quiescence entry efficiency compared to unadjusted YPD, demonstrating that pH, not salt ions, are the most relevant variable. Quiescence entry efficiency and pH are highly correlated between pH 4 and pH 8.24 ($r^2 = .9057$) (Figure 1C). Using simple linear regression, the estimated slope in -16.44, and is significantly non-zero ($p<0.0001$).

To test if the cells produced were truly quiescent, I performed a thermotolerance assay. Quiescence yeast have improved thermotolerance, and can survive heat shock at 51 °C (Allen et al., 2006; Klosinska et al., 2011). Thermotolerance is relatively similar regardless of media pH (Figure 1D). Although the difference is very minor, pH 4.0 and 5.56 seem to survive slightly better than pH 6.72 and 8.24 after 30 minutes 51 °C. This suggests that the increased quiescence entry yields from the media with pH 4.0 and 5.56 are the result of additional *bona fide* quiescent cells.

In contrast to these results, previous reports demonstrated that acetic acid is toxic to yeast, and low pH has been shown to reduce chronological lifespan (Burtner et al., 2009; Murakami et al., 2011). These experiments were performed in auxotrophic strains, which have poor longevity and are not appropriate for studying quiescence (Boer et al., 2008; Breeden & Tsukiyama, 2022). Additionally, BY4741 was used for some experiments, which does not go through the diauxic shift or enter quiescence (Miles et al., 2023). Thus, low pH reduces the lifespan of yeast unable to enter quiescence, but increases quiescence entry in W303 prototrophic yeast.

Method:

A 2-liter batch YEP was made (1% yeast extract, 2% peptone) and split into five 375 mL aliquots. pH was then adjusted with either HCl (pH 4, and 5.5) or NaOH (8.5). As an additional

control, NaCl was added at 25 mM to an aliquot. This concentration was determined based on the amount of HCl added to the pH 4 aliquot. The amount of acid, base or salt added was measured, and a remaining volume of water was added to so that 10 mL of additional volume were added to each aliquot. For the unadjusted control, 10 mL of water were added. All 5 media were autoclaved 1 hour at >120˚C. Glucose was added to a final concentration of 2%, and the pH was re-measured. 10 µl of yeast overnight culture from unadjusted YPD was added to each flask and grown for 7 days to saturation.

All experiments were performed in biological triplicate with independently created stains. The following strains were used:

Strain Number	**Source**	**Complete Genotype**
yTT5781	Tsukiyama Lab	*MATa RAD5+ can1-100*
yTT5782	Tsukiyama Lab	*MATa RAD5+ can1-100*
yTT5779	Tsukiyama Lab	*MAT@ RAD5+ can1-100*

Quiescent cell purification, quiescence entry efficiency, and thermotolerance were performed in 3.5, 3.6 and 3.7. Of note, quiescence entry percent was calculated from the OD of the saturated culture and the final volume and OD of the quiescent cells collected. The saturated culture was in YPD and blanked against YPD, while final Q fraction was in water and blanked against water. In one case this led to the total quiescent cell yield being calculated as greater than 100 percent.

Graphing and statistical analysis was performed in prism (version 10). Paired t-test was used to compare between columns in figure 1A and B. Simple linear regression was used to generate the trend line in figure 1C.

VITA

Alison Greenlaw grew up in Kirkland, Washington. She attended Washington University in St. Louis and graduated with an A.B. in Biology in 2014. Alison worked in the labs of Dr. Erik Herzog and Dr. Hani Zaher while at WashU. During this time, she became interested in RNA biology and gene regulation. Alison joined the Molecular and Cellular Biology program at the University of Washington in 2018, and the lab of Dr. Toshio Tsukiyama in 2019.